Morphing Technologies Design Toolbox and Application to Hydrofoil Design

by
Alexander John Ham

Thesis presented in partial fulfilment of the requirements for the degree of Master of Engineering (Mechanical) in the Faculty of Engineering at Stellenbosch University

Supervisor: Dr M.P. Venter
Co-supervisor: Dr M.T.F Owen

March 2021

Declaration

By submitting this thesis electronically, I declare that the entirety of the work contained therein is my own, original work, that I am the sole author thereof (save to the extent explicitly otherwise stated), that reproduction and publication thereof by Stellenbosch University will not infringe any third party rights and that I have not previously in its entirety or in part submitted it for obtaining any qualification.

Date: 20 November 2020 .....

Abstract

This thesis presents a morphing technology design toolbox and a conceptual design of a morphing centreboard which improves the performance of a 505 class sailing dinghy by eliminating leeway upwind, $\lambda = 0°$, and increasing VMG up to 9.5 %. From specifications stemming from the fluid dynamic investigation, the morphing centreboard concept changes shape from a NACA 0010 to a NACA 4410 profile yielding $C_{l0} = 0.4719$ at $AoA = 0°$. The design toolbox consists of a lexicon, classification and categorisation scheme applicable to fluid dynamic morphing technologies. Over two hundred morphing research entries are filtered in the design toolbox according to the design specifications of the morphing centreboard yielding eleven appropriate research entries. A preliminary structural investigation provides information on the surface (strains of up to 50 % are found) and the substructure and actuation (linear and bending actuators must overcome peak forces and bending moments of 2000 N and 300 Nm respectively). After the preliminary structural investigation multistable composite actuation and structural members together with a segmented composite/elastomer skin are the final conceptual technology solutions proposed for the morphing centreboard.

Uittreksel

Hierdie tesis bied 'n morphende tegnologie ontwerpgereedskapkis en 'n konseptuele ontwerp van 'n morphende-swaard aan. Die morphende-swaard verbeter die werkverrigting van 'n 505 klas seilboot deur die wind-op seilruimte, $\lambda = 0°$, te elimineer en VMG 9,5 % te verhoog. Vanuit spesifikasies uit die vloeidinamiese ondersoek moet die morphende-swaard konsep vorm verander van 'n NACA 0010 na 'n NACA 4410 profiel toe. Die verandering lewer 'n C_{l0} van 0.4719 op teen $AoA = 0°$. Die ontwerpgereedskapskis bestaan uit 'n leksikon-, klassifikasie- en kategoriseringskema wat van toepassing is op vloeidinamiese morphende-tegnologieë. Meer as tweehonderd navorsingsinskrywings word in die ontwerpgereedskapskas gefilter volgens die ontwerpspesifikasies van die morphende-swaard, wat elf toepaslike navorsingsinskrywings oplewer. 'N Voorlopige strukturele ondersoek bied inligting oor die oppervlak (vervorming van tot 50 %) en die struktuur en aktuator (lineêre en buigende aandrywers moet die piek kragte en buigmomente van onderskeidelik 2000 N en 300 Nm oorkom). Na die voorlopige strukturele ondersoek is multistabiele saamgestelde aktuators en struktuuronderdele tesame met 'n gesegmenteerde saamgestelde/elastomeer vel die finale konseptuele tegnologiese oplossings wat vir die morphende-swaard voorgestel woord.

Acknowledgements

I would like to begin by acknowledging the continued support of my supervisors, Dr M. Owen and Dr M.P. Venter. You have helped guide me through the numerous twists and turns of this project and I have learned a great deal from this experience.

I would like to thank my parents for their support, not only during this project but over the course of all of my studies.

Lastly I would like to thank Marz, you have been unwavering in your positivity throughout this project. Thank you for all the help, not least some of the figures in this thesis.

Contents

List of Figures

List of Tables

Nomenclature

Abbreviations

AAW Active Aeroelastic Wing

AFC Artificial Flow Control

AFW Active Flexible Wing

ATFI Advanced Fighter Technology Integration

CE Centre of Effort

CLR Centre of Lateral Resistance

DARPA Defence Advanced Research Projects Agency

DLR Deutsches Zentrum für Luft- und Raumfahrt; German Aerospace Centre

DSYHS Delft Systematic Yacht Hull Series

EAP Electro Active Polymer

LE Leading Edge

MAS Morphing Aircraft Structures

MAW Mission Adaptive Wing

MDA Multidisciplinary Analysis

NACA National Advisory Committee for Aeronautics

NASA National Aeronautics and Space Administration

PZT Piezoelectrics

SMA Shape Memory Alloys

SMP Shape Memory Polymers

TE Trailing Edge

TRL Technology Readiness Level

VMG Velocity Made Good

Abbreviations (Used in Design Toolbox)

ACT Actuation

AES Actuation Energy Source

AF Actuation Frequency

AL Actuation Load

AP Actuation Power

AXI Axis Influenced

DSC Degree of Shape Change

DT Design Target

ENT Entire

FA Focus Area

FD Fluid Dynamics

MECH Mechanics

MEF Morphing Effect

OPR Operating Conditions

PD Physical Description

SCL Scale

SUB Substructure

SUR Surface

SUS Sub-System

Symbols

α_k Keel/Centreboard Angle of Attack

α_{rudder} Rudder Angle of Attack

β_A Apparent Wind Angle

β_{tw} True Wind Angle

δ_r Rudder Trim Angle

λ Leeway Angle

μ Dynamic viscosity

ν Kinematic viscosity

ρ Density

ρ_w Water Density

θ Heel Angle

A_k Keel/Centreboard Surface Area

A_r Rudder Surface Area

A_w Wetted Surface Area

AR Aspect Ratio

AR_{eff} Effective Aspect Ratio

b Wing Span (Double the Span of an Underwater Appendage)

C_f Coefficient of Friction

c_r Root chord length

C_w Wave Drag Coefficient

C_{l0} Two dimensional zero AoA lift coefficient

C_{Lk} Keel/Centreboard Lift Coefficient

C_{Lr} Rudder Lift Coefficient

D	Drag Force
F_A	Total Aerodynamic Force
F_H	Total Hydrodynamic Force
F_m	Driving/Motive Force
F_{oa}	Aerodynamic Heeling/Overturning Force
F_s	Aerodynamic Side/Lateral Force
h	Endplate Height
L	Lift Force
l	Characteristic length (Chord length for airfoils)
M	Pitching Moment
m_c	Crew Mass
m_h	Helm Mass
$Ncrit$	XFoil turbulence transition factor
R	Hydrodynamic Drag Force
S	Hydrodynamic Side/Lateral Force
s	One Half Wing Span (Full Span of an Underwater Appendage)
t	Foil Thickness
V	Velocity
V_s	Boat Velocity
V_A	Apparent Wind Velocity
V_{tw}	True Wind Velocity
y_c	Crew Moment Arm
y_h	Helm Moment Arm
z_a	Distance from waterline to CE
z_h	Distance from waterline to CLR

Glossary of Sailing Terms

Glossary of Sailing Terms

Term	Description
Centreboard	A centreboard is the main underwater appendage producing lift counteracting the aerodynamic side force. It is usually located near the centre of the boat under the hull and is retractable by pivoting around a point inside a centreboard case in the hull.
Close Hauled	Is a point of sail where the boat is sailing on a course as close to opposite the wind direction as possible, approximately 45°. Is often also called beating.
Course	With reference to sailing: The path along which a boat travels.
Crew	The group of people who operate a boat. When referring to a specific sailor on a dinghy it is the sailor whose primary task it is to balance the boat and operate a number of sails and controls.
Sailing Dinghy	A small sailing boat, usually un-ballasted requiring the crew to use their weight to balance the overturning moment produced by the sails.
Heading	The direction that a boat is pointing in, not necessarily traveling in.
Helm	The means by which a boat is steered. When referring to a sailor it is the sailor which is primarily tasked with steering the boat.
Hull	The watertight body of a boat, displacing the water and allowing the boat to float.

Glossary of Sailing Terms - *cont.*

Term	**Description**
Leeway	The sideways drift to *leeward* (towards the side of the boat that is facing away from the wind) of a boat while sailing. The angle that the boats actual course makes with its heading is the *leeway angle*.
No-Go-Zone	The point of sail where the interaction of the forces acting on the boat do not produce any forward component, the sails are unable to drive the boat forward. Usually closer than 45° to the wind.
Point of Sail	A point of sail is a sailing boat's direction of travel under sail in relation to the true wind direction. The main points of sail are close hauled, beam reach and run at 45°, 90°, and 180° from the wind direction respectively.
Rudder	A rudder is a primary underwater appendage used to steer a boat. It is usually located at the back of the boat.
Sail (Noun)	A piece of fabric attached to the superstructure of the boat in such a way that its interaction with the wind drives the boat.
Sloop	A sailing boat with a single mast, typically slightly forward of the centre of the boat with one sail behind the mast and one forward of the mast. The most common rig design for modern sailing boats.
Tack (Verb)	To change a boats course by turning the boat's bow (front) into and through the wind.
Tack (Noun)	The direction of a boat with respect to the trim of her sails. With the sails are on the left or right side of the boat called starboard and port tack respectively
Velocity Made Good	A term used in sailing indicating the speed of a boat towards its target destination. In many cases it is equal to the boat speed but when sailing towards a goal directly upwind it is a component of the boat speed and angle.

Chapter 1

Introduction

1.1 Introduction to Competitive Sailing

Competitive sailing makes use of sophisticated technology and complex aero- and hydro-dynamic interactions to propel a boat around a set course in the minimum possible time. Figure 1.1 shows a high performance 505 class sailing dinghy in a racing situation.

Figure 1.1: High Performance 505 Class Sailing Dinghy Launching off a Wave with the Centreboard Visible (www.int505.org)

To achieve this goal a set of parameters need to be optimised over a range of

operating conditions. To be able to sail *against* the wind lift, and as a consequence drag, is produced by the sails, hull and underwater appendages of the boat. The interaction of these force vectors propel the boat forward as shown in Figure A.5 and Figure A.6 and expanded upon in subsection A.2. [1] Presently sailing boats require compromises in their design to allow for these varying operating conditions. A large area of compromise is in the design of the underwater appendages, specifically the symmetric, un-cambered centreboard which requires leeway of the boat in order to produce lift. Boats need to sail on both tacks requiring all components and systems to either be symmetric about the centre line or be move-able in such a way that they take up a mirrored configuration on the other side of the boat. This requirement for symmetry of the underwater appendages leads to penalties in their hydrodynamic interaction with the water. If the profile shape of the centreboard of a sailing boat can be altered while sailing, in response to changing operating conditions, lift can be produced with reduced induced drag resulting in improved performance. This leads to the idea of a *morphing centreboard.*

1.2 Introduction to Morphing

The concept of the seamless shape change of a body operating in a fluid flow to aid in control, improve performance, or otherwise alter the objective function, is an appealing one given the above context and is by no means new. The shape change of soft sails of sailing boats, whether actively controlled or passively affected is, and has been used in a number of different ways as far back as ancient Mesopotamian times. Within sailing, modern *sloop* rigged boats change the shape of their sails in order to adapt to changing operating conditions or improve performance. The shape changes present in sails include changes in camber, chord length and twist. The higher density of water makes similar applications to the hull and underwater appendages more challenging and consequently examples of shape change of bodies for hydrodynamic applications is far more limited.

Such envisioned shape changing bodies physically *morph* through or between a number of different stable configurations and fall within the umbrella of *morphing technologies.* According to Thill *et al.* (2008) morphing must deal with the change in *shape, form, external structure or arrangement.* The concept of *morph-*

[1] The understanding and comprehension of this thesis relies on a basic knowledge of competitive sailing, the basis for sailing races, terminology, equipment, and interaction of forces that govern the operation of a sailing boat. Appendix A.1 provides a brief outline of the key concepts and information required, should the reader have no baseline knowledge of sailing it is highly recommended this section be consulted and referenced throughout the thesis. Of particular importance are the concepts of upwind velocity made good (VMG) and leeway.

ing as applied to fluid dynamic cases, specifically foils (either *aerofoils* for aerodynamic applications or *hydrofoils* for hydrodynamic applications) encompasses a wide range of definitions, multidisciplinary challenges, and research streams. Appendix C provides a comprehensive outline of the available literature as well as a timeline of morphing technologies.

Research and technology pertaining to the field of morphing aircraft is abundant and diverse, however, due to their inherent changeable nature, morphing technologies are difficult to define and classify, consequently, the field of research contains little consensus on definition, classification, terminology, and applications. These challenges are further amplified with morphing technologies as it is often not obvious to differentiate between the structure and its various sub-structures due to the multi-functionality of many of the components involved (Thill *et al.*, 2008). It is generally accepted that discrete geometry changes arising from conventional hinged control systems or high lift devices (flaps, ailerons, etc.) are not considered morphing technology.Weisshaar (2006) defines the technology as a geometric change to improve performance or aid in control in the relevant application while maintaining a continuous, smooth surface. A number of review papers have collated much of the available morphing research and some seek to define the terms involved and classify morphing technologies, these include Jha and Kudva (2004); Rodriguez (2007); Thill *et al.* (2008); McGowan *et al.* (2009); Sofla *et al.* (2010); Barbarino *et al.* (2011*a*); Li *et al.* (2018).

The scope of potential applications for morphing technologies is broad and extends well outside of simply the aerospace industry. There is some limited literature within the hydrodynamic field specifically, using a variety of terms such as *flexible* (Lauder and Madden, 2007; Zeiner-Gundersen, 2014), *active* (Lagoudas *et al.*, 2014), *morphing* (Chen *et al.*, 2017; hua Hu *et al.*, 2017) and *adaptive* (Young *et al.*, 2016). The one underlying idea which persists in morphing technologies regardless of the application is the increased capability that such technologies can provide. The essence of morphing lies within the ability to drastically change the objective function of the body to which it applied thereby improving performance, expanding operational capability, aiding in control, or achieving optimized performance or control at more than a single operating or design point, (McGowan *et al.*, 2009). A high performance sailing dinghy stands to gain significant improvements in performance from a morphing centreboard.

1.3 Motivation

The goal of a sailing boat in a race is to complete a set course in the minimum time possible. This can be achieved by, (1) increasing the speed of the boat or by, (2) reducing the distance sailed. The motivation for shape change in the centreboard of a high performance sailing dinghy is to improve the performance, specifically, increase the boat speed and reduce leeway by reducing the induced drag produced as a byproduct of the lift it generates. This steepens the lift/drag slope of the centreboard and can be used by the sailors to, (1) sail the boat faster or, (2) sail closer to the wind reducing distance sailed. Appendix A.1 explains the sailing model and provides the terms and equations showing the relationship between a reduction in induced drag and an increase in boat speed or reduction in leeway. It is hypothesised that this shape change may be obtained using *morphing technology*. The morphing centreboard envisioned will seamlessly change from a traditionally symmetric profile shape to a more effective asymmetric shape or number of shapes without major surface discontinuities. It is hypothesised that this will increase sailing performance through increased centreboard lift, reduced boat leeway and hull drag and increased boat speed and VMG.

Morphing Technology, under its various synonymous names, is at the pinnacle of aeronautic design. There is a broad base of research and initial technologies available, however, widespread technological feasibility and use are still a few steps away. Despite this large interest in morphing technologies for aerodynamic applications, there are few other applications of this concept and the field of research for applications outside of aerospace is sparse. Hydrodynamic applications stand the chance of significant performance gains over aerodynamic applications due to the inherent properties of the different operating fluid. Although they pose their unique challenges, there exist solutions within the current field of research which could be suitable to the hydrodynamic case, if only they were easier to find, compare, and build upon.

Presently there are a number of barriers preventing further development and wider application of morphing to generalised cases such as the design of a morphing foil for hydrodynamic applications. These include:

1. A lack of a clear, concise, explicit definition of what constitutes *morphing technology* within the general applied physical science, and more specifically engineering context.

2. A lack of standard lexicon leads to little consistency in both the terms used and their corresponding definitions and connotations within the scope of what is universally accepted as *morphing technology*, definitions and terms

are often either used differently or differ entirely. Consequently, it is difficult to reconcile research spanning different authors, projects, and organizations.

3. The lack of a generic, universal categorisation methodology or scheme facilitating the sorting and consequent comparison and identification of technologies within the literature for application to a given problem.

4. The lack of applications of *morphing* outside of the aeronautic field. The consequent bias towards aeronautic field-specific concepts, principles, and solutions limits trans-disciplinary applications of *morphing*.

The barriers listed above are evident as shortcomings within existing literature when consulting the major review papers within the field of morphing in Chapter 2. These problems within the field's literature make it inconvenient to build on the large, varied base of existing literature to grow the field and, as a consequence, authors tend to provide their own definitions which suit their specific use cases but are often incompatible with other applications, further limiting widespread development. There is a need for some form of universally accepted, inclusive, comprehensive, and explicit categorisation and classification schemes and corresponding standard lexicon for the field of morphing.

1.4 Objectives and Methodology

The overarching vision of this project is twofold: (1) to develop a preliminary conceptual design for a morphing centreboard for a high performance sailing dinghy and, (2) to provide a tool that will facilitate the engineering design process, further development and wider application of *morphing technology* for fluid dynamic applications while providing a framework for the adaptation of the tool to other fields outside of aeronautics. In order to embark on an effective design process for a morphing centreboard and achieve (1), it must first be possible to find, compare and decide on applicable existing morphing technologies (2), consequently this paper aims to:

1. Define a standard lexicon (a proposal of explicit, universal definitions) for *morphing technologies* which will apply to generalised cases and be universally applied within the field. Within this lexicon new definitions of specific, key terms are presented. Specific terms within the field of morphing are stated to use definitions adopted from other standard lexicons (for example the definition of the term *foil* can be adopted from the standard lexicon of the field of aerodynamics.)

2. Provide a classification scheme, the proposal of a gated method for classifying or sorting both existing and future research as: within or outside the scope of morphing (some other technology). The format that is envisioned will sequentially filter all existing research and technology into mutually exclusive classes until only that which is proposed to be considered morphing remains. The scheme will:

   (a) Propose an explicit, clear methodology that defines what constitutes *morphing technology* within the general applied physical science and engineering context.

   (b) Provide suggestions for refinement and further classification of *morphing technologies* within other fields' context-specific applications. In this paper, a refined classification for foil morphing within the field of fluid dynamics specifically is presented but the generalised reasoning and approach can and is proposed to be adapted to any field.

3. Provide a categorisation scheme which can be applied specifically to *foil morphing* for fluid dynamic applications, with the intention of not explicitly limiting the scheme to this field, to sort technologies in a useful manner to both structure the field and allow researchers to find and evaluate applicable technologies for specific applications. This categorisation scheme is chosen to be a vectorised categorisation (to ensure it is computer search-able). Further, it must categorise both research and technology according to a number of fields corresponding to common subsystems or subsets of morphing technology.

4. Utilise the lexicon, classification and categorisation schemes above as a design toolbox to complete a preliminary conceptual design or proof of concept for a morphing hydrofoil, specifically the centreboard of a high performance sailing dinghy. This design will also provide a test case as validation of the utility of the design toolbox developed in (1) - (3). The preliminary design will provide guidance on feasible materials, structure and actuation for the camber morphing of a centreboard profile shape

To present and motivate the toolbox outlined above, (1-3), a review of the available literature in the context of the proposed design toolbox is required to develop fair, representative categorisation and classification schemes as well as present realistic, practical definitions and further provide a basis on which to build the toolbox on. A meta-analysis of existing review papers is undertaken covering subsets within the morphing field rather than a traditional literature review of specific research within the field. The meta-analysis covers prominent review papers, particularly those which have made an attempt at classifying research in the

past. The strengths and shortcomings of any existing attempts at classification are discussed. The design toolbox is not considered a complete, ubiquitous solution, rather it builds on the review papers considered in the meta-analysis Chapter 2 by:

- Adopting concepts on which there is absolute consensus.
- Adapting concepts on which there is some consensus.
- Proposing novel concepts and contributions in areas where there is little to no consensus or a lack of sufficient attention in the existing literature.

The key contribution of this part of the research is that all concepts presented are explicitly defined and generally applicable to *foil morphing* for fluid dynamic applications. With an emphasis on creating a scheme which can be easily adopted and adapted to be generally applicable to any morphing technology and engineering field. The concepts are easily reproducible allowing the classification and categorisation schemes to be adapted, further expanded, and applied within fields other than aeronautics.

The completion of the fourth objective yields a preliminary conceptual morphing design for a centreboard of a high performance sailing dinghy, specifically a 505 class dinghy. The design toolbox along with simplified fluid dynamic and structural investigations, utilising open source software, is used to aid in the design process. The type of morphing, core enabling technologies and validation of the proposed design are presented as a basis for future work on detailed design of such a morphing centreboard. The preliminary design provides a 2D representation of the mechanism and technologies required to achieve the morphing of the profile shape of the centreboard. The design parameters are based on a generic 505 class dinghy centreboard and the typical operating conditions it experiences. Three main steps are undertaken in the design:

1. A fluid dynamic investigation utilising 2D CFD along the with know algebraic equations describing sailing boat systems is undertaken in order to determine a target, morphed profile shape for the centreboard.
2. The design toolbox is used to find candidate technologies for the specific design case.
3. A structural investigation utilising basic FEM simulation is used to scrutinise the candidate designs and determine the suitability of each.

From the steps above a final concept is presented. The conceptual design will include: (1) the base and target profile shapes for the morphing foil, (2) the broad

structure of the foil, (3) candidate materials for the substructure and surface and, (4) an outline of the actuation method for the morphing.

1.5 Outline

The centerboard of a high performance sailing dinghy provides a portion of the equilibrium forces in the operation of a sailing boat via a lift force which facilitates *forward* motion of the boat. The centerboard is traditionally symmetrical due to the requirement of a sailing boat for equal performance on opposite tacks. A symmetrical centreboard, however, relies on a non-zero angle of attack to produce lift leading to drag penalties on the hull and underwater appendages. A centreboard that can change to an asymmetric shape on either tack will provide improved performance at different operating conditions, leading to the idea of a *morphing centreboard*. The hypothesis for this thesis is that existing shape morphing technology can successfully be applied to hydrofoils and hydrodynamic cases, specifically the centreboard of a high performance sailing dinghy in order to improve performance. The use of sailing provides a design case allowing this hypothesis to be tested.

To design the envisioned morphing centreboard the field of morphing literature is approached. The available morphing research found is inconsistent and ambiguous in its definitions and implementation, making conceptualization and design based on existing morphing technologies difficult. A morphing design toolbox is developed to address the problems found in the research. The toolbox takes morphing out of its field specific applications and presents morphing as an enabling technology. The design toolbox consolidates past ideas, proposes new ideas and leaves space for collaboration and addition. This toolbox is then applied to the morphing centreboard case, defined using sailing theory and fluid dynamic study, to identify a concept or number of concepts which are evaluated for applicability using a structural investigation. The design process provides a test case for the validation of the design toolbox and concludes with a preliminary concept for a morphing centreboard. The actual preliminary designs are not intended to be validated, rather are used to show the utility of the toolbox and provide a previously non-existent conceptual design for a morphing centreboard.

1.6 Constraints and Scope Limitations

There are constraints inherent to the design of a high performance sailing dinghy centreboard applied to the conceptualisation phase of the project. The normal

operating conditions of such a boat including typical crew weight, wind range and consequent boat speed range are used to define the design requirements and specifications. Existing centreboard shapes are considered the basis for the design, consequently the un-morphed shape of the centreboard is constrained by current designs which are based on the 505 class rules. This constraint will yield further, implied constraints on the morphed shapes possible for the design. [2] There are constraints applied to the design toolbox including a natural limitation in the amount and variation of research available for the literature survey and meta-analysis, language and access rights further narrow the field of research sine only research that is available in English is considered. The institution from which this research is conducted has certain limitations to research access, this must be taken into account when evaluating the applicability of the proposed lexicon, categorisation, and classification schemes.

Outside of the above constraints, there are a number of specific scope exclusions imposed on this project:

- Centreboard Conceptual Design
  - The design presented in this project is limited to a 2D design of the foil profile based on assumptions from 3D requirements.
  - Physical properties of the design are shown to be *in range* of the physical properties required by the application, however further physical properties such as weight and stiffness in operation are not considered.
  - The preliminary, conceptual design is envisioned to be a first step in the design process, resulting directly from the application of the proposed design toolbox and simple application of engineering design tools. The emphasis is on the process and informing future design work, not on in depth design or validation.
  - The conceptual design will be purely theoretical, motivated mathematically and with results from fluid dynamic and structural investigation. No physical prototype is constructed or tested, however this is seen as the next step for future research.
  - The CFD and FEM simulations conducted are explicitly limited to simplified conceptual models. The goal of which is to demonstrate feasibility of generalised concepts, not to provide case specific information. To this end, highly simplified models are utilised based on core assumptions without the goal of explicit validation. These models are intended to inform the design, not provide specific design specifications.

[2] By limiting the un-morphed shape the possibilities for morphed shapes are naturally limited

  - Only 2D camber morphing of the foil profile will be considered for the design. Camber morphing is considered the most effective way to achieve the desired goal of increasing the lift/drag curve slope. This is motivated in Chapter 4.
  - The morphing is considered to be uniform over the span of the foil, no spanwise differential morphing is investigated.
  - The theoretical cost of the design is not taken into account and no limitations are made in this regard. No cost studies or analysis are performed and this is not seen as a determining factor in the conceptualisation at this stage.

- Design Toolbox
  - This research deals solely with applications of the term morphing within the physical sciences and more specifically, engineering. Uses of the term morphing within computer science (morphing within genetic algorithms etc.), biology and other usages for fields outside of the obvious implied scope are explicitly excluded. The classification scheme will position the boundaries of the use of the term morphing for this specific case.
  - This thesis is not a purely meta-analysis or literature review thesis. The literature survey and meta-analysis are simply presented to provide background and motivate the need for categorisation and classification within the field. Further, the literature survey and meta-analysis provide a number of test cases as a platform (a base of literature currently considered as morphing technology, which may be defined, classified and categorised through the application of the toolbox) as a proof of concept for the decisions made in the categorisation and classification schemes.
  - The intention for the toolbox is that it applies to all existing and future research, however the validation of this intention is not possible within the scope of a single paper. In order to show ubiquity in the use of the toolbox it must be widely adopted into future research in the field. This paper only aims to show utility of the toolbox in the specific design case of a morphing foil for fluid dynamic applications as this is the main area of current morphing applications. Despite this limitation it is the aim of this project to, as far as possible, design the toolbox to allow generalisation. At present only research covered in the literature survey and meta-analysis presented will be categorised and classified.
  - Utility of the toolbox will only be shown by its successful use in the preliminary design of the morphing centreboard. This includes the success-

ful classification and categorisation and successive filtering performed on the description vectors of many of the existing morphing papers reviewed.

– All categorizing and classifying of research and technology is carried out manually. This specific research does not look into or explore the possibilities of using computer software (text recognition etc.) to classify and categorise research. It must be emphasised that the toolbox is specifically designed in such a way that automated/computerised definition, classification and categorization of research and technology should be possible and in fact this is envisioned as the future application of the toolbox.

Chapter 2

Meta-analysis

In the context of this thesis the *meta-analysis* performed refers to the review of multiple papers which are themselves review papers of morphing technologies. Considering the abundance and wide variety of morphing research and technologies the analysis of existing review papers allows large amounts of research to be considered effectively and is appropriate when surveying the field as a whole. The goal of the meta-analysis is to determine whether existing definitions, classification and categorisation exists and if so what each approach's advantages, disadvantages and limitations are. The structure of the literature review undertaken here differs from that of a typical engineering design project. The aim of this chapter is not to review prior existing technologies or concepts, rather to review the contents and context of the entire field of morphing subject to the envisioned design toolbox. To this end the chapter is approached as a meta-analysis collating existing lexicon, attempts at classification and categorisation to inform the development of the design toolbox rather than a literature review of the existing technologies.

2.1 Existing Definitions and Classification

It is impractical to review every single relevant paper's definitions and classification and therefore eleven notable, appropriate, and varied review papers are examined and presented chronologically in the following subsections. [1]. These provide a comprehensive background of the existing literature and consequently the definitions and connotations of the field of morphing under all of its alternative names. The proposed lexicon for morphing technologies evolves out of this discussion and is addressed in the design tool box.

[1] Appendix C provides a far more in depth discussion of these papers amoung others

2.1.1 Defence Advanced Research Projects Agency – Smart Materials and Structures Demonstration Program Overview (Sanders *et al.* (2004))

The Defence Advanced Research Projects Agency (DARPA) has been involved in research both directly in morphing and in fields that are supplementary. In the paper Sanders *et al.* (2004) *morphing* is not directly focused on, the focus is rather on smart materials and structures. The shift towards integration between the sensing, structure, and actuation. *Smart Materials* are suggested to be the key for future morphing technologies. Sanders *et al.* (2004) uses a definition for smart materials similar to the definition proposed by Rogers *et al.* (1988): "A system or material which has a built-in or intrinsic sensor(s), actuator(s) and control mechanism(s) whereby it is capable of sensing a stimulus, responding to it in a predetermined manner and extent, in a short/appropriate time, and reverting to its original state as soon as the stimulus is removed." Sanders *et al.* (2004) concludes with a look at the future of smart materials and structures as applied to aircraft to yield the future, morphing aircraft.

2.1.2 Morphing Aircraft Concepts, Classifications, and Challenges (Jha and Kudva (2004))

The term *morphing aircraft* is used as the basis for the research, defined as "...an aircraft that changes configuration to maximise its performance at radically different flight conditions." No restriction is imposed on the location, extent, or type of configuration change. The paper does acknowledge the fact that morphing of the wing is the most important aspect of aircraft morphing. The definitions and limitations imposed show that the view of morphing given in Jha and Kudva (2004) focuses not on the specifics of the shape change, rather on maximization of performance at multiple operating points. The paper introduces it's application of the field of morphing, provides a short literature survey of past morphing aircraft designs and classifies the respective technologies.

2.1.3 Morphing Aircraft Technology – New Shapes for Aircraft Design (Weisshaar (2006))

Weisshaar (2006) uses the terms *morphing*, variable geometry and polymorphous aircraft, defined as "...multi-role aircraft that change their external shape substantially to adapt to a changing mission environment during flight." The objective of morphing is to change shape and performance substantially during operation to create multiple regime, aerodynamic efficiency. The shape change envisioned only

occurs in the wing. Concepts are limited, possibly unnecessarily, to substantial shape change. The paper gives an overview of a prominent morphing program, the MAS program run by DARPA and its consequent definitions and method of classification.

2.1.4 Morphing Aircraft Technology Survey (Rodriguez (2007))

Rodriguez (2007) provides a well-researched technology survey of all aspects of morphing research, uniquely organizing the research by prominent organizations' projects, structural based approaches, and multidisciplinary optimization and system approaches. The paper does not seek to provide a single, unified definition of the field of morphing, rather acknowledges the variation within the field and deals with each research instance's definitions. A number of terms including: *bird-like*, *shape-shifting*, *variable geometry*, *adaptive structures* and *biomimetric* and several phrases including: "...an ability to perform smooth, continuous stable deformations" and "...an ability to adapt and change shape based on varying flight performance and control requirements", have been used synonymously in some manner under the umbrella term *morphing*. Rodriguez (2007) quotes from a course provided by the University of Bristol: "These different applications are all regarded as morphing; however, each is very different in terms of the magnitude of the shape changes required, and time constants necessary for these changes. Fortunately, large changes for improved performance are only required at low frequency, and very fast changes for vibration control only need to be small amplitude. This does mean that there is never going to be a single solution for a morphing aircraft, and the technology employed will be vastly different depending on the application required. However, all applications require that morphing achieves the objective of improved performance and/or functionality." In this paper the objective of morphing is centered on the improvement of performance and functionality rather than the specifics of the actual physical shape change which takes place. The literature and projects surveyed are organized in a logical, novel manner by their specific area of focus within morphing.

2.1.5 Morphing Skins (Thill *et al.* (2008))

Thill *et al.* (2008) presents a review of morphing concepts with a strong focus on the surfaces or skins to be used in such applications. The paper deals solely with applications in aircraft wings although no limitation to this application is imposed in the definition of *morphing* presented. Thill *et al.* (2008) defines the field of *morphology*, as discussed in the Chapter 1, and follows that only continuous shape

change with no discrete discontinuities is considered *morphing*. No reference to solely fluid dynamic applications is made and therefore it can be envisioned that morphing, in this case, can be applied to technologies with a shape change utilised outside the realm of fluid dynamics. It should be noted that the distinction given between *active* and *passive* structures in this paper is completely different from the conventional use of the terms within the field. Thill *et al.* (2008) proposes that: "An active structure can be defined as possessing an ability to change shape whilst maintaining a continuous form, whereas a passive structure, such as a hinged aileron, has discrete components which move relative to each other." This is in contrast to the widely accepted definition of the terms wherein there is no reference to the type of shape change, rather the emphasis is on the differences in sensing, control, and actuation Rogers *et al.* (1988); Gardiner (1993); *active* is taken to mean that the structure utilises some sort of control or actuation system which modifies its geometric or material properties in response to an electric, thermal or magnetic field, thereby acquiring an inherent capacity to transduce energy. *Passive* is the term used for any structure which is not active.

2.1.6 Perspectives on Highly Adaptive or Morphing Aircraft (McGowan *et al.* (2009))

McGowan *et al.* (2009) proposes that much of the disagreement over a universal definition for morphing stems from the fact that the discussion focuses on how the morphing is done. It is proposed that, to avoid artificial constraints on the field, the definition focuses on the capability provided by a morphing vehicle. McGowan *et al.* (2009) utilises the definition of *morphing* provided by the NATO Research and Technology Organization, Applied Vehicle Technology (AVT) Technical Team on Morphing Vehicles (AVT-168): "Real-time Adaptation to Enable Multi-point Optimized Performance. This includes morphing applied to air, land, and sea vehicles." Here, similarly to Rodriguez (2007), the definition of morphing is focused on the performance rather than the specifics such as method, degree, or location of the application.

2.1.7 Efficient Multidisciplinary Analysis Approach for Conceptual Design of Aircraft with Large Shape Change (Chwalowski *et al.* (2009))

Chwalowski *et al.* (2009) is not a true review paper but does present a definition for morphing which differs from many other definitions presented and supports NASA's ideas of a less stringent definition of the technology to avoid artificial constraints being applied. "Technologies that can address multi-mission requirements

range from little or no shape-change, such as micro flow control and variable bumps to moderate shape change such as variable airfoil shape (including camber change) and wing twist; to large scale shape change such as variable span, sweep, and fold angle" is the definition provided for morphing. According to Chwalowski *et al.* (2009) the field of morphing has also been referred to in literature as: "...reconfigurable, multifunctional, adaptive". The report collects all of these terms under the umbrella of *morphing*. The paper goes further to include that morphing may also be defined as in McGowan *et al.* (2009) as: "...efficient, multi-point adaptability."

2.1.8 Shape Morphing of Aircraft Wing: Status and Challenges (Sofla *et al.* (2010))

Sofla *et al.* (2010) presents a paper classifying recent activity in the field of *shape morphing wings*, dealing specifically with concepts which include smart materials such as shape memory alloys (SMA), piezoelectric actuators (PZT), and shape memory polymers (SMP). The paper does not provide its own definition for morphing but states that: "In the field of aeronautics, shape morphing has been used to identify those aircraft that undergo certain geometrical changes to enhance or adapt to their mission profile." it goes on to state that: "... there is a general agreement that the conventional hinged control surfaces or high lift devices, such as flaps or slats that provide discrete geometry changes cannot be considered as morphing."

2.1.9 A Review of Morphing Aircraft (Barbarino *et al.* (2011*a*))

Barbarino *et al.* (2011*a*) emphasizes that *morphing* is a promising enabling technology for the future of aircraft, basing the definition used upon the idea that an integration between structure and function (this distinction is an important, continuing theme in modern morphing concepts), as seen in birds, is the key characterization. This *integration between structure and function* remains an underlying idea of the field. The definition proposed for *morphing* is "...a set of technologies that increase a vehicle's performance by manipulating certain characteristics to better match the vehicle state to the environment and task at hand", this definition is taken from Weisshaar (2006). Under this definition, established technologies such as flaps or retractable landing gear fall within the scope of morphing, Barbarino *et al.* (2011*a*) however suggests that under the connotations carried in the field this is not the case. The paper goes further to suggest that morphing carried

the additional connotation of radical shape changes [2] or shape changes that are only achievable through near-term or futuristic technologies. This is a potentially limiting definition as warned against by McGowan *et al.* (2009) but does allow Barbarino *et al.* (2011*a*) to effectively gate concepts that are considered within or outside the specific definition of morphing.

2.1.10 Realization of Morphing Wings: A Multidisciplinary Challenge (Vasista *et al.* (2012))

Vasista *et al.* (2012) motivates the idea that the field requires a multidisciplinary approach to produce successful technologies. Here the basic term used is *morphing wing*, defined as a wing that changes shape in flight in a controlled manner to improve aircraft performance. The paper notes that there is no formal definition within the field and that the consensus of morphing is that of a "...smooth, continuous shape change, flexibility and the art of mimicking birds." Vasista *et al.* (2012) suggests that a move away from distinguishable substructure, skin and actuator components towards a more integrated system such that functions such as carrying loads and changing shape are shared between a single comprehensive system is the future of the technology. Consequently it is suggested that the trends within the field tend towards smart material-based systems and topology optimized compliant mechanism designs.

2.1.11 A Review of Modelling and Analysis of Morphing Wings (Li *et al.* (2018))

The review presented in Li *et al.* (2018) is unique since it focuses on the modelling and analysis of morphing wings. *morphing wings* are the focus of this paper, however, it defines *morphing* as "...the ability to transform shape or structure", an open-ended definition backed up by the proposal that the overarching idea behind a morphing wing is to: "...adapt its aerodynamic shape to each flight condition to obtain better performances, such as flight envelope, flight control, flight range." This limits morphing concepts in this paper to applications specifically within aircraft wings and focuses on the performance as an indicator of the morphing rather than the specifics of the shape change.

[2] Barbarino *et al.* (2011*a*) does not provide much information on what is considered *radical* shape change, however the scope may be implied from the reading of the paper

2.1.12 Summary and Shortcomings

From the review of available literature it is difficult to determine whether a single objective, well defined, structured, universal system for classifying research and technology as *morphing* or not exists. There are however clear overlaps between approaches across different papers. The lexicon of the field of fluid dynamics and more specifically, aerodynamics, often for aircraft-specific applications are used widely within existing research, this is largely appropriate but does, in some cases, lead to artificial constraints within the realm of the possible application of morphing technologies. For example, it is more appropriate and inclusive to speak of shape changes according to the axes/planes in which they occur rather than the structure specific terminology as this reduces the likelihood of constraints from the terms used, opening up the field to various applications. Clear descriptors are also required to consistently and effectively ensure information is being clearly defined and translated. One key area is the axes and planes corresponding to the structures involved in morphing. Figure 2.1 gives the axes related to a foil. *Wing morphing*, a term used in much of the reviewed literature, refers specifically to morphing technology applied to the wing of an aircraft. Since artificial limitations on the application of the field need to be avoided the term *foil* can be used as an alternative (to aeronautic specific terms). The term *foil morphing* then naturally follows as it takes the application of morphing outside of field specific terms relating to aircraft only.

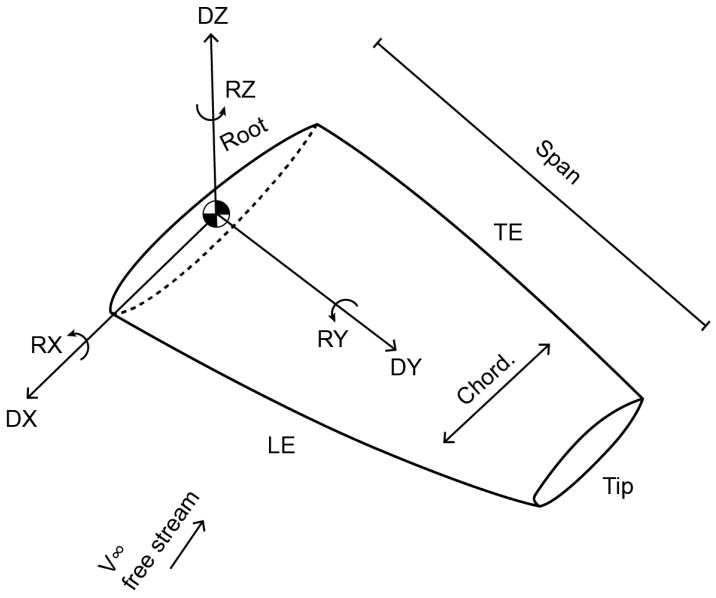

Figure 2.1: Foil Axes

Despite these review papers covering a large portion of the existing morphing research as well as unanimously recognizing the lack of clear definitions and consensus within the field, many of the definitions proposed or used are not generic or inclusive frameworks and the definitions do not make the research field more structured or allow collective continuation between various researchers.

2.2 Categorisation vs Classification

The terms *categorisation* and *classification* are often used interchangeably in the literature reviewed. There is often no clear distinction between the two and the implications of each to the information they aim to sort are seldom fully explored or explicitly explained. Most papers within the literature seem to treat the terms synonymously, illustrated by one of the most commonly used expressions following along the lines of: *classification* as a method of sorting into specific *categories*. This subsection aims to explicitly define each term and consequently highlight the differences and appropriate uses of each. Jacob (2004) gives a breakdown of the differences between the terms, explicitly defining each and outlining the implications of the definitions. A summary of the breakdown can be seen in Table 2.1. Categorisation and classification systems are both mechanisms for establishing order through the grouping of related phenomena. There are however, fundamental differences between the terms. Classification is a rigorous process mandating that an entry is monothetically assigned to a class. Categorisation is more flexible, drawing non-binding associations between entities with associations based on similarities existing within a set, (Jacob, 2004).

The terms have been used incorrectly throughout literature, leading to the very issue faced here, the introduction or utilisation of the correct terms in the correct context seem to cause confusion and inconsistency when presented alongside the review of existing literature. It must be noted that the term *classification* as used in computer science carries its own definition, numerical classification problems have very stringent definitions of their own and it should be made clear in what context the terms are used to avoid ambiguity. The explicit, correct definition of the terms, according to Table 2.1 are required and used in the following sections.

2.3 Existing Categorisation

Five review papers, within the reviewed literature, propose explicit categorisation methods for morphing research or technology, these are Jha and Kudva (2004); Sofla *et al.* (2010); Barbarino *et al.* (2011*a*); Vasista *et al.* (2012); Li *et al.* (2018) and are expanded upon in chronological order below. It is important to note that

Table 2.1: Comparison of Categorisation vs Classification (Jacob, 2004)

Categorization	Classification
Process	
Creative synthesis of entities based on context or perceived similarity	Systematic arrangement of entities based on analysis of necessary and sufficient characteristics
Boundaries	
Because membership in any group is non-binding, boundaries are "fuzzy"	Because classes are mutually-exclusive and non-overlapping, boundaries are fixed
Membership	
Flexible: category membership is based on generalized knowledge and/or immediate context	Rigorous: an entity either *is* or *is not* a member of a particular class based on the intension of a class
Criteria for Assignment	
Criteria both context-dependent and context-independent	Criteria are predetermined guidelines or principles
Typicality	
Individual members can be rank-ordered by typicality (graded structure)	All members are equally representative (ungraded structure)
Structure	
Clusters of entities; may form hierarchical structure	Hierarchical structure of fixed classes

each paper utilises its own, unique terms for the field and accompanying definitions. The schemes reviewed here deal with some manner of sorting of research within the field of morphing, whether the categories within the sorting scheme are mutually exclusive [3] or not.

2.3.1 Morphing Aircraft Concepts, Classifications, and Challenges (Jha and Kudva (2004))

Jha and Kudva (2004) provides novel method for high-level categorisation of morphing technologies. Figure 2.2 shows the systematic categorisation. Initially all morphing within aircraft systems are divided between their location on the airframe. Morphing within the wing specifically is divided into a) robotic design, and

[3]Many of these papers either incorrectly refer to these schemes as *classification* when they are in fact *categorisation* schemes by nature. In this section the emphasis is on schemes which sort research or technology which has already been classified as *morphing technology*. Consequently the schemes will be referred to as categorisation schemes irrespective of the terminology used by the authors.

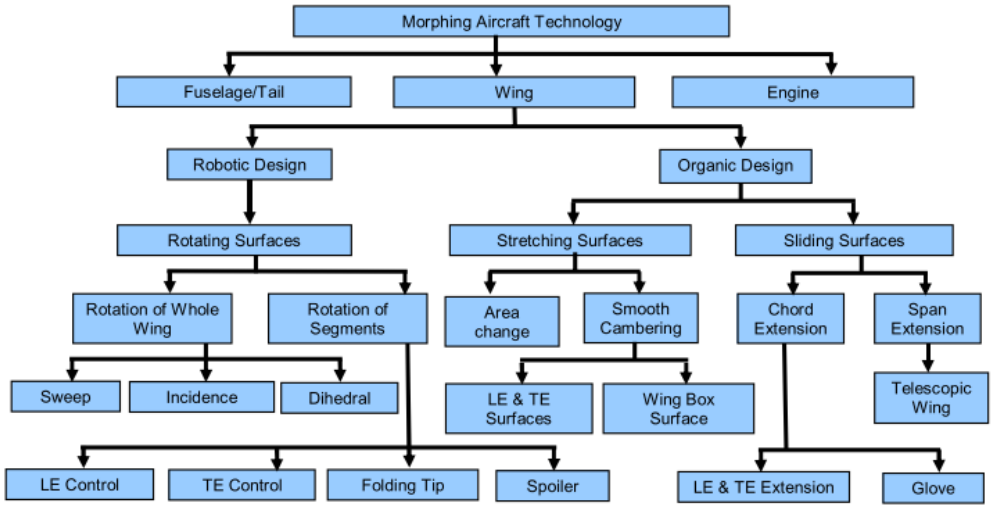

Figure 2.2: Categorisation of Morphing Aircraft Technology Jha and Kudva (2004)

b) organic design.

Robotic design refers to wings which undergo morphing that does not change the planform area of the wing. This means that wings of robotic design can only undergo a rotation of either the whole wing or a part thereof along any axis [4]. Rotation of the whole wing will lead to variable-sweep (Z-axis), variable incidence (Y-axis), and variable dihedral (X-axis). Rotation of parts of the wing will lead to leading and trailing edge control surfaces (Y-axis), folding wingtips (X-axis), and spoiler mechanisms. In an *organic design* a mechanism allows the overall surface area of the wing to vary. This change in surface area is proposed to take place either by stretching the wing or sliding part of the wing over the other. Concepts with stretching wings will require flexible skins or surfaces, no further detail is given in this section, however, it can be seen in Figure 2.2 that the concepts are further categorised into area change and smooth cambering concepts. The latter of which can be divided into changes of the leading edge (LE) and trailing edge (TE) surfaces or the wing box surface. Sliding wing designs require some parts of the wing to be hidden within others, retracting or expanding during operation. Here wings can have sliding surfaces that extend in the chordwise direction or the spanwise direction. Telescopic wings are explicitly mentioned as wings where the complete wing is divided into two parts in the spanwise direction, with one part hiding within the other. The paper does provide a categorisation for a rather unusual case of morphing wherein tandem wings are covered to yield a single, longer

[4]No axes are given in the paper, they are inferred here for clarity by the type of rotation described according to the standard aircraft axes.

chord wing, this is referred to as a glove wing.

The scheme is reasonably inclusive of the appropriate technology and successfully categorises a large body of existing research. Only morphing within the wing is categorised in successive detail, morphing in any other part of the aircraft is simply categorised by its location with no indication of the type, extent, or detail of the morphing. The distinction of robotic and organic design serves its purpose within the proposed scheme, however, it is unclear as to where the terms originated and the connotations behind the terms are often in contrast to the definitions provided by the paper. There does not seem to be any inherently *robotic* features of rotational deformations over stretching or sliding ones. For reference, birds make use of all three deformations in their wings to adapt to different flight conditions, optimize their flight performance, and aid in control. Because of this the distinction, although useful, seems unnecessary the division of concepts based solely on the type of deformation: *rotating surfaces*, *stretching surfaces*, *sliding surfaces* is equivalent.

This method is different from many others presented in that it focuses first on how the actual wing surface deforms rather than the axes on which the deformation takes place or the aeronautic terminology thereof. The axes on which the shape change acts are inferred at a later stage of categorisation by the aeronautic terms used to define the shape change. The order in which the categorisation takes place does allow technologies applied to the surfaces or skins of the structures to be universally applied within each category (rotating, stretching, and sliding). It does in some cases create a distinction between the type of morphing which may have very similar underlying technologies, for example, the difference between a discrete LE and TE control surface and smooth cambering of a wing through deflecting a portion of the LE and TE is very small, yet these technologies are separated very early on by the scheme.

2.3.2 Shape Morphing of Aircraft Wing: Status and Challenges (Sofla *et al.* (2010))

Morphing of aircraft, and in particular wings can fall into three categories as is quite common in existing schemes, these are presented in Sofla *et al.* (2010) among others. From here the method takes on a tree structure filtering concepts into successively narrowing categories. Figure 2.3 shows a breakdown of these shape parameters with their corresponding demonstrative sketches as defined and expanded upon by Galantai (2010).

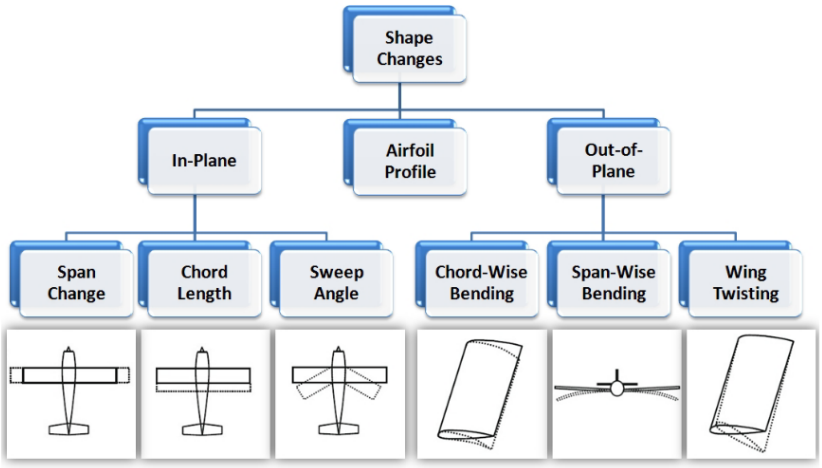

Figure 2.3: Existing Morphing Shape Parameter Categorisation taken from Galantai (2010), adapted from Sofla *et al.* (2010)

The type of morphing can initially be categorised according to which plane the geometric shape change takes place within since the definition of the paper explicitly mentions a geometric change under the definition of shape morphing. Planform alteration refers to all geometric changes which occur within the main, reference plane of the wing. This includes planform area changes and changes to the wing sweep. Out of plane transformations can occur on any plane other than the reference plane, however, they are distinctly different from changes to the actual airfoil profile shape. Airfoil adjustment is used to categorise designs that make changes to the actual airfoil profile shape without significantly changing the camber. The airfoil profile changes are, by nature also out of plane transformations but are categorised separately due to their unique position in airfoil design. For example, with certain airfoil profile designations it is possible to choose an airfoil profile and then change the camber without technically changing the profile you are using, this is in contrast to using two different profiles each with the same camber. Sofla *et al.* (2010) goes on to expand upon each of the final categorisations, presenting a number of technologies in a tabular format for each with additional information such as: the standard aeronautic terms for the wing geometry morphed, the actuator type used, the skin or surface type and a broad TRL (whether the technology had undergone prototyping, wind tunnel testing or flight testing).

The scheme presented categorises morphing as a geometric change applied to wings of traditional aircraft. The categorisation and further expansion upon existing research within each of the final categories are extremely useful in compar-

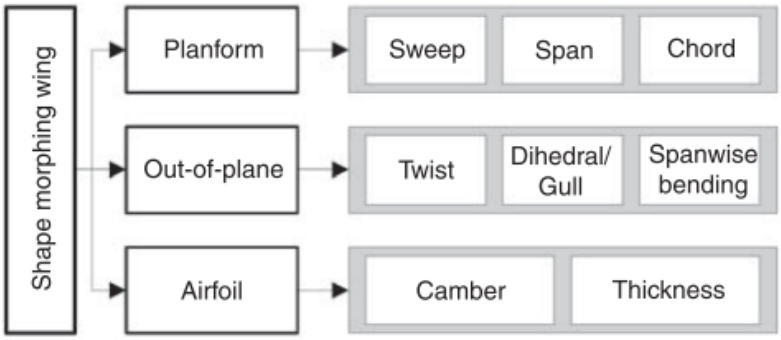

Figure 2.4: Organisation of the Review. Barbarino *et al.* (2011*a*)

ing similar morphing concepts. The distinction between *airfoil profile adjustment* and *out of plane transformation*, particularly when contrasted with *planform or in-plane transformation* can become unclear. It is a case of being exceptionally clear in idealized, standard cases within the aircraft wing application, however, the distinction is sufficiently unclear that certain transformations may either be motivated to fall within both categories simultaneously or in either depending on the point of view taken. Similarly, when the distinction between the *airfoil profile adjustment* and *planform alteration* is probed it can be seen that there are inherent ambiguities. For example, the extension of the chord of a wing will, by its nature lead to significant changes in the airfoil profile, yielding a far thinner airfoil.

2.3.3 A Review of Morphing Aircraft (Barbarino *et al.* (2011*a*))

Barbarino *et al.* (2011*a*) categorises wing morphing technologies in a different and more intuitive way than that of Sofla *et al.* (2010). A tree structure is utilised as shown in Figure 2.4.

The first step in the categorisation is to divide the concepts by the plane in which the shape change occurs. In the case of Barbarino *et al.* (2011*a*) the distinction of the three categories, *planform or in plane*, *out of plane* and *airfoil* is done well as the majority of sub-categories conform to and consequently motivate their respective parent categories. Planform alteration is seen as in-plane shape change and includes changes in sweep, span, and chord exactly as before. However, out of plane transformations now refer mainly to change in the YZ plane, span-wise twisting, dihedral/anhedral or gull configurations, and span-wise bending. The third category suggested by Barbarino *et al.* (2011*a*) is *airfoil* which intuitively includes camber and thickness changes of the airfoil shape used in the wing, changes

in the XZ plane.

Barbarino *et al.* (2011*a*) gives a comprehensive review of available morphing technologies, categorizing them in a tabular format and presenting a number of papers within each final category with additional information. The paper is, however mainly concerned with the application of the technology to aircraft. Within the tabular expansion of technology in each morphing category a number of pieces of information are summarised; the relevant meta-data of each piece of literature is given, the corresponding aeronautic term for the geometric parameter changed is given, details on the vehicle the technology is applied to are given such as whether it is a fixed or rotary craft and its rough size, the method of actuation, the type of skin or surface used and the main purpose behind the shape change are also provided. Further details are given as to the TRL of the technology by summarising whether the technology has undergone numerical investigation, prototyping, wind tunnel testing, and flight testing. A complete table is given for every subset within the categorisation scheme and in some cases different tables are given according to specific actuation mechanisms.

The categorisation scheme presented in Barbarino *et al.* (2011*a*) shares aspects with that of Sofla *et al.* (2010) and utilises the same first step of distinction. The distinction between categories is robust and logical and fewer conflicting cases can be found. The issue of airfoil profile chord changes and wing planform chord changes being the same geometric change in different categories in Sofla *et al.* (2010) is partially solved here by specifying airfoil profile changes as camber and thickness changes rather than open-ended profile changes. Most shape changes given in the subcategories occur within the plane given by the initial categorisation step: sweep, span and chord changes all occur mainly in the XY plane; airfoil profile camber and thickness changes occur in the XZ plane; changes to the dihedral or gull configurations of the wing as well as spanwise bending occur in the YZ plane, out of plane to the reference plane.

2.3.4 Realization of Morphing Wings: A Multidisciplinary Challenge (Vasista *et al.* (2012))

The paper aims to synthesize many different approaches and categorises the technology in terms of three main categories: 1) the shape parameters (*What to morph?*), 2) the performance benefits (*Why to morph?*) and, 3) the enabling technologies (*How to morph?*). In contrast to many other methods the categorisation does not make use of a tree structure, rather associates certain categories with technologies based on various internal properties of the morphing concept. This

categorisation is useful in the study and analysis of available literature as the field is extremely broad and many sources deal with multiple categories interchangeably.

Vasista *et al.* (2012) follows a similar approach to that of Sofla *et al.* (2010) and Barbarino *et al.* (2011*a*) by dividing the shape parameters affected according to the plane in which they act. Here the shape parameters are only broken down into two categories: 1) in-plane parameters and, 2) out of plane parameters. The paper provides a comprehensive yet concise description of each by formalizing the planes and deformations associated with each. Morphing of the shape parameters can be described as either small, medium, or large scale. The paper describes the scale of shape change as the percentage change of wing geometry with respect to the overall baseline wing geometry. Table 2.2 and Table 2.3 give the in-plane and out of plane shape parameters and the performance benefits corresponding to an increase or decrease of the property respectively, linking the shape change it's effect on performance.

Table 2.2: In Plane Shape Parameters and Performance Benefits

		Benefits due to Changes in Parameter	
Parameter	Axis Influenced	Increasing	Decreasing
Wing area	(DX, DY)	Increased lift, Decreased wing loading	Decrease drag
Aspect ratio	(DX, DY)	Increase spanwise efficiency, Decreased induced drag	decreased parasitic drag, Decreased wing root bending moment
Chord length	(DX)	Increased wing area, decreased aspect ratio	Increased aspect ratio, Decreased wing area
Span length	(DY)	Increased wing area, Increased aspect ratio	Decreased wing area, Decreased aspect ratio
Sweep angle	(RZ)	Increased longitudinal stability	Increased lift curve slope
Taper ratio c_t/c_r	(DX)	Improved tip stall performance	Increased spanwise efficiency when used in conjunction with twist

Table 2.3: Out of Plane Shape Parameters and Performance Benefits

		Benefits due to Changes in Parameter	
Parameter	Axis Influenced	Increasing	Decreasing
Camber	(DZ, RY)	Increased lift	Decrease drag
Thickness	(DZ)	Increase lift, Improved low speed performance	Improved high speed performance, Decreased drag, Decreased chance of flow separation
Dihedral angle	(RX)	Increased dihedral effect, Increased dutch roll mode stability, Increased manoeuvrability	Decreased wing area, Decreased aspect ratio
Twist	(RY)	Wash-in: increased lift	Wash-out: increased efficiency, improved tip stall performance, decreased wing root bending moment
Taper	(DZ)		Decreasing wing root bending moment
LE radius	(DX, DZ)	Improved low speed performance	Improved high speed performance
Winglet cant angle	(RX)	Increased lift, improved low speed performance	Increased spanwise lift efficiency

The structural system utilised for many morphing concepts, specifically morphing wing applications is, according to Vasista *et al.* (2012), traditionally composed of three distinct subsystems, these are: 1) a substructure, 2) a skin or surface and, 3) and actuation subsystem illustrated in Table 2.4. Vasista *et al.* (2012) groups the enabling technologies behind the substructure and the skin of a morphing concept together, inferring that much the same technology goes into the two subsystems. The paper states that there have been two main approaches taken in existing morphing technologies, these are termed *conventional mechanisms* and *compliant mechanisms*. For compliant materials the paper follows the material categorisation scheme of Thill *et al.* (2008), the particulars of which are given as parameters in Table 2.4. The actuation subsystem may either consist of conventional actuators or may be smart material based (see Table 2.4). The actuation subsystem in this case refers specifically to the actuators themselves, the mech-

anisms involved in the actuation of the structure are categorised as *conventional compliant* within the substructure or surface descriptors.

Table 2.4: System Combination

Index	Parameter
	Structural System Combination $Su_iSk_jA_k$
Su	Substructure
Sk	surface
A	Actuator
	ij values
1	Conventional Mechanism
	Compliant Materials
2	Stretchable
3	Rollable
4	Collapsible
5	Foldable
6	Inflatable
7	Stacked
8	Stiffness Change
9	Tailored Stiffness
10	Active Substrate or surface
11	Compliant Mechanism
NS	Not Specified
	k values
1	Conventional
2	Smart Material Based
NS	Not Specified

The paper categorizing specific wing morphing concepts clearly and logically in a way that is easy to understand, analyze, and compare. The system used leads to little ambiguity within the categorisation and a broad range of concepts are catered for. The structure of the categorisation method proposed by Vasista *et al.* (2012) is far more appropriate to the type of classification/categorisation problem encountered within morphing research. One possible area of improvement would be the restructuring of the descriptors in a manner that they may be presented as vectors, this would allow the set of technologies to be computer searchable and open the door to further computational operations supporting the comparison and analysis of various concepts yielding a powerful design tool for future research. In terms of the actual categorisation, the breakdown of the problem into *what*, *why*, and *how* is a novel, logical approach and gives the entire method a comprehensible

structure. Only the shape parameters and the enabling technologies for the three subsystems are given in the final categorisation and the performance benefits are inferred from the morphed shape, this perhaps indicates that the *why* has qualitative rather than quantitative connotations within the scheme.

The shape parameters given constitute the furthest refinement of these ideas within the reviewed literature. The utilisation of only two categories, *in plane* and *out of plane* as well as the explicit description of the axes of displacement and rotation corresponding to each is clear and completely describes any conceivable morphing shape change. It would be easy to apply this categorisation of shape parameters to structures outside of just aircraft wings. The performance benefits corresponding to various shape parameters presented cover typical improvement to aircraft performance when increasing or decreasing the shape parameter. These are a mixture of direct and indirect impacts by the change. Many of these performance benefits, such as *increased wing fuel volume*, only correspond to traditional fixed-wing aircraft. The performance benefits proposed can be significantly simplified into only their key components which are directly impacted by the shape change, this will lead to the scheme being far more applicable, not only to aircraft but any technology that's goal it is to produce significantly more lift than drag when operating within a fluid flow. Breaking down a morphing wing into three discrete subsystems has benefits in terms of dramatically simplifying the categorisation but does also potentially introduce artificial constraints in the design of a morphing system. A fully integrated structure making use of SMA's for its surface, actuation, and load-carrying, for example, would be entirely categorizable in Vasista *et al.* (2012)'s system, proving that despite potential shortcomings, it is able to deal with integrated systems. It may be better, in this case, to sort enabling technologies by properties rather than the specific type of technology implemented. Practically this means perhaps stopping the scheme at the *conventional mechanism, compliant mechanism* and *compliant material* level.

2.3.5 A Review of Modelling and Analysis of Morphing Wings (Li *et al.* (2018))

This paper provides an alternative reasoning to the categorisation of morphing concepts. The paper is not concerned with the categorisation of actual morphing concepts, rather the categorisation of existing research in the field based upon its TRL, analysis, and modelling methods. The shape change incurred in the morphing of a wing is divided into two categories, airfoil level morphing, 2D, and wing level morphing, 3D. Table 2.5 shows the table given, mapping the morphing strategy to its purpose or objective. Included is a rough categorisation of the

Table 2.5: Mapping between Morphing Strategies (Design Solutions) and Objectives (Design Problem). Li *et al.* (2018)

Morphing strategy	Purpose	Morphing level
Variable Camber	Performance C_L/C_D Noise reduction Flight control (roll, pitch, yaw)	Low
Variable thickness	Performance C_L/C_D Low-speed performance improvement	Low
Twist morphing	Flight control (roll, pitch)	Medium
Span morphing	Performance C_L/C_D Flight control (roll)	High
Variable sweep	Performance C_L/C_D Flight control (turn radius) Disturbance rejection (crosswind)	High
Folding wing	Performance C_L/C_D	High

morphing level, either low, medium, or high. The first two entries correspond to airfoil level - 2D morphing while the remaining four correspond to wing level morphing - 3D.

The paper goes on to categorise a number of papers, all of which produced working prototypes, according to the methods deployed for the analysis of the morphing wings. In this categorisation the methods used for the analysis and modelling of the structural, aerodynamic, control, and optimization aspects are summarised. The categorisation, in this case, is applied to the papers reviewed and the research conducted rather than the actual physical morphing concept contained within.

Li *et al.* (2018) defines morphing as an ability to transform shape or structure with an overarching idea of improving an aircraft's overall flight performance. The summarisation presented is useful and effective in presenting the key properties of various research papers to facilitate effective searching and comparison. The distinction between the three morphing levels proposed is rather unclear, further explanation is required in this regard to realize the utility of that specific categorisation. The paper and it's categorisation scheme is useful in the sense that it provides an extremely contrasting approach to the categorisation of morphing technology research when compared to many of the other papers. It approaches

the problem from a more research-based side, focusing on the supporting research and projects undertaken around a morphing concept rather than the specifics of the morphing itself. This method leads to insights into the real-world readiness of concepts as well as the design methodology followed and required to yield a fully functioning morphing design of arbitrary shape change.

2.3.6 Shortcomings and Problems with Existing Research

There are a number of overall, main shortcomings with the proposed categorisation schemes within morphing. These issues stem from shortcomings within the classification of morphing, the standard lexicon, and the definitions within the field as well as the inherent structure imposed on many of the schemes reviewed. Table 2.6 shows a high-level summary and some properties of the categorisation schemes reviewed.

Jha and Kudva (2004); Sofla *et al.* (2010); Barbarino *et al.* (2011*a*) propose categorisation methods following a tree structure, essentially a gated method where concepts can only fall into a single category. There are inherent limitations with this structure for a complex set of technologies such as morphing aircraft since many applications fall into multiple categories and the subsystems enabling the morphing are oftentimes indistinguishable. Although the method is exceptionally clear, discrete categories are not necessarily the best approach. All of the categorisation schemes within the reviewed literature deal with morphing applied to aircraft, and specifically wings an consequently utilise much of the aeronautic standard lexicon. Sofla *et al.* (2010); Barbarino *et al.* (2011*a*); Vasista *et al.* (2012) use the typical distinction of wing planes in order to guide the categorisation. This is a useful characteristic when only categorizing a small subset of potential morphing applications, however, it is limiting to potential morphing applications. Categorisation by this method for an arbitrarily shaped object which has no dominant plane would be impossible, and a number of such structures can be envisioned as wings. Many of the proposed schemes, Jha and Kudva (2004); Sofla *et al.* (2010); Barbarino *et al.* (2011*a*), struggle to handle certain difficult to categorise morphing cases. It is often unclear whether *grey area* applications such as retractable landing gear (mounted on the fuselage or wing), virtual flow control, aeroelastic tailoring, and discreet control surfaces constitute morphing, and can consequently be categorised.

Table 2.6: Summary of Categorisation Schemes

Review Paper	Title	Year	Categorisation		
			Description	Structure	Mono-thetic?
Jha and Kudva (2004)	Morphing aircraft concepts, classifications, and challenges	2004	Morphing Aircraft Technology: Sorted by location on aircraft, novel but confusing "robotic" vs "organic" distinction, further distinction by aircraft specific terms.	Tree	Y
Sofla *et al.* (2010)	Shape morphing of aircraft wing: Status and challenges	2010	Shape Morphing Wing: Categorised into three major types: planform alternation, out-of-plane transformation, and airfoil adjustment, issues with consequent fields corresponding to parent bins.	Tree	Y
Barbarino *et al.* (2011*a*)	A review of morphing aircraft	2011	Shape Morphing Wing: Categorised into three major types: planform, out-of-plane, and airfoil. Logical further distinction based on aircraft specific terms.	Tree	Y
Vasista *et al.* (2012)	Realization of Morphing Wings: A Multidisciplinary Challenge	2012	Morphing wings can be categorised in terms of shape parameters (what to morph), performance benefits (why morph), and enabling technologies (how to morph). Done by two categories; Shape parameters and structural system combination each with specific alphanumeric string descriptor.	Alpha-numeric String Descriptor	N
Li *et al.* (2018)	A review of modelling and analysis of morphing wings	2018	Categorised according to TRL, analysis and modelling methods. More of a summarisation.	Tabular	N

Chapter 3

Design Toolbox

3.1 Morphing Lexicon

The lexicon development has been an evolving theme throughout the paper rather than a distinct standalone item. Table 3.1 presents a summary of some key terms and their definitions discussed throughout the paper. The list is by no means exhaustive and in many cases research specific terms will have to be introduced, it is however suggested that when new terms are used or proposed they be as descriptive, concise, and field-independent as possible.

Table 3.1: A Summary of Key Terms making up the Proposed Morphing Lexicon.

Term	**Definition**
Categorisation	Categorisation divides the world of experience into groups or categories whose members bear some immediate similarity within a given context. That this context may vary—and with it the composition of the category—is the basis for both the flexibility and the power of cognitive categorisation. In the context of this research categorisation refers to some manner of sorting of entities within the scope of morphing.
Classification	Classification divides a universe of entities into an arbitrary system of mutually exclusive and non-overlapping classes that are arranged within the conceptual context established by a set of established principles. In the context of this research classification refers to the rigorous definition of an entry as morphing or not.
Morphing	The act of changing of shape, form, external structure, or arrangement.
Foil	A solid structure with a shape such that when placed in a moving fluid at an appropriate angle of attack (AoA) it generates substantially more lift than drag.
Foil Morphing	Physical morphing of a foil structure.

Table 3.1: A Summary of Key Terms making up the Proposed Morphing Lexicon. - *cont.*

Term	Definition
Objective function	A function that describes the goal or output of a physical system or component within a system. To optimize the system the objective function should be minimised or maximised within the bounds of certain constraints. The objective function describes what the system or component is supposed to do.
Smart Materials	Materials, which possess the ability to change their physical properties in a specific manner in response to specific stimulus input. Rogers *et al.* (1988). Stimuli include changes in pressure, temperature, or electric and magnetic fields and the associated changeable physical properties include shape, stiffness, viscosity, or damping. Gardiner (1993).
Smart System/ Structure	A system or structure which has a built-in or intrinsic sensor(s), actuator(s) and control mechanism(s) whereby it is capable of sensing a stimulus, responding to it in a predetermined manner and extent, in a short/ appropriate time, and reverting to its original state as soon as the stimulus is removed Rogers *et al.* (1988).
Active	Systems/structures/materials/actuators which posses the capacity to respond under the application of electric, thermal, or magnetic fields. In essence active structures have an inherent capacity to transduce energy. The utility of such active structures is that of force transducers and actuators.
Passive	Systems/structures/materials/actuators which are not active, lacking the inherent capability to transduce energy.
Characteristic Length	A dimension that both defines the scale and provides a reference of a physical system. A generic dimension widely accepted as being characteristic of a certain system within a specific context. This dimension has both a definition and a magnitude and informs scale but also reference. As an example, within the field of fluid mechanics there exists a multitude of standardized definitions for characteristic lengths of various shapes (chord length for foils). The characteristic length must be generally agreed upon and are easy to find and compare.

3.2 Classification Scheme

3.2.1 Overview and Starting Point

The classification scheme proposes a clear definition of what constitutes morphing and provides suggestions for refinement of classification within the context

of field-specific morphing. The underlying vision is to be universally applicable to generalised cases while also allowing for field specific refinement in the later stages of the scheme. According to the scope of this project only the branch of classification leading to foil morphing for fluid dynamic applications is developed here. Once an entry is classified as outside of the scope no further effort will be made to classify *what* exactly that technology is. The classification scheme follows a hierarchical, decision tree structure with successive, mutually exclusive classes with fixed boundaries. This provides a significant improvement on existing classification by providing a structured, objective methodology for standardisation of the field. Entries, technologies or other candidate entities, are rigorously sorted, an entry either *is* or *is not* a member of a particular class. Figure 3.1 shows a visual representation of the decision tree structure.

The classification scheme can be approached from a system, subsystem or component level. It is important, however, to remain consistent with the scope of the technology and its respective objective function throughout the classification process. For example, an entire aircraft, a wing, a control surface, an internal structural member, or even an actuator may all be classified along with their respective objective functions using the scheme. This distinction allows systems, sub-systems and / or enabling components to be individually classified as morphing or not and further sub-classified within the relevant contexts. To set the starting point, research within the applied physical sciences and engineering is considered. The classification scheme consists of three distinct *levels*: level 1 deals with the question: *is this morphing?*, this acts as an overall classification of a technology as morphing or not, level 2 deals with the type of morphing or disciplinary classification of morphing technologies, and then level 3 is specific to the relevant discipline it is a specific sub-classification of a type of morphing within a discipline.

Morphing Technologies - After level 1 entries are considered to be *morphing technology*. This classification is field and technology independent. The following further refinement of the field is in line with the scope of this project and serves as an example of the process for other applications of morphing. The reasoning and approach can be adapted to any field. This scheme may be used as a tool for the further application and wider development of *morphing*. Many of the existing classification schemes view morphing as a *science* within a certain context (e.g. aircraft), the method proposed here is that morphing be defined as a science or field in and of itself. This is an important philosophical departure that will allow for the further development of morphing technologies as *things that enable morphing* rather than things that change a specific systems performance.

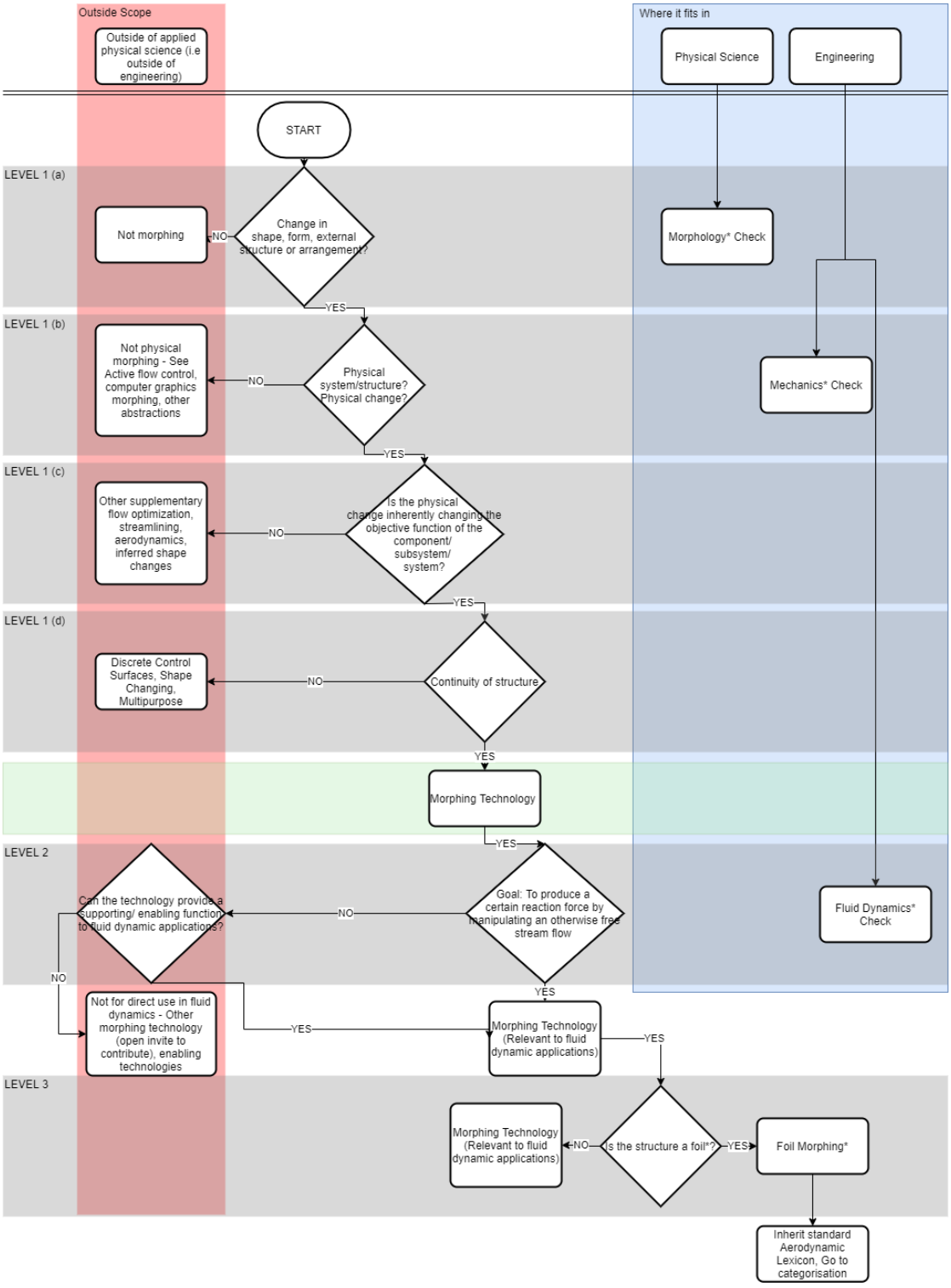

Figure 3.1: Foil Morphing Classification Decision Tree

3.2.2 Individual Level Descriptions

Level 1(a) - *Morphology Check*
A **change** in *shape, form, external structure or arrangement* is required. The change is broad and no constraints are imposed at this level as to the extent, type or reason of change.

Level 1(b) - *Mechanics Check*
The next binary classifier considers whether the entry deals with a physical structure or system and whether the change considered is a ***physical*** *change in shape, form, external structure, or arrangement* essentially enforcing the mechanics component. This excludes any abstractions of the term of morphing. At this level many existing research and technologies termed as morphing, such as artificial flow control or virtual aerodynamic shaping, are excluded from the proposed definition and subsequent classification of the field. This is motivated by the fact that this field of artificial flow control (AFC) is a large, stand-alone field within engineering and the boundaries between AFC and morphing should not be blurred to the detriment of either field.

Level 1(c)
The next decision block asks: *is the shape change inherently changing the objective function if the component/subsystem/system?*. Many papers require a *positive gain* for a technology to be defined as morphing. This may however be a limiting, constraining definition since it is often difficult to define improvement. The key idea with looking at the objective function is simply to enforce a change in function or performance, rather than an ambiguous *positive* change. This step rigorously evaluates whether a shape change to the entry in question is meant to influence the objective function of that entry, or simply inferred due to some other supplementary function. Retractable landing gear, for example, could pass all of the levels above, however, the change in shape is in most cases not inherently changing the objective function of the landing gear and therefore is excluded here. It is important to note that this is meant to be a logical distinction rather than a rigorous mathematical one.

Level 1(d)
Continuity of structure despite the shape change is enforced at this level. The idea of continuity of structure is important and is reflected as its own level. The vast majority of research and technology into morphing requires that there is some manner of continuity of structure, discrete, in the case of fluid dynamic morphing, hinged control surfaces causing surface discontinuity are excluded at this step.

Level 2 - *Fluid Dynamics Check*

At level 2 concepts are divided into fluid dynamic applications or not. The goal of the technology represented in the entry must be *to produce a certain reaction force by manipulating an otherwise free stream flow.* The morphing entity needs to operate within a flow field and have an objective function related to the reaction force produced by the manipulation of otherwise free stream, external flow. The goal of the physical deformation specifically, must be to directly affect the flow. The shape change must have a direct link to the fluid dynamic effect. The fluid dynamic change cannot simply be inferred by the shape change. For example flying cars which *morph* from a land-based vehicle to an aircraft would be excluded here, an example of such is a recent patent by Toyota of a *Dual-mode vehicle with wheel rotors* Nam and Uehara (2018). The main goal of the physical shape change, in this case, would be to change the mode of the vehicle, not necessarily to produce a reaction force by manipulating free stream flow. At this level there is an opportunity for other researchers to add their own developments of the classification of morphing under the branch outside of fluid dynamics since, in this paper, only the fluid dynamic branch will be developed further as outlined in the scope.

Level 3

The distinction made here is between *morphing* and *foil morphing* which is entirely dependent on whether the structure involved either is a foil or is directly involved in the morphing of a structure that is a foil. It is possible to inherit the standard aeronautic lexicon and proceed to the categorisation of the technology within the field. In this sense *foils* have their own specific terminology and standard definitions (characteristic length etc.) that can be used to complete the categorization. Concepts which are only classified as morphing, not foil morphing are difficult to categorise further due to the sheer number of possible implementations of the technology, it is impossible to predict or foresee the direction in which the field of morphing will move and consequently the type of structures and systems it will be applied to. To avoid any artificial constraints on the technology and field the realm of *morphing* outside of applications on structures which could be classified as foils is left purposely open-ended and will no doubt be filled in the future. Further research in the field of morphing outside of foils and fluid dynamics is encouraged and it is suggested that the classification scheme presented here serve as a basis for further development. At present the greatest potential for the technology and its application is seen in structures that aim to produce significantly more lift than drag: foils.

3.3 Categorisation Scheme

The categorisation scheme will categorise concepts which are classified as foil morphing for fluid dynamic applications, as set out in the scope of the thesis. Care is taken in the development of the categorisation scheme to explain the process as well as make each entry into the vector as field independent as possible. Here categorisation divides morphing concepts, using a description vector, into groups or categories whose members bear some immediate similarity within a given context. Membership to any group is non-binding and therefore boundaries are *fuzzy*, category membership is based on generalised similarity or immediate context. Table B.1 shows the application of the categorisation scheme to a number of papers. It is envisioned that the a table consisting of the categorisation results for all of the papers review in this project will be made available as an online repository at a later stage allowing researchers to utilise the design toolbox by comparing existing research for application to new research.

3.3.1 Description Vector

The effective description and consequent sorting, categorisation, and comparison of all research is done through a *description vector* which can be set up for each entry and used to directly compare any research within the field. Components of the description vector may be a single value or a vector in itself. The motivation behind the format of the description vector is twofold, it is easy and logical to have separate entries which each relate to some physical quality or descriptor of the technology and secondly, a vectorised format allows for computational operations such as searching or sorting which make categorisation of a large number of entries practical. Figure 3.2 gives a visual representation in a tree structure of the format of the vector, in this case all of the fields will be populated (provided the information is available). The first level provides the nine entries into the vector while successive levels describe those entries which themselves are vectors. The description vector is set up as follows:
$Description\ vector = [FA\ DT\ MEF\ PD\ AXI\ ACT\ SUR\ SUB\ OPR]$

Focus Area [FA] - The first category contains the field-specific focus areas such as: *fluid dynamics* [FD], *mechanics* [MEC] and general *system* [SYS] focus. Also given is the relevant system level focus area, distinctions are made between system, subsystem [SUS] and component [COMP] level entries. *Subsystem* and *component* level entries can be further categorised as focusing on the *surface, substructure* or *actuation*. This category provides a useful guideline for the broad goal of the entry in question and filtering by focus area yields entries that are easier to compare directly with one another. The entry is a two-column array, the first

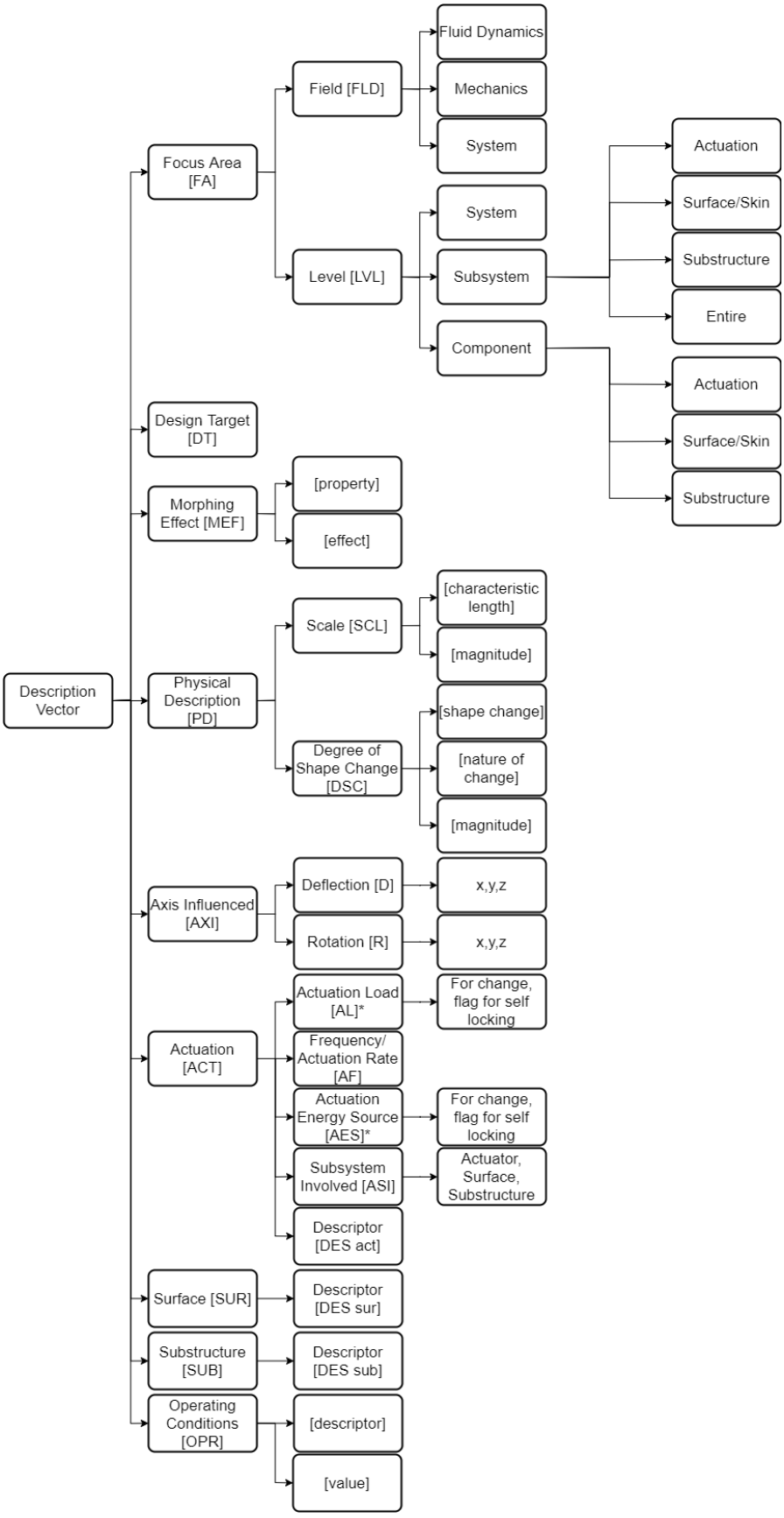

Figure 3.2: Tree Diagram of the Structure of the Description Vector

column corresponding to the field and the second to the system level focus areas.

Design Target [**DT**] - During the review of literature it was found that the vast majority of technologies and corresponding research efforts chose a single or a number of design targets guiding the entire research process. The design target entry is a column vector with text entries corresponding to the various design targets stipulated. The shortest standard notation will be used for fluid dynamic specific terms.

Morphing Effect [**MEF**] - The objective function and the extent to which it is affected by the morphing is presented here. This identifies which aspect of performance is improved and by how much. The effect entry is an array with two columns, the length of the array corresponds to the number of claimed properties that are affected by the shape change. The first and second entries relate to the property (lift or drag coefficient, L/D ratio, flexural rigidity, etc.) and corresponding claimed improvement, respectively. This improvement is normalised against the base value of the unmorphed shape. A value of 0 indicates 0 % improvement while 1 indicates a 100 % improvement.

Physical Description [**PD**] - The third entry is a two-row vector that describes the key physical properties of the technology. It describes the absolute size of the structure in question and the extent of the morphing.

Scale [SCL] - This entry is represented by an array of two columns, the length of which is governed by the number of entries. The first column in the scale array is a text entry describing the geometric property representing the characteristic length of the structure, in the case of multiple components with different characteristic lengths there will be multiple entries in successive rows of the first column (examples include LE/TE segment chords, overall wing chord, etc.). The second column deals with the corresponding magnitude of characteristic length of each geometry. Meters are used as the unit of measurement ensuring consistency and uniformity throughout entries.

Degree of Shape Change [DSC] - The degree of intended shape change is represented by a three-column array of varying length. The first column specifies the property of the structure that is being changed, for example, length, camber or area. The second column describes the type or nature of change, this is described by a text entry of the most simple term possible, expand, contract, twist, rotate, etc as an example. The last column gives the corresponding magnitude of the shape change in each case. For any translational shape change it is the maximum deflection through the shape change normalised by the characteristic length. For

a rotational shape change the entry is the maximum degree of rotation normalised by 90 degrees. [1] The characteristic length is defined as per convention as used in the aerodynamic dimensionless numbers, such as the Reynolds Number [2].

Axis Influenced [AI] - The entry for the axis influenced is a 2×1 column vector. The entry deals with deflections in the x, y,, and z axes while the second represents rotations about the three axes.

Actuation [ACT]

Actuation Load [AL] - The entry for actuation load is a numeric scalar entry of maximum actuation force encountered, measured in Newtons. The entry is the load on the actuator for *shape change*. In some cases the actuation load may be represented by a torque in this case the unit will be newton-meters. An asterisk (*) is used to flag that the actuator takes no load to hold the shape, indicating a form of locking.

Actuation Frequency [AF] - The actuation frequency is represented as a scalar value, calculated as the inverse of the time taken to complete one cycle or full range of shape change.

Actuation Energy Source [AES] (Active/Passive distinction) - The actuation energy source entry categorises whether the energy for the *shape change* comes purely from the flow (passive) or purely from an energy source within the system (active). An entry of 0 represents purely passive action, all of the energy comes from within the fluid flow. An entry of 1 represents purely active action, in this case all of the energy comes from a component within the system. Here an asterisk (*) is again used to flag that there is no energy required to hold shape. [3]

Subsystem Involved [ASI]- Here the component, subsytem, or system directly involved in or responsible for the actuation is identified. this distinction provides important insight into the level of integration of the technology. The entry can be any of the following: surface, substructure or a dedicated non-structural actuator component.

Descriptor [DES act] - The actuation technology is effectively described by Table 2.4 Vasista *et al.* (2012). The corresponding notation and descriptions are

[1] 90 degrees was chosen as the reference for rotational shape changes as this constitutes a full orthogonal change.

[2] The entry will be a fraction where 0 is no shape change and 1 is a shape change equal to the characteristic length for translations and 1 is a shape change of 90 degrees for rotations.

[3] The key difference between the flag in this category and in the actuation load category is that, in the case of a flag in the AL category, the actuator itself takes no load, in other words the rest of the structure somehow locks into position. When the AES is flagged as having no energy required to hold the shape change it could indicate, as with AL, that the structure locks independently of the actuating member or has internal locking.

used here.

Surface [SUR], Substructure [SUB] - Table 2.4 Vasista *et al.* (2012) gives the details of the surface and substructure technologies and provides corresponding categorisation. The notation and method will be used here.

Operating Conditions [OPR] - The entry is generalised to non fluid dynamic cases by incorporating some descriptor of the operating conditions of the technology and its corresponding value to allow for some form of scale independent categorisation. The entry is a two-column vector, the first column corresponding to the descriptor and the second to its value. It is suggested that the descriptor be chosen as a common non-dimensionalised number providing some insight into the operating conditions of the entry. For fluid dynamic cases this entry would correspond to the Reynolds number range encountered in the application. This category would, for example, make applications across different operating fluids easier.

3.3.2 Utility

Supplementary categories including the meta-data of all entries are included in the table in order to facilitate utility. Operations can now be applied to concepts with populated description vectors, including sorting, comparison, and categorisation. This process is illustrated in Chapter 4 and the resulting table given in Table B.1. It is envisioned that this part of the design toolbox be used in one of two ways:

1. Existing research can be sorted, compared, and categorised into categories that match the design specifications of an envisioned morphing technology or project. From here the individual entries within the desired category bounds may be further studied to guide the initial design phase. This approach is followed during this project. A description vector is set up from the design requirements for a morphing centreboard, this description vector acts as a target for the description vectors of existing research to be filtered by. This will yield specific existing technologies and concepts which may be directly implemented in the design of the morphing centreboard.

2. The description vector, and supplementary categories as required, may be applied to a new design within the realm of morphing as presented by the classification scheme. From here it can be determined which categories the new design falls within and which existing technologies have similarities, allowing comparison as well as possible ideas or suggestions leading to improvements to the design. It also provides a useful tool for positioning a new technology within the field of morphing.

Chapter 4

Morphing Centreboard Conceptualisation

In this chapter the conceptualisation of a morphing foil for a hydrodynamic application, specifically the profile of centreboard of a 505 class sailing dinghy, is undertaken together with the application of the design toolbox presented. To develop design requirements and specifications the the theory of a sailing boat is covered and the governing equations are presented and solved with physical parameters of the 505 class sailing dinghy and variables describing the operating conditions as inputs. A fluid dynamic investigation, the design toolbox Chapter 3 and a structural investigation are used to complete the design requirements and generate concepts. The use of the design toolbox both enables the conceptualisation of the morphing hydrofoil and acts as a case study proving the efficacy of the lexicon, categorisation and classification schemes.

4.1 Mathematical Model of a Sailing Vessel

In this section the principles behind a mathematical model are introduced, the specific aerodynamic forces on the sails and the hydrodynamic forces on the hull and underwater appendages are discussed in subsection A.2. The force balance between the aero- and hydro- forces, the heel and yaw moment equations and balances are presented and the overall mathematical model is given here. This section provides the link between camber change of a foil profile used in a centreboard, and the performance of the sailing boat by deriving and presenting equations which link properties of the foil profile to performance metrics of the boat. This motivates the hypothesis of using a camber morphing centreboard to improve the performance of a sailing boat. The assumptions, equations and methodology presented are used, along with typical operating conditions of a high performance

sailing dinghy, in order to determine the design requirements and specifications of the proposed morphing centreboard.

4.1.1 Principles

A sailing boat operates dynamically, with a complex interaction between aero- and hydro-dynamic, gravity and inertial forces, the resulting motions can only be described by a six *degree of freedom* (DOF) axis system as presented in Figure 4.1 (Knudsen, 2013). In theory it is possible to identify all of the forces and moments which act on a boat and, according to Newton's second law, must balance for a steady state sailing case. Many of these forces and moments have little influence on the speed of the boat or are extremely difficult to determine. As outlined by Philpott *et al.* (1993) the sailing model will consist of a number of force and moment balance equations which must sum to zero in a steady state sailing condition. What follows here and in subsection A.2 are the assumptions made in order to present the equations governing the equilibrium of a sailing boat. For the purposes of this chapter and the sailing background presented here, a significantly simplified approach to the sailing boat model is taken according to that presented by Philpott *et al.* (1993). Far more elaborate, detailed and consequently accurate formulations can be found in research, such as those of Gerritsma and Keuning (1992) and Mason (2010).

The first simplifying assumption is that both the vertical force balance and the pitching moment balance are always satisfied, removing them from further consideration. The vertical force balance can be disregarded since there is little movement in this plane and for the most part the yacht weight equals the sum of the buoyancy and vertical aero- and hydro-dynamic forces. [1] In a similar way the pitching moments are assumed to balance, the overall force from the sails creates a moment, depressing the bow and causing a longitudinal imbalance in buoyancy which, in turn, opposes this pitch. The restoring moment from the buoyancy imbalance is large and consequently the system is very stable in pitch, therefore assuming forces balance on this axis is maintained. [2] The remaining forces include those which lie in the plane of the water surface, the forces in the plane causing roll and the forces in the plane causing yaw. For all of these planes, equilibrium

[1] In practice there are fluid-dynamic forces induced by the motion of the boat as well as a slight dynamic change in displacement, this displacement is, however very small since the buoyancy changes rapidly with small vertical displacement. Consequently it is assumed that the boat operates at a fixed displacement.

[2] It must be noted that rough water conditions as well as extremely unstable wind conditions can significantly affect these assumptions and consequently the boat speed, Philpott *et al.* (1993) suggests that this may later be accounted for by adding an extra drag increment to the steady state condition.

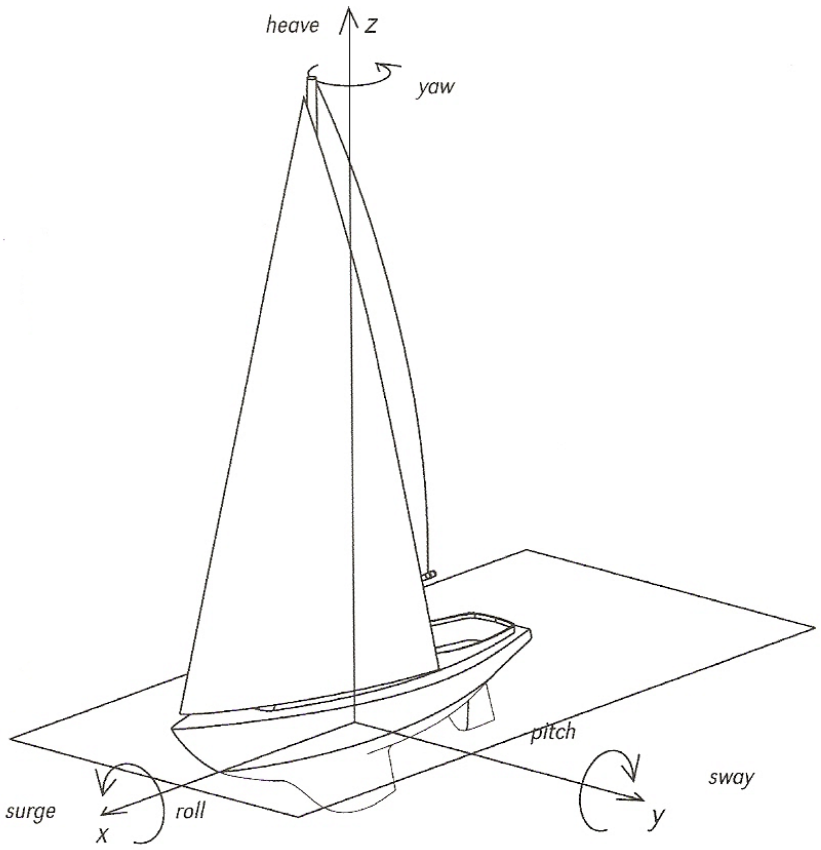

Figure 4.1: Sailing Vessel Axes (Fossati, 2009)

is required. The force and moment balances of the components above yield the other 4 DOF equations.

4.1.2 Force and Moment Balances

The forces lying in plane with the water surface are required to be equal in magnitude and opposite in direction. In principle this requires the total aerodynamic and hydrodynamic forces to be equal and opposing. Figure 4.2 shows this equilibrium. This equilibrium further leads to the conclusion that the motive force equals the resistance force, $F_m = R$, and the aerodynamic side force equals the hydrodynamic side force, $F_s = S$.

The assumption that both the hull and rudder produce no lift is made in order to satisfy the yaw moment balance of the boat. If the rudder and hull only produce resistance opposing the boat's velocity (it is assumed this resistance is balanced

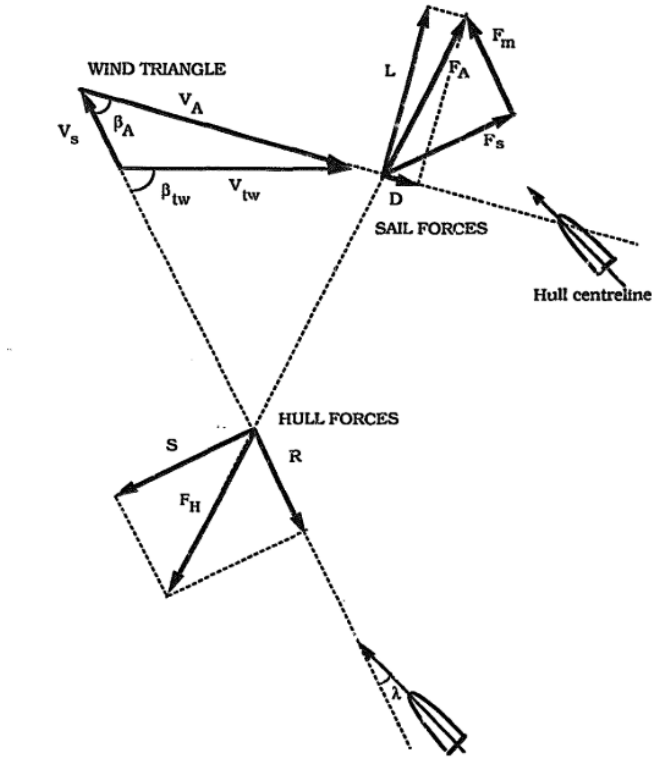

Figure 4.2: Total Aero- and Hydro-dynamic Forces on a Sailing Boat in Equilibrium (Philpott *et al.*, 1993)

about the yaw axis of the boat), then the only components producing a moment about the Z or yaw axis of the boat are the aerodynamic side force and the hydrodynamic side force (the lift from the centreboard). From the force balance in the horizontal plane it is known that the aerodynamic and hydrodynamic side forces must be equal in magnitude and opposite in direction, therefore both these forces must be acting in the same vertical YZ plane (the CE is in plane above the CLR, see Figure A.8). Further, if the boat is sailed at zero heel angle the CE will be directly vertically above the CLR. Leaving only their distances above and below the horizontal plane to be used in further calculation.

Finally, the critical moment balance required for centreboard design, the rolling moment balance can be evaluated, yielding the required hydrodynamic side force and, consequently the design centreboard lift. Figure 4.3 illustrates the forces involved in the roll moment balance. The aerodynamic drag and side force as well as the hydrodynamic resistance and side force produce overturning moments about

the X or roll axis of the boat. Ignoring any hydro-static roll forces from the hull as is applicable at zero heel angle, the only opposing moment is termed the *righting moment* (M_r). On a dinghy the righting moment is produced solely by the crew weight which is positioned on the windward side of the centre line creating a crew roll moment (M_c). Figure 4.4 shows a high performance sailing dinghy sailing upwind at zero heel angle with one crew on trapeze and the other hiking in order to produce the required righting moment in order to keep the boat in equilibrium about the roll axis.

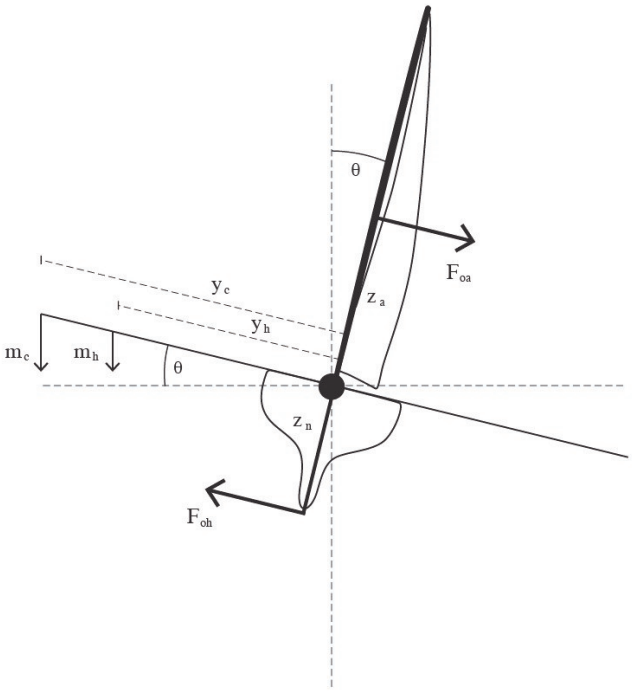

Figure 4.3: Sailing Boat Roll Moment Components

The only remaining variables to be determined in order to perform the roll moment balance are the distances of the CE and CLR from a reference point on the boat, or simply, the distance between the CE and CLR. It follows that with the relevant parameters of the boat known the distance between the waterline and the CLR (z_h) and the waterline and the CE (z_a) are determined as shown in Figure A.8. Multiplying the sum of these distances with the overturning force the roll moment equilibrium equation can be expressed as follows:

Figure 4.4: Righting Moment Illustration - 505 Dinghy Sailing Upwind at Zero Heel Angle (Favereau, 2016)

$$\begin{aligned} M_r &= M_c = F_o\,(z_a + z_h) \\ F_{oa} &= F_{oh} = F_o = L\cos\beta_A + D\sin\beta_A \end{aligned} \tag{4.1}$$

The overall model, summarising the force and moment balances derived in the above equations is then the the motive force, resistance force balance:

$$F_m = R = F_f + F_w + F_i\,(V_s, \theta, \lambda) \tag{4.2}$$

where F_f, F_w, F_i are components of the hydrodynamic resistance of the entire hull and underwater appendage system. appendix A.2 outlines each term.

The aerodynamic side force and hydrodynamic side force balance:

$$F_s = S \tag{4.3}$$

and the roll moment balance:

$$M_r = M_c = F_o\,(z_a + z_h) = (L\cos\beta_A + D\sin\beta_A)\,(z_a + z_h) \tag{4.4}$$

High performance sailing dinghies' upwind performance is often governed by the amount of righting moment that can be generated by the crew. The overturning moment generated by the sails is managed by the crew through inputs to the sail shapes and relative AoA's in such a way that the roll moments are held in

equilibrium. This leads to the assumption that, in all operating conditions the roll moment balance is maintained. Since the righting moment of the crew is known through typical crew weights and positions, and the distances to the CE and CLR, z_a and z_h are known, the overturning force, F_o and consequently F_{oa} and F_{oh} can be calculated. Equation 4.1, Equation A.4, and Equation 4.3 can now be used to calculate the hydrodynamic side force S (equivalent to the centreboard lift). This yields centreboard lift targets at various operating conditions. These assumptions and equations are used along with 2D CFD in the following section to determine a target for the morphed foil profile shape.t

4.2 Design Requirements and Specifications

4.2.1 Preliminary Force and Moment Balances

The force and moment balances given in Equation 4.2, Equation 4.3, and Equation 4.4 are now used along with parameters associated with a 505 class high performance sailing dinghy to determine the requirements of the morphed profile shape for the centreboard. This is done in five steps:

1. Determine the geometry and basic physical properties associated with foils for existing 505 class dinghy centreboards: planform shape (including chord length, span, area and aspect ratio) and profile shape (including thickness, position of maximum thickness, LE and TE shapes).

2. Compare the profile shape to existing NACA profiles and select a basic four digit NACA 00– series profile shape which represents the shape sufficiently.

3. Determine basic operating conditions based on typical 505 class dinghy sailing conditions. This includes the operating conditions required to complete the force and moment balances: boat velocity based on wind velocity, crew weight, boat geometry. Operating conditions relating to the operating fluid including: density, viscosity, temperature, Reynolds number range are also included.

4. Calculate centreboard lift target force based on operating conditions, 505 class dinghy parameters and calculation of the force and moment balances.

5. Determine the target 2D C_l from the 3D C_L

4.2.1.1 Geometry

Most modern 505 centreboard designs have converged and have similar planform shapes with only small differences in certain specific design parameters. A generic

all condition, high aspect ratio, centreboard from producers such as Milanes Foils (2014); Segelsport Jess (2020) and Pinnell & Bax (2020) is used. Table 4.1 shows the measured planform shape and specifics of the centreboard. For the purposes of this project it is assumed that the planform is sufficiently similar to a perfectly elliptical planform. Figure 4.5 shows a modern 505 centreboard planform with an elliptical shape overlaid, motivating the above assumption. Hoerner, Sighard (1985) provides the particulars of elliptical wing theory which can be used in the analysis of the centreboard.

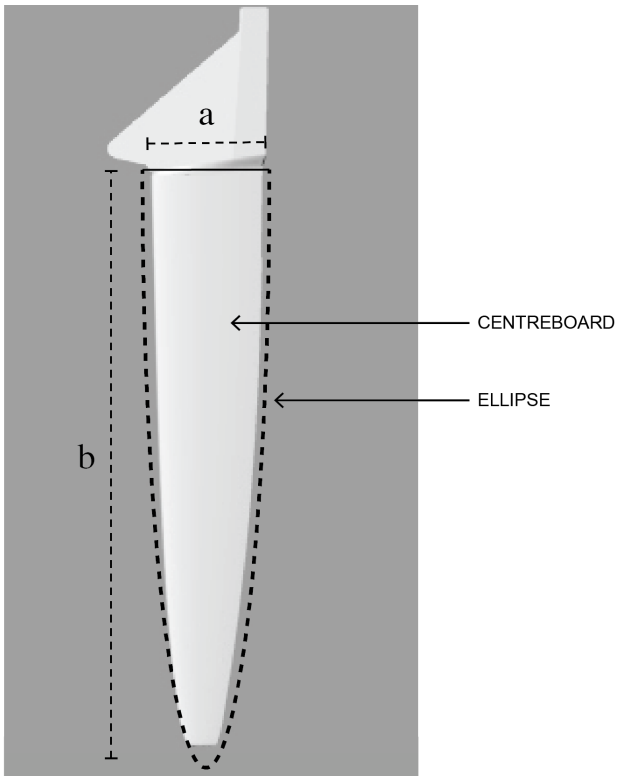

Figure 4.5: 505 Centreboard Planform Shape adapted from Competition Composites Inc. (2020)

The aspect ratio is calculated as per Equation 4.5. Since the centreboard is effectively a wing with an end-plate at the foil-hull junction an end-plate correction factor is included in the effective aspect ratio calculation. According to Hoerner, Sighard (1985) the effective aspect ratio of a wing increases when fitted with an endplate according to Equation 4.6

$$AR = \frac{s^2}{S} \tag{4.5}$$

$$AR_{eff} = AR\left[1 + 1{,}9\frac{h}{b}\right] \tag{4.6}$$

Table 4.1: 505 Class Sailing Dinghy Centreboard Geometry

Planform Shape			
	Root Chord (m)	c_r	0.3
	Span (m)	s	1.45
	Planform Area (m^2)	A_k	0.3416
	Aspect Ratio	AR	6.1540
Profile Shape			
	Thickness (mm)	t	30
	Thickness/Chord		10 %
	Position of max. Thickness		30 %

4.2.1.2 NACA four digit equivalent

An in depth explanation of the NACA four digit profiles and their applicability to low Re cases is provided by Hoerner, Sighard (1985). Representing the centreboard profile as an NACA profile allows a large base of existing research to be used. This representation is appropriate since many low Re number foils follow the profiles closely, in fact Milanes explicitly state that they use un-cambered NACA 00– profiles in their centreboard design Milanes Foils (2014). The NACA four digit series allows parameters of the foil profile to be individually changed simply by changing digits in the four digit code of the foil. XFoil, an open source 2D CFD program expanded upon in subsection 4.2.2, includes a NACA foil profile generator in the software package allowing rapid editing and simulation of multiple different profile shapes. The symmetrical 505 centreboard has a root chord length of 300 mm, an a maximum thickness of 30 mm. These measurements can be represented by a NACA 0010 profile shape as shown in Figure 4.10 (together with the cambered foil profile).

4.2.1.3 Basic Operating Conditions

The operating conditions provide inputs into the algebraic equations describing the force and moment balances as well as inputs for the fluid dynamic investiga-

tion to follow. Appendix A.3 provides supplementary information to this section including explanations and formulae. There is limited documented research that exists describing the particulars of 505 crew combinations as well as their positions transversely within the boat at different wind speeds. Since the author has extensive experience in competitive 505 class dinghy sailing the above variables are described based on observations of the sailors and techniques typically encountered in competitive regattas. The particulars of the crew are shown in Table 4.2.

Table 4.2: Typical 505 Sailor Particulars

		Weight kg	Height m
Heavy Crew Combination			
	Helmsman	70	1.7
	Crew	100	1.9
Light Crew Combination			
	Helmsman	60	1.6
	Crew	90	1.8

The righting moments produced by the sailors at different wind speeds is calculated according to subsection A.3 shown in Table 4.3 together with the relationship between boat speed and heading angle at various wind speeds for a sailing boat. The table gives the basic upwind speed targets in for a 505 dinghy at a number of wind speeds. [3]

The operating conditions for hydrodynamic applications are generally harsher than for aerodynamic applications, water is far more dense, incompressible, corrosive and conductive than air. Water's properties at $20°C$ are used ((values from Engineering Toolbox (2020)) in Equation 4.7:

$$Re = \frac{\rho V_s l}{\mu} = \frac{V_s l}{\nu} \approx 750000 - 1000000 \tag{4.7}$$

where ρ is the density of the operating fluid, in this case sea-water, approximately 1000 kg/m^3.The boat velocity, V_s, ranges from 5 knots to 7 knots or 2.6 m/s to 3.6 m/s at typical sailing conditions. l is the characteristic length of the foil, in this case the chord length of an existing foil is in the range of 0.3 m. μ is the

[3]The boat velocity used as one of the operating conditions' variables is determined from research and not calculated according to the motive force, resistance force balance equation, Equation 4.2. This calculation would require the particulars of the sail shapes and trim configurations as well as all of the drag components of the hull and underwater appendages to be calculated according to section 4.1, this is considered outside of scope of the work done here.

Table 4.3: 505 Polar Targets (Upwind Speed vs Wind from Buell Software (2019))

True Wind Speed [kts]	6	8	10	12	14	16	20
Upwind Speed [kts]	5.0	5.3	5.6	6.0	6.5	7.0	7.0
Crew Position	Inside	On Gunwale	On Gunwale, Weighted Trapeze	On Trapeze, Crouched	On Trapeze 75 %	On Trapeze Flat	On Trapeze 100 %, Arms Out
Heavy Combination Righting Moment (Upwind) [Nm]	1567.6	1616.8	1800.6	2155.0	2680.0	3375.7	3375.7
Light Combination Righting Moment (Upwind) [Nm]	1566.7	1616.9	1801.3	2154.1	2678.0.0	2898.3	2898.3

dynamic viscosity of the fluid, which is 0.001 kg/(m s). This puts the operation of the foil in the Re range of 750 000 - 1 000 000.

4.2.1.4 Centreboard Lift Target

The assumptions and equations presented up to this point are now used to calculate the centreboard lift targets as a function of wind speed for both crew combinations. The lift force or centreboard load is calculated by solving for F_o (and according to the assumptions made in section 4.1, F_{oa}) in Equation 4.4, the boat's roll moment balance. The results are shown in Figure 4.6, the centreboard load increases with wind speed and consequently (according to Table 4.3) boat speed, righting and overturning moments. There is a breakpoint in the graph where the lighter sailor combination is unable to produce a higher righting moment and consequently has to maintain their overturning moment despite the increase in wind speed. Since the limiting factor to the high wind performance of the light sailor combination is the righting moment they are able to produce, the lift requirement of the heavy sailor combination will be taken as the applicable case.

The calculation of the target centreboard lift force over a range of wind speeds provides an important design requirement for the morphing centreboard. Currently the lift force is generated by a symmetrical foil at a non-zero AoA, the morphing centreboard must produce the target lift force over all operating conditions at zero AoA, eliminating boat leeway.

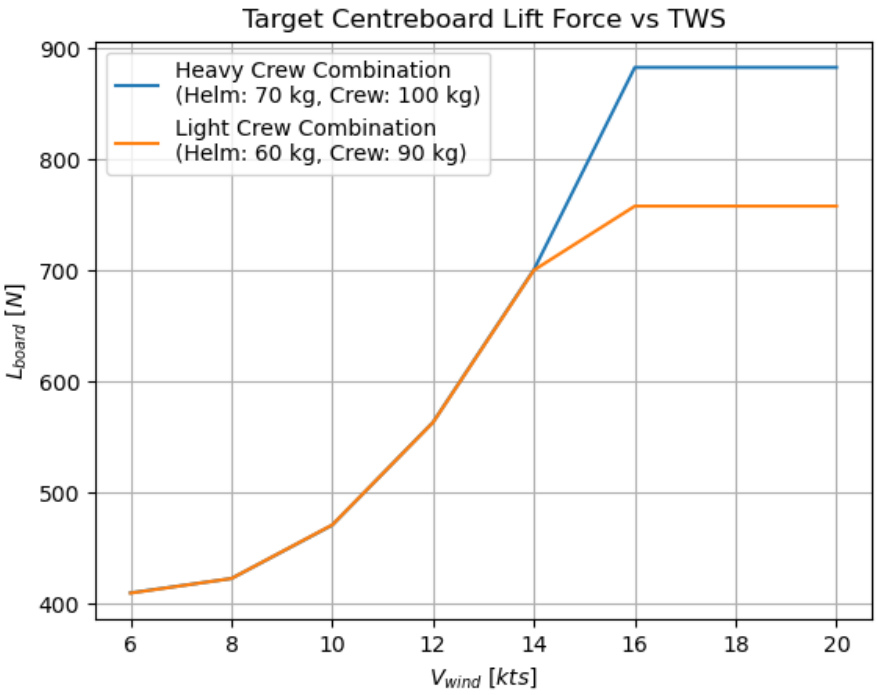

Figure 4.6: Centreboard Load vs True Wind Speed

4.2.1.5 Lift Coefficient

Pope (1951) provides a method of relating a 3D lift coefficient of a finite span elliptic wing with the 2D lift coefficient of the profile. First the 3D lift coefficient, C_L for the centreboard is calculated using Equation A.2. Then a theoretical ratio of $\alpha_{2D}/\alpha 3D$ can be used to correlate the 2D and 3D coefficients. There are two parts to the method provided by Pope (1951), the first deals with the lift curve slope change caused by circulation of flow over a finite wing and the second, with reference to Jones (1941), provides an edge correction factor for spanwise flow due to the "sweep" created by the LE of an elliptical planform shape. The resulting equation with correction factors providing the slope of the lift curve for a 3D elliptic wing is given in Equation 4.8.

$$\alpha_{3D} = \alpha_{2D} k \left(\frac{AR_{eff}}{EAR_{eff} + 2k} \right) \tag{4.8}$$

where

$$k = \frac{1+\epsilon}{1+\epsilon^2}, \tag{4.9}$$

$$\epsilon = \frac{4}{3\sqrt{3}} \times airfoil\ thickness\ ratio \tag{4.10}$$

and

$$E = \frac{wingsemi - perimeter}{wing\ span}, \tag{4.11}$$

A target 2D zero AoA lift coefficient, C_{l0} is calculated at each wind, and corresponding boat speed, this provides a specification for the morphing foil profile shape. Typically 2D profiles have lift curve slopes of $\alpha = 2\pi$ in radians, it is commonly accepted that NACA 00– sections have a 2D lift curve slope of 0.12 for small $AoAs$, (Hoerner, Sighard, 1985). The relationship between lift coefficient and wind speed is shown in Figure 4.7. [4]

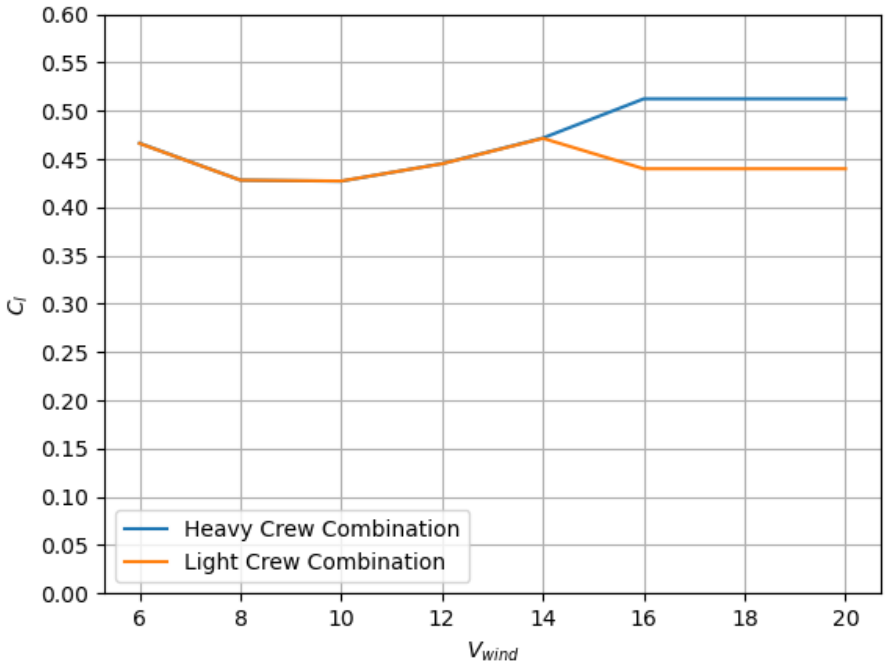

Figure 4.7: Required 2D Lift Coefficient vs True Wind Speed

[4]When dealing with the analysis of sailing boats the wind speed is often the independent variable. True wind speed, not boat speed, is therefore represented on the x axis when representing properties of sailing boats and their components.

Figure 4.7 shows that the required 2D lift coefficient for a 505 centreboard foil profile stays relatively constant throughout the wind and boat speed range. The target C_l's range from 0.42 to 0.51 with the average lying at 0.4719 for the heavy crew combination. The reason for the last three points remaining constant is the limitation of available righting moment and the consequent maintaining of aerodynamic overturning moment and boat speed. This C_l range provides a design specification for the 2D profile shape of the morphing centreboard. It must have a zero AoA lift coefficient, C_{l0}, within this range, and ideally equal to the average. [5] This design requirement means that a boat equipped with the morphing centreboard will have zero leeway angle.

4.2.2 Fluid Dynamic Investigation and Application

The fluid dynamic investigation done uses results from section 4.1 and subsection 4.2.1 which are inputted into basic CFD simulations which determine the target, cambered 2D profile for a morphing centreboard. XFoil is be used to run all of the flow simulations, profile design and analysis. XFoil is an interactive panel-based 2D CFD program developed in 1980 by Mark Drela for the design and analysis of subsonic airfoils.[6]. The program uses a full potential flow method to solve the bulk flow around a foil section. A number of corrections based on well-established experimental data are then applied to the solution to approximate the effect of the boundary layer. The method is effective at simulating low Re flows with little or no laminar flow separation. XFoil performs well against experimental data when dealing with viscous analysis of airfoils and allows the user to specify forced transition or calculate the free transition point. Limited trailing edge separation and transitional separation bubbles can also be simulated effectively, (Drela, 1989). The XFoil design environment consists of four main menu driven routines, the panel generator, the flow solver, the inverse flow solver or editor and the geometry manipulation. There are also a number of *batch mode* operations possible. For the design presented here the XFoil panel generator, geometry manipulator and flow solver are the only modules used. XFoil is written in Fortran and can be run from the terminal, this is used in order to run multiple automated simulations through Python. Since the computation requirements required to run XFoil simulations are relatively low the maximum number of panel nodes allowed by the software is used in each simulation. This ensures that there are no errors from inadequate *mesh refinement*.

[5] The average is chosen since it assumed that the morphing centreboard will only actuate between stable positions with no proportional actuation between. In this case designing for the average lift coefficient will provide the most benefit across operating conditions.

[6] For more information on XFoil consult Drela (1989)

Figure 4.8 gives the XFoil predicted C_l vs AoA curves for a symmetric and asymmetric foil profile. It can be seen that the asymmetric profile generates higher lift at the same AoA than the symmetric profile. It is important to note that the asymmetric foil produces lift even at zero AoA. Figure 4.8 shows that the drag produced by a symmetric and asymmetric profile is similar at low AoA. The combination of these two relationships is given in Figure 4.8, shows the lift to drag ratio over a range of AoA's for similar symmetric and asymmetric foils at a Reynolds number that can be expected in underwater applications. See Equation 4.7 for a basic Reynolds number calculation as it applies to the expected applications in this project. From Figure 4.8 [7] it can be seen that the absolute value of the lift to drag ratio of the asymmetric foil is higher than that of the symmetric foil, concluding that the asymmetric foil produces lift more effectively than its symmetric kin over most $AoAs$, it does this by producing higher lift with similar induced drag.

Utilising 2D CFD simulation through XFoil, typical NACA four digit cambered profile shapes are simulated at the expected operating conditions. Through using the software to design according to a target C_l, a cambered profile is found which meets the lift targets. There are a number of ways to achieve an asymmetric, cambered profile derived from a symmetric profile, for example: one may alter a single side (or surface) of the profile while maintaining the shape of the other, creating a thicker or thinner cambered profile, alternatively the thickness may be maintained and the profile *curved* along the camber line. The latter of the solutions is chosen for this application as it allows for the most direct comparison, using the NACA 4 digit designation, of differently cambered profiles. This solution also carries structural advantages such as minimal strain within the foil surface, the structural aspects are addressed further in subsection 4.3.2. Figure 4.9 shows the relevant foil profile terminology and dimensions.

Section 4.2.1 shows that the target cambered airfoil profile must produce a zero AoA lift coefficient of 0.4719. XFoil allows a user to specify a direct operating point for any 2D profile shape and solve for C_l or α with the other as an input. Additionally the software includes a NACA airfoil generator capable of generating and paneling the profile shapes of non-standard NACA foils. To determine the appropriate NACA profile a simple python script is written which utilised the command line to run a number of automated XFoil simulations. This script cycles through NACA designations altering the first and second digits from 2 to 5 and, in each iteration, solving for the AoA required to achieve a C_l of 0.4719. Since the lift coefficient is a design specification the goal of the simulation is to determine which NACA four digit profile achieves this C_l at the lowest AoA. The operating

[7] Ncrit is simply a turbulence transition factor used in XFoil. See (Drela and Harold, 2001) for a description of the Ncrit parameter in the XFoil software.

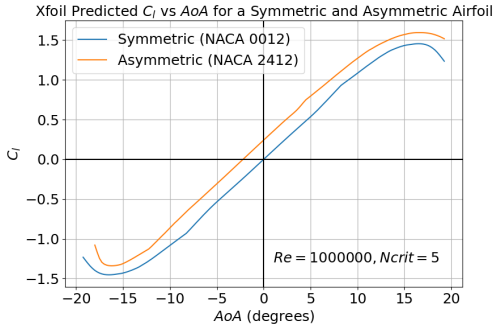

(a) Lift curves for Symmetric and Asymmetric Foil Profiles

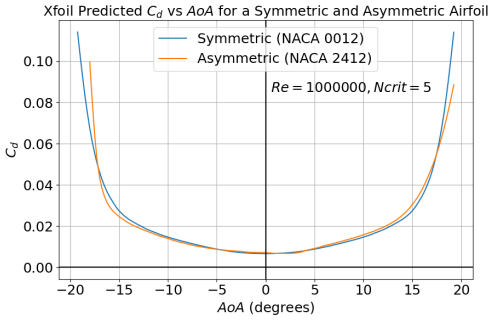

(b) Drag curves for Symmetric and Asymmetric Foil Profiles

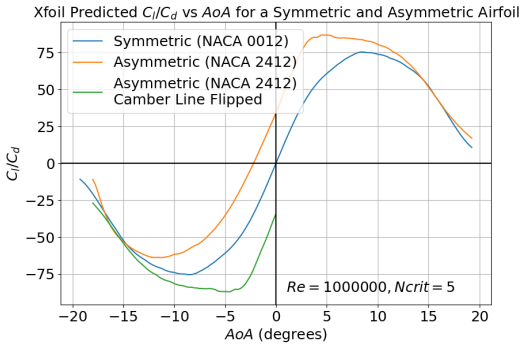

(c) Lift/Drag Curves for Symmetric and Asymmetric Foil Profiles

Figure 4.8: Symmetric vs Asymmetric Foil Curves (profile data provided by Airfoil Tools (2020))

conditions and inputs remained constant in each simulation, only the profile shape is changed. Table 4.4 shows a table of the constant variables. The results of these simulations are shown in Table 4.5. Included in the results are the corresponding drag coefficients. [8]

The ideal profile will show zero AoA in Table 4.5. The NACA 4410 profile achieves the required C_l at and AoA of 0,0398°. This is the closest to zero AoA by nearly a factor of 10 over all the other simulated shapes. The AoA reduction from the NACA 0010 profile to the NACA 4410 profile is 4,35°. The NACA 4410 profile

[8]The moment coefficient is excluded from the results since a 505 class sailing dinghy has the ability to change the sweep angle of the centreboard, this may be used to move the effective CLR forward or aft and consequently balance out any minor pitching moments created by a cambered foil. subsection A.4 gives details on the forward sweep of the centreboard required to balance the moment produced by the asymmetric foil.

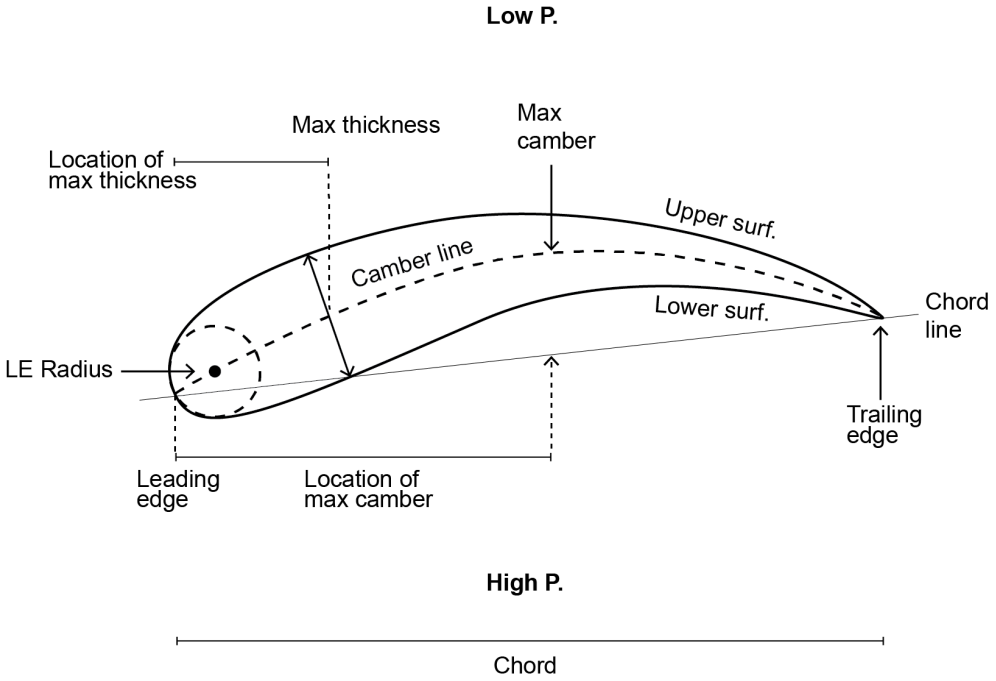

Figure 4.9: Foil Profile Descriptors

Table 4.4: XFoil Simulation Constant Input Variables

Input	Value
Viscous / In-viscid Simulation	Viscous
Reynolds Number, Re	1 000 000
Turbulence Critical Amplification Ratio, $Ncrit$	5
Mach Number, Ma	0
Number of Airfoil Panel Nodes	494
Target Lift Coefficient C_l	0.4719

does not have the lowest drag coefficient despite having the lowest AoA. This low AoA will, however lead to the minimum possible hull drag which is the largest component of the total boat drag, (Milgram, 1998). Some of the lower cambered profiles such as NACA 2610 have lower C_d values at the expense of AoA, however in terms of total system efficiency these do not achieve the goal of the morphing foil. The cambered profile does have a lower C_d than the symmetric foil leading to reduced drag on the foil itself.

Most of the profiles do not encounter flow separation, or when there is separa-

Table 4.5: XFoil Simulation Results, Target C_l of 0.4719

Camber %	Camber Position	α, °	C_d
0	0	4.3920	0.00836
2	2	2.4804	0.00701
2	3	2.3296	0.00639
2	4	2.2381	0.00605
2	5	1.9717	0.00627
2	6	1.7061	0.00672
3	3	1.3797	0.00667
3	4	1.0890	0.00654
3	5	0.7530	0.00633
3	6	0.3091	0.00578
3	7	-0.3028	0.00539
4	2	0.6166	0.00974
4	3	0.3649	0.00852
4	**4**	**0.0398**	**0.00745**
4	5	-0.3967	0.00657
4	6	-0.9703	0.00603
5	2	-0.2550	0.01024
5	3	-0.5642	0.00895
5	4	-0.9741	0.00779
5	5	-1.5108	0.00691
5	6	-2.1915	0.00653

tion the flow becomes re-attached relatively quickly. This is due to the fact that all of the cambered profiles simulated are run at very low *AoA*s under the simulated conditions. It should be noted that large separation is undesirable for a dinghy centreboard as it can quickly lead to stall if the flow is unable to re-attach. The $Ncrit$ value used in the simulation also has a pronounced effect on the likelihood of laminar flow separation. The lower the $Ncrit$ value, the later the transition from laminar to turbulent flow and the higher likelihood that laminar flow separation may occur. subsection A.4 provides more information on the particulars of flow separation for this case.

The NACA 4410 profile is found to be the most suitable cambered foil shape according to the constraints, assumptions and design requirements for the morphed high performance dinghy centreboard. The initial shape of the morphing centreboard is a NACA 0010 and the target morphed shape is a NACA 4410, the properties of which are shown in Table 4.5. From this section it can be concluded that there are far more possibilities and considerations both inside and outside of the NACA 4 digit series used in this analysis which may also be suitable for

the application. These are discussed in Chapter 5. As an illustration, if a typical value of $\lambda = 3°$ can be reduced to zero a 9.5 % increase in VMG can be expected according to Equation 4.12.

$$VMG_{upwind} = V_s \cos(45° + \lambda \tag{4.12}$$

4.3 Concepts

Morphing centreboard concepts are now generated which meet the design requirements and specifications in section 4.2. The final concepts are generated by: (1) Utilising the design toolbox, and (2) preliminary structural investigation. The utilisation of the toolbox in this case consists of: (1) applying the classification scheme to both the proposed foil and the existing technologies reviewed in order to ensure the design is within the field of morphing and the proposed lexicon can be used, and (2) using the categorisation scheme to set up description vectors for the design requirements of the morphing centreboard and existing morphing technologies from which concepts can be directly informed.

4.3.1 Classification and Categorisation Results

The design toolbox presented in Chapter 3 is now used as a design tool to guide the technology selection based on existing morphing concepts. The proposed foil passes the three classification scheme levels (section 3.2) and can be considered within the realm of foil morphing. This allows the standard lexicon proposed in section 3.1 to be used to describe the design. This leaves the morphing categorisation scheme (section 3.3) which is the main tool used to aid in the design of the new morphing foil. The significant contribution of the categorisation vector proposed is its computer searchability. Provided enough research and morphing technologies are categorised and added to a database, one will be able to sort, search, filter and compare based on any of the vector entries. In the design case presented here the physical and the fluid dynamic properties are used to populate most of the description vector. These populated fields are then used to search all of the research and technologies in the database so far in order to *fill in the blanks*. Essentially find existing technologies which closely relate to the specific case and identify appropriate concepts for the actuation, surface and substructure for the morphing centreboard to be built upon in subsection 4.3.2. The morphing centreboard details are inputted into the categorisation scheme and the description vector is set up according to Figure 3.2 as follows.

4.3.1.1 Description Vector Setup

Focus Area [FA] - The field specific focus area of the design is in the fluid dynamic operation of the foil as well as the mechanics of the shape change. The system level focus is on the entire centreboard sub-system including the actuation, the surface and the sub-structure (not on the entire boat *system* or on *components* within the centreboard enabling the morphing). This yields the entry into the description vector [*FD, MECH*; [*SUS; ACT, SUR, SUB, ENT)*]].

Design Target [DT] - The design requirements and specifications of the centreboard are to produce the required C_l of 0.4719 at an AoA of 0°. The other design requirements are that the morphing centreboard follow the geometry and physical properties of existing centreboards, this is covered in the physical description entry. The resulting entry is [AoA ; 0°] , [C_l ; 0,4719].

Morphing Effect [MEF] - The morphing effect entry describes the change to key properties of the objective function and their change from the unmorphed to the morphed shape. In this case the AoA required to meet the C_l decreases from 4,392° for the NACA 0010 profile to 0,0398° for the morphed NACA 4410 profile, a decrease of 99 %. The C_d of the profile is another property of the objective function, to reduce overall boat drag, it is decreased from 0.00836 to 0.00745 in the unmorphed and morphed profile respectively, a decrease of 10.8 %. The MEF entry is then [AoA ; −0,991] , [C_d; −0,108].

Physical Description [PD] - The characteristic length of the foil in this design is the root chord length of 0.3 m. The shape change that is envisioned for the design is an increase in camber of 40 % of the chord length. Together this yields: Scale [SCL] - [c_r; 0,3], and Degree of Shape Change [DSC] - [*camber ; increase ;* 0,4].

Axis Influenced [AI] - The way in which the camber changes in the envisioned design can be broken down into a translational component as well as a rotational component, the movement of panels along the profile surface from the symmetric to cambered profile can be described entirely by translation along the z axis and rotation around the y axis. In reality there will be a component of translation in the x axis but this will be minor compared to the movement in the other axes. This results in the entry [DZ] and [RY].

Actuation [ACT] - Many of the actuation properties are not explicitly specified for the design at this point. The particulars of appropriate actuation systems are found by filtering a number of morphing technologies' description vectors by

the entries that are specified in the design (Morphing Effect, Pysical Description and Axis Influenced). The structural and actuation designs are then compared in subsection 4.3.2. The first entry is the actuation load [AL] on the actuator for shape change. This property is not known at this stage in the design. Actuation frequency can be inferred from some operational properties of a 505 class sailing dinghy. The morphing centreboard will flip its camber line over its chord line during a *tack* going from asymmetrically cambered on one side of the chord line to the same asymmetric camber on the other side. It is envisioned that the full morphing cycle consisting of two sub-cycles from NACA 0010 to 4410 will complete in the time it takes to complete the tack. From video footage of the author sailing a 505 in a competitive regatta, a fast tack is seen to take around 2.5 seconds. This means the foil must complete two sub-cycles in this time leading to a frequency of 0,8 Hz. The actuation energy source [AES] is not know or specified for the morphing centreboard design. [9] There is no limitation placed on the subsystem involved [ASI] in the actuation. Rather it is one of the properties which are determined through the comparison of existing technologies' description vectors within the research database. The descriptor of the actuation, following Table 2.4 according to Vasista *et al.* (2012) is not specified for this design leading to $[A_{NS}]$. This leaves $[NS; > 0{,}8 \text{ Hz}; NS; NS; A_{NS}]$ as the actuation entry into the vector.

Surface [SUR] and Substructure [SUB] - Neither of these entries is specified at this point in the design, there are however certain potential entries which are disqualified due to the operating conditions for the morphing centreboard. The list of potential parameters for the surface and substructure according to Vasista *et al.* (2012) is given in Table 2.4. It can be concluded that the incompressibility of water as well as the nature of the desired shape change excludes rollable materials since we are not looking at *deployable* concepts. Stretchable materials are also unlikely candidates for the final solution as they inherently lack any out of plane stiffness which would be required to some extent for operation in water. For now the entry remains $[Su_{NS}; Sk_{NS}]$.

Operating Conditions [OPR] - Since the operating conditions deal with a fluid dynamic case the Reynolds number will be used to describe the operating conditions, this simply leads to the entry $[Re; 0{,}75 - 1 \times e^6]$.

The full description vector for the morphing centreboard is now presented as:

[9] An ideal design however will have purely passive actuation since this would fall within the 505 class rules Adherence to the class rules was however excluded from the scope early in the project since the design presented here is a preliminary proof of concept as well as a test case for the design toolbox.

$$\left[\begin{bmatrix} FD,\ MECH \\ SUS-ENT \end{bmatrix}\begin{bmatrix} AoA & 0^\circ \\ C_l & 0{,}4719 \end{bmatrix}\begin{bmatrix} AoA & -0{,}991 \\ C_d & -0{,}108 \end{bmatrix}\begin{bmatrix} c_r & 0{,}3\ m \\ camber & 0{,}4 \end{bmatrix}\begin{bmatrix} DZ \\ RY \end{bmatrix}\begin{bmatrix} NS \\ > 0{,}8\ Hz \\ NS \\ NS \\ A_{NS} \end{bmatrix}[Su_{NS}][Sk_{NS}][Re1e^6]\right]$$

4.3.1.2 Application

Potential candidate technologies or solutions for the actuation method, surface and substructure of the morphing centreboard are now found by filtering the existing morphing description vector database by the morphing effect and physical description. The database of description vectors created in Chapter 3 [10] is filtered successively by:

1. Design target. This category is consulted initially to determine whether any existing technology or research has the same design targets as the current design. This step is more of a check than a filtering step as technologies with other design targets may still meet the requirements or specifications of the specific case.

2. Axis Influenced, only concepts which include shape change along at least one of the axes influenced in the morphing centreboard shape change, $[DZ]$ and/or $[RY]$. This will automatically include all of the camber change concepts but also concepts which aim to change particular properties of the airfoil shape such as thickness.

3. Physical description

   (a) *Camber* in the degree of shape change entry, only camber change is relevant to this design. Camber change along the same order of magnitude is also enforced, $\approx 45 \times e^{-1}$.

   (b) A scale entry in the same order of magnitude as the morphing centreboard, 3×10^{-1} m

The first three filtering steps ensure the morphing entries that remain meet the physical requirements for the morphing centreboard. These entries are further filtered by their fluid dynamic properties:

4. Entries are filtered by morphing effect requiring a decrease in AoA, which may also be expressed as an increase in C_l at a set AoA. The C_l increase from NACA 0010 to NACA 4410 at zero AoA is 0.4719. Entries are further

[10] The database contains around 200 entries in an excel spreadsheet format, it is envisioned that this database may be made into a live online repository available to researchers to use in guiding new morphing designs.

filtered by a decrease in C_d. All of these parameters result in an increase of L/D. Since this is a preliminary design any decrease in AoA and C_d or increase on C_l at a set AoA is accepted. [11]

5. The operating conditions also provide a parameter to filter entries by. Candidate entries should have a Re in the similar order of magnitude as expected by the morphing foil, around e^6.

Some of the entries in the database have previously been considered morphing technology but, according to the classification scheme proposed here, fall outside of the class of morphing technologies, the meta-data for these entries is included in the database however they do not have a description vector. This excludes 38 entries. There are no entries which perfectly match the design targets of the morphing centreboard so the filtering begins at step 2. After filtering for the axes influenced, 78 morphing concepts remain, all of these concepts have at least a translational component in the Z axis or a rotational component about the Y axis. From here entries are filtered as per step 3(a) into camber morphing only, 57 entries remain. There are many camber morphing concepts which focus solely on leading or trailing edge shape change, although not exactly what is envisioned for the morphing centreboard design it is assumed that many of their technologies may be extrapolated into camber change of the entire foil. The scale category is now used to filter concepts leaving 29 entries. All of these 29 concepts should be able to achieve the physical parameters required by the morphing centreboard and will be further filtered according to the fluid dynamic parameters. Quite a number of concepts are excluded based on high Reynolds number design conditions, leaving 15 entries, this is due to the fact that much of the existing research is centred around high speed aerodynamic applications. The restrictions on actuation load and frequency are now imposed on the remaining entries. It must be noted that almost all of the SMA concepts are excluded at this step because of their inherently low actuation frequency. This is due to the relatively low thermal conductivity properties of air, for which they are all designed. Water as an operating fluid has a far higher thermal conductivity and it is hypothesised that SMA's may realise higher actuation frequencies in hydrodynamic applications. This analysis is outside of the scope of this research but is a promising field for further research. 12 entries, 3 of them patents, pass through all of the criteria, these include Kiceniuk (1964); Dorfman *et al.* (1978); Eggleston *et al.* (2002); Cadogan *et al.* (2004); Cooper (2006); Diaconu *et al.* (2008); Daynes *et al.* (2009); Peel *et al.* (2009); Viresh *et al.* (2009); Kota *et al.* (2013); Wigley (2018). The patents are given leeway to pass through certain filtering steps such as scale and operating condi-

[11] At a later stage in the design process entries may be filtered more stringently by their morphing effect.

tions since they often present conceptual designs without many design specifics. These concepts are however useful in providing initial concepts for the design of the morphing centreboard. Appendix B shows the results of the filtering on the populated research table. Each of the entries is sorted according to the Vasista *et al.* (2012) criteria for actuation, sub-structure and surface in the ACT, SUB and SUR categories in the description vector. This sorting provides an indication of the manner in which all of the appropriate concepts physically achieve their morphing.

Actuation - 9 concepts use conventional actuators, Kiceniuk (1964); Dorfman *et al.* (1978); Eggleston *et al.* (2002); Cooper (2006); Diaconu *et al.* (2008); Daynes *et al.* (2009); Kota *et al.* (2013); Wigley (2018), and 4 use smart material based actuators, Eggleston *et al.* (2002); Cadogan *et al.* (2004); Peel *et al.* (2009); Viresh *et al.* (2009). The conventional actuator concepts include linear, Dorfman *et al.* (1978); Kota *et al.* (2013); Wigley (2018), and rotational, Eggleston *et al.* (2002); Cooper (2006); Wigley (2018), mechanical actuators using mechanical mechanisms to drive the morphing. Also included are bistable or multistable composites, Diaconu *et al.* (2008); Daynes *et al.* (2009), whose stable shapes are achieved through conventional actuation. A single hydraulically actuated, Kiceniuk (1964), and a single pneumatically actuated, Peel *et al.* (2009), concept are also included. The smart material based actuator concepts primarily make use of PZT, Eggleston *et al.* (2002); Cadogan *et al.* (2004); Viresh *et al.* (2009), also included are a single SMA actuator, Eggleston *et al.* (2002), and an electro-active polymer (EAP) skin actuator, Viresh *et al.* (2009). Cadogan *et al.* (2004) and Peel *et al.* (2009) also provide informatin on nastric structures for bending and linear actuation respectively. Conventional linear actuators and bending piezoelectric actuators make up the majority of the concepts and are chosen for further investigation for application to the morphing centreboard. These actuators either drive mechanical mechanisms or multistable composites to achieve morphing.

Surface: All of the concepts' surfaces, bar one, Viresh *et al.* (2009), use a form of compliant materials to cover and conform to the morphing of the substructure. Two of these concepts, Diaconu *et al.* (2008); Daynes *et al.* (2009), using multistable composites within the actuation subsystem, have composite surfaces which rely on tailored stiffness or stiffness change within the surface in order to achieve the morphed shapes. There are two concepts, Cadogan *et al.* (2004); Viresh *et al.* (2009), which use active surfaces through the implementation of PZT's and EAP's respectively, which are also involved in the actuation. Compliant materials are the preferred solution for a morphing foil surface and are investigated further.

Substructure: The most variation among filtered concepts is found in their

substructure. 5 concepts utilise some form of conventional mechanism as a morphing substructure, Dorfman *et al.* (1978); Eggleston *et al.* (2002); Cooper (2006); Kota *et al.* (2013); Wigley (2018) . In most cases these concepts make use of a classic wing spar or wing box to carry structural, spanwise loads and a number of ribs along the span to enforce the shape of the foil profile. Cooper (2006) makes use of conventional mechanisms in order to change the stiffness of the foil and achieve aeroelastic morphing. This is similar in concept to the multi-stable composite substructures, Diaconu *et al.* (2008); Daynes *et al.* (2009), which blur the line between substructure and actuator, making use of tailored material stiffness to both carry load and enforce shape change while being considered compliant mechanisms. Eggleston *et al.* (2002); Viresh *et al.* (2009) also make use of compliant mechanisms in their substructure, both relying on pre-made PZT laminated materials capable of carrying both in and out of plane load and actuating in the form of out of plane bending. There are two concepts which make use of inflatable segments as substructure, Kiceniuk (1964) utilises hydraulic pressure to both support the structure and actuate the shape change while Cadogan *et al.* (2004) simply uses inflatable segments as the structure of the foil. Conventional mechanisms often provide the easiest solution to a morphing foil substructure and will be investigated further. Compliant mechanisms, particularly multi-stable composites and PZT laminates which provide both structure and actuation in the form of bending also have promise for the morphing centreboard application.

4.3.2 Structural Investigation and Application

4.3.2.1 Outline

To complete the design conceptualisation process and further filter the concepts presented in **??** three simplified 2D FEM simulations are conducted on the potential enabling technologies for the morphing centreboard. The aim of the simulations is to develop representative FEM models of the broad approaches to the surface, substructure and actuation and extract variables which will provide insight into the applicability of each approach. The models are all actuated using the known unmorphed and morphed foil surface shapes shown in Figure 4.10.

Certain limitations and scope exclusions are enforced on the FEM simulations according to the guidelines presented in section 1.6. Aerodynamic or aeroelastic loads are not considered in the simulation. No pressure gradient over foil or representative aerodynamic load is included in the boundary conditions. Only the loads involved in the planar, 2D morphing of a profile section of the foil are considered. The investigation is focused on how shape change occurs throughout profile by

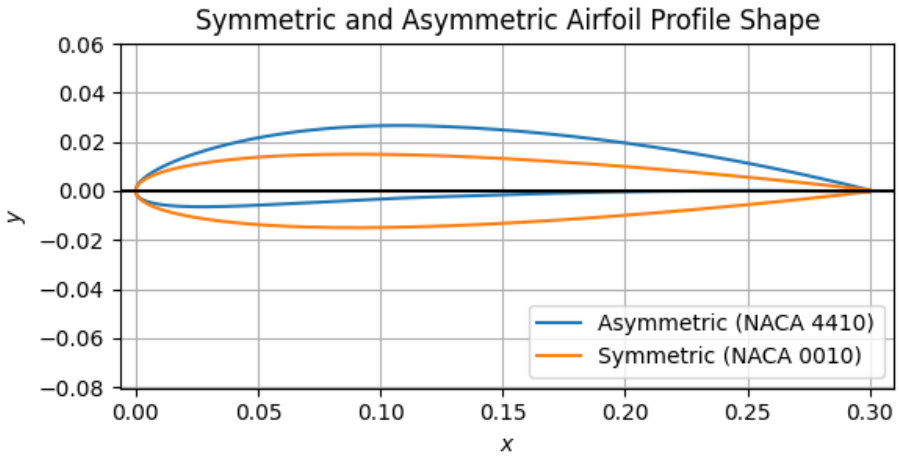

Figure 4.10: NACA 0010 and NACA 4410 Profile Shapes

enforcing displacement of the surface, the resulting stresses and strains on the surface and chosen representative internal structure are the desired outcomes. The surface, substructure and actuation members are, in each case, modelled using one-dimensional elements. Two dimensional surface elements were considered and preliminary models with 2D elements were tested, however 2D mesh cells as representations of the profile and internal structure lead to overly specific geometries in the FEM simulation. The aim of the simulation is to keep each model as generalised as possible with it's representation of the relevant morphing solution. This informs the design as to the type of morphing solution rather than the specific technology.

The french open source FEM solver *Code-Aster* is used together with *Salome*, a pre and post processor for code aster. The Salome-Meca software package includes both Salome and Code-Aster and is run on Linux for the all of FEM simulations completed here. Aubry (2013) provides a comprehensive resource on the utilisation of Salome and Code Aster. Due to the limitations of the Salome GUI when running automated simulations with complicated boundary conditions, the ASTK package is run through the command line via python in order to run the Code-Aster simulations. ASTK collects input files for Code-Aster including the command, mesh and output files, all written in the Code-Aster syntax. This allows automation, data manipulation and management through Python as well as creating a direct pipeline from XFoil, which is also run through the command line, to the Salome geometry and meshing module, GEOM and SMESH. Appendix D provides some simplified code sections for the first model, illustrating the Code-Aster command file. All of the code is written in a generalised manner allowing parameters, such as

morphed and unmorped shapes, mesh particulars, boundary conditions and results to be changed without affecting the stability of the code.

4.3.2.2 Simulation Particulars

The simulation process runs as follows[12]:

1. The algebraic equations for the morphing centreboard operating conditions and specifications are solved in Python and passed to XFoil,
2. 2D NACA profile geometry is generated in XFoil and passed to back to Python.
3. The displacement required at each node is calculated from the unmorphed and target morphed shape and is later used as an enforced displacement boundary condition in the FEM simulation.
4. The geometry is passed to Salome and manipulated as required through the Salome GEOM module and meshed in the SMESH module.
5. An external command file, (COMM) is written containing all of the FEM simulation parameters in the Code-Aster syntax. See section D
6. The mesh and command files are passed to ASTK which is run through the command line via Python.
7. ASTK runs the FEM solver, Code-Aster, and passes the results back to Python.
8. The results are interpreted in Python and where necessary post-processed in the ParaVis module of Salome.

Geometry - A .csv file containing the nodal coordinates of the unmorphed geometry, NACA 0010, with a chord length of 0.3 m is used as the initial geometry. Geometry groups for the leading and trailing edge nodes as well as the surface nodes and edges are created. See section D for the basic implementation.

Mesh - A one-dimensional mesh is generated using the nodal coordinates from XFoil as the mesh nodes. The number of segments between each node is changed for the mesh refinement study presented in section 4.3.2. The nodal coordinates generated by the panel mesh in XFoil are found to be appropriate as a starting point for the FEM meshing. This carry over from XFoil is useful as the meshing

[12]The simulation particulars are outlined in the following paragraphs, for the exact implementation of each parameter consult the code in section D

algorithm in XFoil already refines the mesh in areas of high curvature, allowing the meshing in SMESH to simply define requirement for number of elements between nodes.

Models - The solver is set to a linear static, mechanical case. Straight 1D Timoshenko beam or simple bar elements are used to model the mesh. The material properties and element cross sections are varied in each of the simulations. Appendix D shows the command file for Code-Aster which contains the model, boundary conditions and results parameter implementation. The Eularian beam model was tested and found to introduce additional stiffness in the surface, particularly in the nose of the profile. This is due to the fact that the elements in that area, due to the high curvature of the geometry they are representing, in some cases have a L/t ratio of less than 10 leading the the assumptions made in the Euler beam model being inappropriate, (Labuschagne *et al.*, 2009). [13]

Boundary Conditions - A Python function within the Code-Aster command file creates and enforces nodal displacements along the profile boundary based on the difference between the unmorphed and morphed shapes. The leading edge node is fixed in the remaining rotational and translational degrees of freedom to fully constrain the model. Enforced displacement boundary conditions are chosen over using forces to yield displacement since the required shape change is considered an independent variable of the design while the forces involved are dependent variables.

Results - The required result types are selected in each model simulation. The displacements are enforced and the corresponding strains automatically calculated.

4.3.2.3 Mesh Refinement

A basic mesh refinement study is conducted to ensure the size of the elements being used is appropriate. The study is run on the first model which is further expanded upon in the following subsection. The mesh is initially made as coarse as possible and refined increasing the number of elements per node in successive simulation runs. The results of the stress components and nodal forces at each

[13] The assumption of Euler-Bernoulli beams, that the cross section remains in plane, disregards shear deformation effects. In elements with lower L/t ratios or with high shear, such as in the nose of the morphing profile, the assumption leads to inaccurate stress concentrations, thus the Timoshenko beam theory is used. Timoshenko beam theory accounts for the rotation of the cross section with respect to the neutral axis, including shear deformation in an additional equation of motion and is considered accurate, according to Labuschagne *et al.* (2009), even in slender beams.

node are recorded and the mesh is considered sufficiently refined when the absolute maximum error between successive refinements reaches less than $1e-6$. Table 4.6 gives an outline of the results from the mesh refinement study. Since the mesh nodes for both the unmorphed and morphed shapes are created and carried over from XFoil, the displacement boundary conditions are generated according to the XFoil nodes. This forces the mesh used for the FEM to be at least as fine as the XFoil mesh (162 elements) since the displacements can only be enforced at a node and not an arbitrary position along the beam element.

Table 4.6: Mesh Refinement Study Results

Run	Number of Beam Elements	Max Absolute Difference from Previous Run
1	162	(Spurious stress concentration)
2	324	$2e^{6}$ (No stress concentrations)
3	486	$6e^{-5}$
4	648	$2e^{-5}$
5	810	$2e^{-6}$
6	972	$-1e^{-6}$

Using five elements between each of the nodes exported by XFoil provides the required level of mesh refinement and will be used in all of the simulations. The element lengths range from 0.0065 mm to 0.95 mm with 810 elements in total for model 1.

4.3.2.4 Model 1: Surface

The first model is the most simplified, it makes use of one dimensional beam elements to represent only the surface of the foil. This model is used in order to determine the strain in the surface and the results provide insight into the type of compliant surface materials which may be applicable. It is found that the surface strains required limit the use of the active surfaces proposed in **??**. Additionally this model is used as the basis for the mesh refinement study in section 4.3.2 and is used to check that the boundary conditions are correctly implemented from XFoil, through Python, onto the mesh in Code-Aster. The strain values analysed in this section correspond to the axial strain values of the beam elements which represent in plane strain values of the surface.

A simple analytical strain calculation is done in python by dividing the relative displacement between nodes (from the unmorphed to morphed shapes) by the initial distance between the nodes along the surface of the profile. The maximum absolute stain value is found to be 0,5180. This agrees with the maximum

displacement strain value found in FEM of 0,5135. In both cases the maximum strain comes from elongation of elements localised on the top surface near the LE as shown in Figure 4.11.

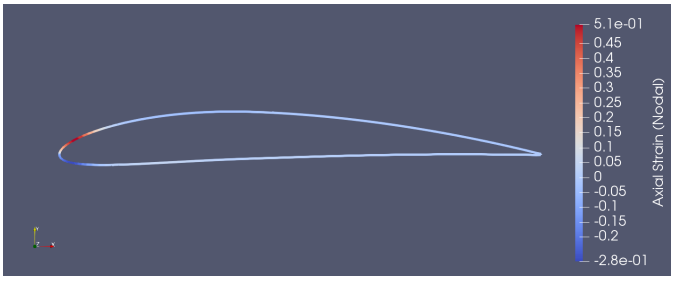

Figure 4.11: In Plane Edge Strain

This localisation of the area of maximum strain is partly due to the nature of the shape change and partly due to the assumption made in how the surface will be morphed. From analysis of Figure 4.12 [14], the nose of the profile undergoes the largest shape change in the morphing, the top section of the nose elongates and increases in curvature, becoming more convex. In contrast, the lower section of the nose must contract while changing from a convex shape to a concave shape. As one moves along the surfaces towards the trailing edge a more constant strain is encountered. After the point of maximum camber, 30 % along the chord, the lower surface undergoes an increase in curvature from the unmorphed to the morphed shape, yielding positive strain values, while the top surface undergoes little change in curvature near the tail, and consequently near zero values for strain.

Further, the way in which the morphing is enforced, by nodal displacements with the leading edge node fixed in translation, forces the nose of the foil in particular to change shape. In contrast, if the skin is given an axial degree of freedom and the shape change is not forced on a particular segment of the shin (i.e. the skin can *slide* from high to low strain areas) the surface strain values will be lower. This is particularly true in the nose of the profile where there is an area of large negative strain near an area of large positive strain. The assumption of fixed nodal displacements of the surface is applicable for morphing solutions where the surface is rigidly attached or integrated into the substructure. For morphing solutions where the surface is allowed to slide over an underlying substructure the assumptions made in the simulation will overestimate the amount of surface strain. If the areas of maximum strain concentration are excluded the strains required after the point of maximum camber are in the order of $0 - 0{,}05$, 10 % lower than the

[14] Areas of large gradients in the displacement values of nodes will yield areas of high stress, while areas of constant displacement yield lower stress values.

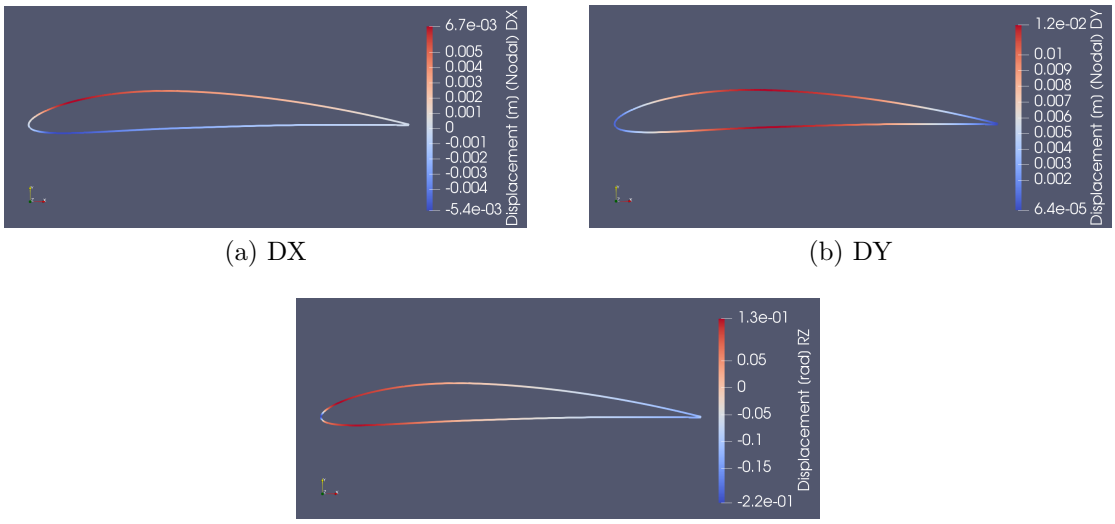

(a) DX

(b) DY

(c) RZ

Figure 4.12: Displacements of the Nodes on the Surface of the Profile

maximum. This finding informs why many many morphing concepts employ a *segmented* approach, where only the trailing edge or a segment of the tail of the profile are involved in the morphing and a rigid, symmetric leading edge either remains constant or is rotated about a point on the chord line. The total length of the edges representing the surface of the profile are 0.6093 m and 0.6117 m for the NACA 0010 and 4410 profiles (with a chord length of 0.3 m respectively. This yields a total, overall surface strain of 0,0039, this is a relatively small strain, representing an overall increase in length of less than a percent, well within the capability of all materials considered in **??**.

Due to the underlying assumptions leading to the high strain areas in the surface, the choice of surface for the morphing centreboard design depends on the choice of substructure. If a substructure is chosen which forces the nose of the foil to change shape only materials capable of strain values in the region of 0,5 are appropriate. If the substructure allows some translation of the surface material in plane then a maximum design strain value of 0,05 are considered. Latex and elastomer based materials often have elastic strain limits well into the hundreds of percent strain (Bhattacharyya *et al.*, 2008), therefore the surface material used by Eggleston *et al.* (2002) and Viresh *et al.* (2009) will easily achieve the strain requirements. Low density polyethylenes, such as those used for the surface by Cooper (2006) and Peel *et al.* (2009) have a elastic strain limit in the range of 40 %, (Jordan *et al.*, 2016) when blended with certain elastomers. These surface materials

have potential applicability to the morphing centreboard depending on the nature of the substructure. Diaconu *et al.* (2008); Peel *et al.* (2009) and Daynes *et al.* (2009) all use laminated composites as the surface materials for their morphing concepts and both have a total laminate thickness of around 1 mm. Typical fibre reinforced polymers have ultimate strain values between 0,5 % (for high modulus carbon fibres) to around 4,5 % for some Aramid fibre reinforced polymers (Prince Lund Engineering PLC, 2020). Fibre reinforced laminated composites have the lowest workable strain properties but, depending of the substructure, could be applied at least partially to the surface of the morphing foil.

Due to the localised areas of high strain in the surface together with the large majority of the surface experiencing strain less than 5 % a segmented surface approach is a good candidate for a solution. This *segmented* surface will use a flexible elastomer over a substructure on the nose of the profile. The rest of the surface will be made of material with higher out of plane stiffness, such as a composite. This is particularly important in the hydrodynamic case due to the incompressibility and consequent increased normal force on the surface stemming from the pressure distribution over the profile. The fluid dynamic loads are not included in the FEM simulation as this is considered out of scope, however the implications of operating in water are taken into account in the selection of surface material.

4.3.2.5 Model 2: Substructure (Compliant Mechanism), Actuation (Bending)

The second model represents the concepts which make use of compliant mechanisms within their substructure, more specifically central chordwise members which undergo a bending deformation during actuation. It consists of a surface and a central member, connected to the surface at the leading and trailing edges and at a number of stations along the profile. The connections between the central member and the surface are modelled as bar elements which do not transfer any moments, only axial forces, between the surface and the central member. The connecting elements are given a high elastic modulus relative to the rest of the structure (200 GPa equivalent to steel) since their purpose is to transfer movement between the central actuating structure and the surface of the foil. The surface for this model is assumed to be made of a thin flexible skin (latex or elastomer as used by Eggleston *et al.* (2002) and Viresh *et al.* (2009)), these materials have elastic modulii in the range of MPa rather than GPa, the skin is modelled with $E = 1,2$ MPa, a typical value for latex. The section properties for the edge beam elements represent the span, 1450 mm and the skin thickness, 1 mm in the relavent element axes. The central member representing the compliant bending actuator is modelled as

a composite plate with similar properties to those of Diaconu *et al.* (2008) and Daynes *et al.* (2009). No effort is made to model the bistable nature of the plate, rather the displacement and bending moment results from the simulation will inform the viability of this solution. The central member is set to have a elastic modulus of 100 GPa, a representative value for different fibre reinforced polymers (Prince Lund Engineering PLC, 2020). The thickness is set to 2 mm, in line with the specifications of Diaconu *et al.* (2008) and Daynes *et al.* (2009).

Figure 4.14 show the nodal forces in the central member, the results from the surface and connecting elements are not shown as they are not of interest in this model. The central member undergoes a large bending deflection with little axial deflection, this results in maximum absolute bending moments of 300 Nm and small normal forces, less than 3 N at any point on the element. The maximum bending moment occurs at the point of maximum curvature, where the first connecting element meets the central member. The small positive bending moments, <0.016 Nm, at the leading and trailing edges are caused by the fact that the central member is considered to have a fixed connection to the surface at these points. This assumption is considered valid in this case since this type of connection will aid in the function of such a central bending actuator and does not result in erroneous results in the model.

The bending moment results in Figure 4.14 show the force required to deflect the central member to the required shape. Figure 4.13 shows the rotational deflection necessary along the central member from -0.096 rad to 0.02 rad, a total deflection of 6,5°. The idea being that in application with the substructure shown, the central member will be deflected according to the simulation results and consequently the surface will deflect from the unmorphed to the morphed shape. If one was to use conventional means of bending the central member a bending moment of 300 Nm would need to be produced and sustained as long as the morphed shape must be held. Multistable composites are capable of reaching the required deflection [15] and require bending moments in the range of 10^1 Nm, (Diaconu *et al.*, 2008), to trigger their snap through behaviour. Traditional actuators or smart material actuators such as EAPs, (Viresh *et al.*, 2009), or macro fibre composite PZT actuators, (Eggleston *et al.*, 2002; Cadogan *et al.*, 2004; Viresh *et al.*, 2009), can be used to trigger the snap through effect as they have actuation bending moments in the appropriate range. A multistable composite central member will also provide much of the structural requirements of the foil while significantly reducing the actuation requirement. Further investigation is necessary on the central multistable composite bending concept as the fluid dynamic loads have not been taken into

[15] Diaconu *et al.* (2008) reach a deflection of 8°, Daynes *et al.* (2009) reach a deflection of 10°

account in the actuation force requirements, this would be done by including the XFoil pressure distribution into the FEM boundary conditions. [16]

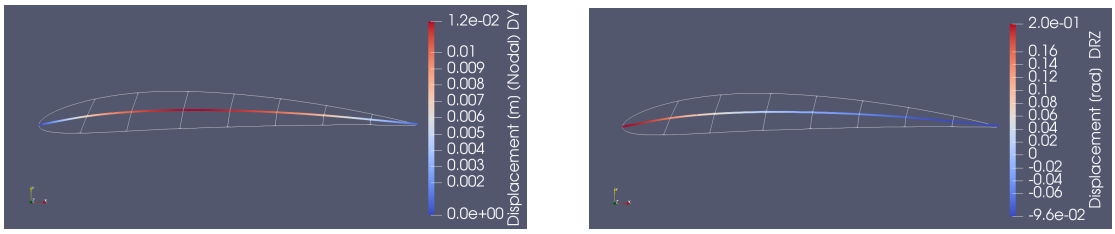

(a) DY (b) RZ

Figure 4.13: Deflection of the Central Member

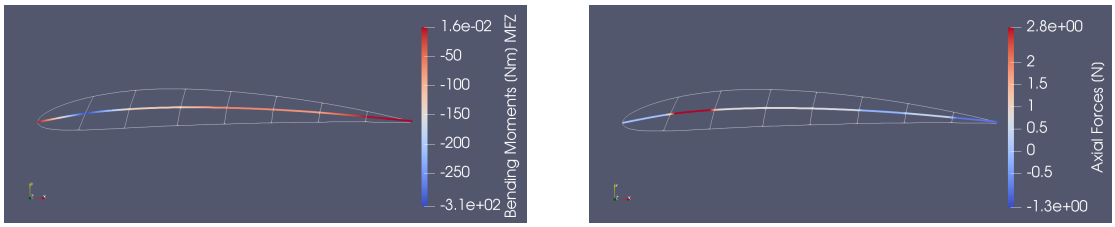

(a) Bending Moments (b) Normal Forces

Figure 4.14: Nodal Forces on the Central Member

A multistable composite central member with three stable positions [17] is envisioned as a possible solution to the substructural subsystem of the morphing centreboard. This multistable plate will either be actuated passively, by the pressure distribution over the profile, or actively by an integrated smart material actuator such as an EAP or PZT laminated composite actuator.

4.3.2.6 Model 3: Substructure (Conventional Mechanism), Actuation (Conventional Linear)

The third model once again makes use of 1D beam elements, however a simple conventional truss like substructure as well as linear actuator elements are included

[16] It is envisioned that the force required to actuate the multistable plate may come from the flow and consequent pressure distribution over the profile. This is outside of the scope of this study but is envisioned as the next point of investigation.

[17] A flat plate would yield a symmetric, uncambered foil, while a bent plate will yield positive and negatively cambered profiles

internally. This model is based on that of Parker (1920) as it represents the underlying concept behind a wide variety of more modern morphing concepts making use of linear actuators driving conventional mechanisms to achieve morphing. In this model both the structural requirements of a conventional substructure and the stroke and force requirements of the linear actuators are determined for the 2D profile. Enforced displacement boundary conditions actuate the surface of the model and the strains in the actuation elements as well as their nodal reaction forces are used in order to determine the actuator stroke and force requirements. The idea being that if actuators are able to produce the stroke and force requirements at between their connection points the unmorphed foil profile will be morphed to the final shape. In this model only the actuating elements which act in tension for a one way camber change are included, this is considered valid since it is assumed that the design will not make use of an antagonistic actuation mechanism and the inactive actuating members will be free to extend.

The surface and connecting elements are modeled as in model 2 with the same physical properties. In this case the central member is modelled using bar elements with nodes at the junctions of the connecting elements running to the surface. Linear actuation elements are added which run diagonally between the surface and the central junctions, they are orientated in such a way that under actuation they will contract linearly causing the morphing shape change. These elements are modelled as bar elements and given zero stiffness since their presence should not interfere in the nodal force results at their connection points. The elements are included in the model in order to generate strain results as well as normal directions for each actuating member and illustrate the location and orientation of the envisioned linear actuators.

Figure 4.15 shows the strain within the actuation members these strain results are saved in a tabular format together with the actuation element node coordinates and the actuator stroke for each is calculated. All of the strains are negative, indicating shortening of the members, for some elements the strain values are near zero, this is due to the shape change between the upper and lower skin being minimal during morphing. The tail mostly maintains its shape and rotates slightly about the Z-axis from the unmorphed to the morphed shapes. This result again informs why many morphing technologies utilise rotating segments on the trailing edge of the foil in order to achieve camber change. The maximum actuator stroke required is 2,6 mm on an actuator of 44 mm in length, this correlates to the maximum strain shown in the figure of 6 %. This is well within the requirements of conventional actuators such as micro electric or hydraulic linear actuators. The *nastic* actuators used in Peel *et al.* (2009) achieve strains of 6,7 % while the *Nitionl*

SMA actuators from Eggleston *et al.* (2002) achieve strains of 8 %, both achieve the strain required and have the added advantage of being easily integrated into the structure due to their adaptability to many different size actuators.

Figure 4.15 shows the nodal reaction force vectors at the connection points of the actuation elements. The force vectors and the actuation element coordinates are output in a tabular form and the resulting component of the forces acting along the axes of the actuation elements is calculated. The maximum nodal force is 2008,5 N [18] acting vertically, this equates to a maximum actuator force of 684 N. The highest actuation force is found at the node with the highest change in surface curvature. The average actuator force is found to be 127 N. It should be noted that the rest of the forces are resolved within the structure, the results of which are not shown in the figure.

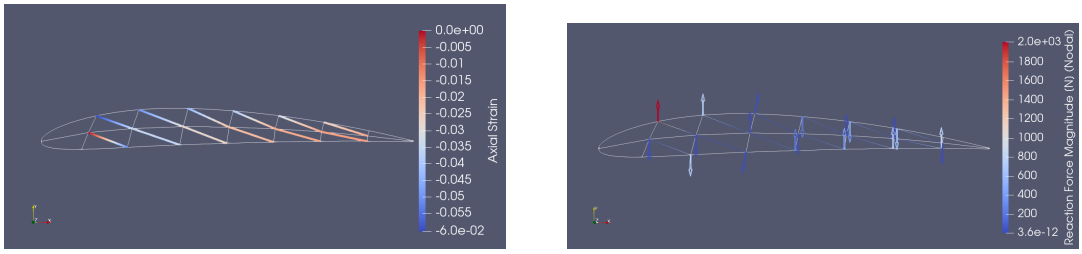

(a) Axial Strain on Actuator Elements

(b) Nodal Reaction Forces on Actuator Elements

Figure 4.15: Results of Simulation of Model 3

A range of micro linear electric actuators can be found from various suppliers, such as Actuonix Motion Devices Inc. (2020), with actuation forces ranging from 10 N up, similarly other conventional linear actuators of the required specification can be found. Most of the *nastic* linear actuators tested by Peel *et al.* (2009) are able to reach peak actuation loads of around 890 N. SMA wires, despite their issues with low actuation frequency, are able to achieve actuation forces of 550 N, with SMA ribbons producing significantly more force, around 8000 N according to Barbarino *et al.* (2009). Although the model used here is simplistic it is able to provide an operational range required for linear actuators for a morphing centreboard. The main constraint, however is not the actuator performance properties but rather the physical size limitations within the morphing foil shell. Further investigation is necessary on the model and concept presented here.

[18] This force is quite high when compared to similar concepts in literature, such as Peel *et al.* (2009). This comes from the nature of the substructure being stiff due to the large number of stiff connecting elements.

4.3.2.7 Results

Following the results and discussion within the structural investigation on the most appropriate technologies from **??**, a proposal is made for the most appropriate conceptual design of a morphing centreboard profile, the details of which are shown in Table 4.7. It is envisioned that this result will be the starting point of further study on the concept of a morphing centreboard for a high performance sailing dinghy.

Table 4.7: Morphing Centreboard Concepts from FEM

Sub-system	**Concepts**	**Descriptor**	**Reference**
Surface	Segmented Approach (High strain elastomer nose together with flexible composite tail)	Sk_1	(Peel *et al.*, 2009)
Actuation	Bistable Composite (Either actively actuated by a nastic or PZT smart material actuator or passively actuated by the flow)	$A_{1,2,6,10}$	(Diaconu *et al.*, 2008; Daynes *et al.*, 2009)
Sub-structure	Central structural member with conventional supporting structure	$Su_{1,8,9}$	(Cooper, 2006; Diaconu *et al.*, 2008; Daynes *et al.*, 2009; Wigley, 2018)

Chapter 5

Conclusions and Recommendations

The objectives outlined in section 1.4 are shown to be achieved in the project and in the following chapter, subject to the limitations imposed on the scope in section 1.6. The idea of increasing a high performance sailing dinghies performance through changing the shape of the centreboard is shown to be valid by increasing the C_{L0} of the centerboard leeway is reduced or eliminated and VMG is improved. Morphing is found to be an appropriate method for achieving the shape change. The issues with the existing field of literature are addressed in the design toolbox and the final morphing centreboard concept is generated.

In conclusion, the objectives (1) - (4) in section 1.4 are all met in the Thesis and a number of recommendations for future study are made. Objectives (1) - (3) are met with the successful formulation of the design toolbox, outlined in Chapter 3. The toolbox is built upon the in depth meta-analysis (Chapter 2) of the field of morphing as it currently stands and adopts concepts on which there is absolute consensus, adapts concepts with little consensus and proposes a number of novel concepts where necessary. It outlines a lexicon which is discussed as a continuing theme throughout the meta-analysis and the key terms of the morphing lexicon as they pertain to foil morphing for fluid dynamic applications are outlined in table 3.1. A classification scheme is proposed which provides explicit, clear methodology that defines what constitutes morphing technology. A refined classification for foil morphing within the field of fluid dynamics specifically is presented. Other branches of the scheme may be refined for use in different fields of morphing applications. The toolbox proposes a categorisation scheme which is applied existing research within the field of foil morphing for fluid dynamic applications.The categorisation scheme does not explicitly limit its application to this field alone, however requires further validation to prove its ubiquity. Its utility

for the specific case is demonstrated by its ability to categorise a large range of existing morphing research and consequently be used as an effective design tool through selective filtering and searching of the populated description vectors. A live repository of the populated research table is envisioned to be the next step in making the toolbox available and useful to researchers in the field. In addition to the current toolbox it is envisioned that the underlying structure may be applied to the broader field of morphing, outside of fluid dynamics. The toolbox provides a, previously non existent, explicit method to define technology or research as *morphing*, further it builds on existing, ambiguous methods of categorisation within the field by proposing the description vector whereby morphing concepts may be directly compared over a number of metrics.

Objective (4) is met with the initial conceptual design for the profile of a morphing centreboard of a high performance 505 sailing dinghy, presented in Table 4.7, consisting of a segmented surface material approach and a multistable composite bending actuator which forms an integral part of the substructure of the foil. This conceptualisation reached through application of the design toolbox (**??**) and preliminary fluid dynamic and structural investigation in subsection 4.2.2 and subsection 4.3.2 respectively. Both the concept and the design process followed serves as a test case for validation of the utility of the morphing design toolbox within the specific field. The preliminary, un-validated design is considered sufficient as a proof of concept and further, the concept provides a *jumping off point* for future investigation and detailed design of the morphing centreboard including more specific, sophisticated FEM and CFD analysis and validation as well as physical testing as per the limitations set out for the scope of this project.

The process outlined in section 4.3 is successful in utilising the design toolbox to inform the conceptualisation of a morphing centreboard. This design falls well within the field of foil morphing for fluid dynamic applications and, as a successful test case, motivates the utility of the toolbox for other cases within this field. The ubiquity of the toolbox is not explicitly shown as per the limitations on the scope, however, since the process of developing the toolbox is clearly outlined and field specific concepts are avoided in favour of generalised descriptors it is envisioned that the toolbox may be applied to other applications of morphing.

The toolbox is created in such a way that it flows first from the adoption of *morphing lexicon* to the classification of technology as within or outside the scope of *foil morphing* and then to the categorisation of *foil morphing technologies for fluid dynamic applications*. It is set up in such a way that earlier steps are more universal and consequent steps are more project specific. Although effort was made

to make all steps in general universally applicable, it is left up to others to add to the work, adopting the same methodology or framework of the toolbox, where different field specific details are needed.

A number of specific recommendations for additional future work are made:

- The preliminary design for a morphing centreboard can be assumed to be in the proof of concept phase and can thus be seen as a basis for further study. Validation of the initial design, further refinement and physical testing are seen as natural progressions.
- Different foil profile shapes, such as the NACA 5 and 6 series profiles and the Eppler profiles (particularly suited to hydrofoils) can be investigated as the target morphed shape for the centreboard.
- An investigation into the actuation rate of SMAs when used in an operating fluid with a high thermal conductivity could lead to acceptable actuation frequencies for the morphing centreboard case since many of the other properties of SMAs are favorable for this application.
- The concept of passive actuation with the conceptual design presented can be investigated. This could yield a morphing centreboard which is not only effective but class legal and open to use in racing situations.
- Foil morphing for other hydrodynamic and sailing applications, such as submarines or lifting hydrofoils, can be investigated using the design toolbox and morphing centreboard conceptualisation test case as a basis.

References

505 International Class Association (2020). International 505 Sailing. Available at: https://www.int505.org/about-the-505/

Actuonix Motion Devices Inc. (2020). Actuonix. Available at: https://www.actuonix.com/category-s/1934.htm

Airfoil Tools (2020). Airfoil Tools. Available at: http://airfoiltools.com/

Anderson, B.D. (2008). The physics of sailing. Tech. Rep. 2, JILA and Department of Physics, University of Colorado, Boulder, Colorado 80309-0440, USA. arXiv: 1011.1669v3.

Aubry, J.-p. (2013). Beginning with code_aster. Available at: http://framabook.org.

Barbarino, S., Bilgen, O., Ajaj, R., Friswell, M.I. and Inman, D.J. (2011*a*). A review of morphing aircraft. *Journal of Intelligent Material Systems and Structures*, vol. 22, no. 9, pp. 823–877. ISSN 1045389X.

Barbarino, S., Pecora, R., Lecce, L., Concilio, A., Ameduri, S. and Calvi, E. (2009). A novel SMA-based concept for airfoil structural morphing. *Journal of Materials Engineering and Performance*, vol. 18, no. 5-6, pp. 696–705. ISSN 10599495.

Barbarino, S., Pecora, R., Lecce, L., Concilio, A., Ameduri, S. and De Rosa, L. (2011 jul*b*). Airfoil structural morphing based on S.M.A. actuator series: Numerical and experimental studies. *Journal of Intelligent Material Systems and Structures*, vol. 22, no. 10, pp. 987–1004. ISSN 1045389X.

Bhattacharyya, S., Sinturel, C., Bahloul, O., Saboungi, M.L., Thomas, S. and Salvetat, J.P. (2008). Improving reinforcement of natural rubber by networking of activated carbon nanotubes. *Carbon*, vol. 46, no. 7, pp. 1037–1045. ISSN 00086223.

Bonnema, K. and Smith, S.B. (1988 may). AFTI/F-111 Mission Adaptive Wing flight research program. In: *4th Flight Test Conference*. American Institute of Aeronautics and Astronautics, Reston, Virigina.

Buell Software (2019). The Solent Routing Software.
Available at: `https://www.buell-software.com/`

Cadogan, D., Smith, T., Uhelsky, F. and Mackusick, M. (2004). Morphing Inflatable Wing Development for Compact Package Unmanned Aerial Vehicles. *AIAA Journal*.

Campanile, L. and Sachau, D. (2000 mar). The Belt-Rib Concept: A Structronic Approach to Variable Camber. *Journal of Intelligent Material Systems and Structures*, vol. 11, no. 3, pp. 215–224. ISSN 1045389X.

Chen, F., Liu, L., Lan, X., Li, Q., Leng, J. and Liu, Y. (2017 may). The study on the morphing composite propeller for marine vehicle. Part I: Design and numerical analysis. *Composite Structures*, vol. 168, pp. 746–757. ISSN 02638223.

Chopra, I. (2002 nov). Review of State of Art of Smart Structures and Integrated Systems. *AIAA Journal*, vol. 40, no. 11, pp. 2145–2187. ISSN 00011452.

Chwalowski, P., Samareh, J.A., Horta, L.G., Piatak, D.J. and Mcgowan, A.-M.R. (2009). Efficient Multidisciplinary Analysis Approach for Conceptual Design of Aircraft with Large Shape Change. Tech. Rep., NASA.

Competition Composites Inc. (2020). Competition Composites Inc.
Available at: `http://cci.one/site/marine/foils-a-z/505-international/?doing{_}wp{_}cron=1603303840.06360697746276855468 75`

Cooper, J.E. (2006 oct). Adaptive Stiffness Structures for Air Vehicle Drag Reduction. *Multifunctional Structures / Integration of Sensors and Antennas*, pp. 15–1 – 15–12.

Davidovits, P. (2019 jan). Static Forces. In: *Physics in Biology and Medicine*, pp. 1–20. Elsevier.

Day, A.H. (2017 may). Performance prediction for sailing dinghies. *Ocean Engineering*, vol. 136, pp. 67–79. ISSN 00298018.

Daynes, S., Nall, S., Weaver, P.M., Potter, K.D., Margaris, P. and Mellor, P. (2009 may). On a Bistable Flap for an Airfoil. In: *AIAA/ASME/ASCE/AHS/ASC Structures, Structural Dynamics, and Materials Conference*, vol. 50. University

of Bristol, American Institute of Aeronautics and Astronautics, Palm Springs, California.

Decamp, R. and Hardy, R. (1984 aug). Mission adaptive wing advanced research concepts. In: *11th Atmospheric Flight Mechanics Conference*. American Institute of Aeronautics and Astronautics, Reston, Virigina.

Diaconu, C.G., Weaver, P.M. and Mattioni, F. (2008 jun). Concepts for morphing airfoil sections using bi-stable laminated composite structures. *Thin-Walled Structures*, vol. 46, no. 6, pp. 689–701. ISSN 02638231.

Dorfman, J.W., Nisbet Carson, D.M. and Rolston, G.A. (1978). Variable Foil Keel and Sailboat.

Drela, M. (1989). XFoil: An Analysis and Design System for Low Reynolds Number Airfoils. Tech. Rep., MIT, Cambridge, Massachusetts. `CA`.

Drela, M. and Harold, Y. (2001). XFOIL 6.9 User Primer.
Available at: `http://web.mit.edu/drela/Public/web/xfoil/`

Eggleston, G., Hutchison, C., Johnston, C., Koch, B., Wargo, G. and Williams, K. (2002). Morphing Aircraft Design Team Report. Tech. Rep., Virginia Tech.

Engineering Toolbox (2020). The Engineering Toolbox.
Available at: `https://www.engineeringtoolbox.com/sea-water-properties-d{_}840.html`

Favereau, C. (2016). SAP 505 WORLDS.
Available at: `https://www.yachtsandyachting.com/news/191367/SAP-505-Worlds-at-Weymouth-day-5`

Fossati, F. (2009). *Aero-Hydrodynamics and the Performance of Sailing Yachts: The Science Behind Sailing Yachts and Their Design*. ISBN 9781408113387.

Fowler, H.D. (1942 apr). Lift, Load and Landing. *Flight*, p. 353.

Galantai, V.P. (2010). Design and Analysis of Morphing Wing for Unmanned Aerial Vehicles. *Master of Science Thesis, University of Toronto*, pp. 1–87.

Gardiner, P. (1993). Smart Structures and Materials Systems. *Automatic Control in Aerospace 1992*, , no. 1987, pp. 127–135.

Gentry, A. (1981). A Review of Modern Sail Theory. In: *11th AIAA Symposium on the Aero/Hydrodynamics of Sailing*, April. Boeing Commercial Airplane Company.

Gerritsma, J. and Keuning, J.A. (1992). Sailing Yacht Performance in Calm Water and Waves. *12th HISWA International Symposium on Yacht Design and Construction*, pp. 233–245.

Goecke Powers, S., Webb, L.D., Friend, E.L. and Lokos, W.A. (1992). Flight test results from a supercritical mission adaptive wing with smooth variable camber. Tech. Rep., National Aeronautics anc Space Administration, Edwards, California.

Gulf Port Yacht Club (2019). Parts of the Boat.
Available at: `https://gulfportyachtclub.webs.com/PartsoftheBoat.jpg`

Hoerner, S. (1965). *Fluid-Dynamic Drag*. Bakersfield. ISBN 9993623938.

Hoerner, Sighard, F. (1985). *Fluid Dynamic Lift - Practical Information on Aerodynamic and Hydrodynamic Lift*. ISBN 9789998831636,9998831636.

hua Hu, J., wei Xu, B., fu Feng, J., Qi, D., Yang, J. and Wang, C. (2017). Research on water-exit and take-off process for Morphing Unmanned Submersible Aerial Vehicle. *China Ocean Engineering*, vol. 31, no. 2, pp. 202–209. ISSN 21918945.

Jacob, E.K. (2004). Classification and Categorization: A Difference that Makes a Difference Elin. *Library Trends*, vol. 52, no. 3, pp. 515–540.

Jha, A.K. and Kudva, J.N. (2004 jul). Morphing aircraft concepts, classifications, and challenges. In: Anderson, E.H. (ed.), *Smart Structures and Materials 2004: Industrial and Commercial Applications of Smart Structures Technologies*, vol. 5388, p. 213. International Society for Optics and Photonics. ISBN 0-8194-5305-6. ISSN 0277-786X.

Jones, R. (1941). Correction of the lifting-line theory for the effect of the chord. Tech. Rep., Langley Memorial Aeronautical Lacoratory, Washington.

Jordan, J.L., Casem, D.T., Bradley, J.M., Dwivedi, A.K., Brown, E.N. and Jordan, C.W. (2016). Mechanical Properties of Low Density Polyethylene. *Journal of Dynamic Behavior of Materials*, vol. 2, no. 4, pp. 411–420. ISSN 21997454.

Keuning, J.A. and Vermeulen, K. (2003). The transactions of the Royal Institution of Naval Architects. Part A. *International Journal of Maritime Engineering*, vol. 145, no. A2, pp. 36–60.

Keuning, J.A. and Verwerft, B. (2009). A new method for the prediction of the side force on keel and rudder of a sailing yacht based on the results of the Delft Systematic Yacht Hull Series. In: *19th Chesapeake Sailing Yacht Symposium, CSYS*, March, pp. 19–29.

Kiceniuk, T. (1964). Control and Propulsion Fluid Foil.

Knudsen, S.S. (2013). *Sail Shape Optimization with CFD*. Ph.D. thesis, DTU.

Kota, S., Osborn, R., Ervin, G., Maric, D., Flick, P. and Paul, D. (2013 nov). Mission Adaptive Compliant Wing - Design, Fabrication and Flight Test. Tech. Rep., NATO.

Labuschagne, A., van Rensburg, N.F. and van der Merwe, A.J. (2009). Comparison of linear beam theories. *Mathematical and Computer Modelling*, vol. 49, no. 1-2, pp. 20–30. ISSN 08957177.

Lagoudas, D.C., Garner, L., Rediniotis, O.K. and Wilson, N. (2014). Modeling and Experiments of the Hysteretic Response of an Active Hydrofoil Actuated by SMA Line Actuators. *Smart Structures*, pp. 153–162.

Larson, R.R. (1987 feb). AFTI/F-111 MAW Flight Control System and Redundancy Management Description. Tech. Rep., National Aeronautics and Space Administration, Edwards, California.

Lauder, G.V. and Madden, P.G. (2007 nov). Fish locomotion: Kinematics and hydrodynamics of flexible foil-like fins. *Experiments in Fluids*, vol. 43, no. 5, pp. 641–653. ISSN 07234864. `arXiv:1011.1669v3`.

Li, D., Zhao, S., Da Ronch, A., Xiang, J., Drofelnik, J., Li, Y., Zhang, L., Wu, Y., Kintscher, M., Monner, H.P., Rudenko, A., Guo, S., Yin, W., Kirn, J., Storm, S. and De Breuker, R. (2018 jun). A review of modelling and analysis of morphing wings. *Progress in Aerospace Sciences*, vol. 100, pp. 46–62. ISSN 03760421.

Mason, A.P. (2010). *Stochastic Optimisation Of Americas's Cup Class Yachts*. Ph.D. thesis, University of Tasmania.

McGowan, A.-M.R., Vicroy, D.D., Busan, R.C. and Hahn, A.S. (2009). Perspectives on Highly Adaptive or Morphing Aircraft. Tech. Rep., NASA.

Milanes Foils (2014). Milanes Foils Technical.
Available at: `http://www.milanesfoils.co.uk/technical.html`

Milgram, J.H. (1998). Fluid mechanics for sailing vessel design. *Annual Review of Fluid Mechanics*, vol. 30, no. Milgram 1996, pp. 613–653. ISSN 00664189.

Monner, H.P. (2001 oct). Realization of an optimized wing camber by using formvariable flap structures. *Aerospace Science and Technology*, vol. 5, no. 7, pp. 445–455. ISSN 12709638.

Monner, H.P., Bein, T., Hanselka, H. and Breitbach, E.J. (2000 feb). Design aspects of the adaptive wing - The elastic trailing edge and the local spoiler bump. *The Aeronautical Journal*, vol. 2454, no. 1032, pp. 89–95. ISSN 00019240.

Nam, T. and Uehara, Y. (2018). Dual-Mode vehicle with wheel rotors.

Parker, H.F. (1920). The Parker Variable Camber Wing. Tech. Rep. 77, National Advisory Committee for Aeronautics, Washington.

Peel, L.D., Mejia, J., Narvaez, B., Thompson, K. and Lingala, M. (2009 sep). Development of a Simple Morphing Wing Using Elastomeric Composites as Skins and Actuators. *Journal of Mechanical Design*, vol. 131, no. 9, p. 091003. ISSN 10500472.

Perry, B., Cole, S.R. and Miller, G.D. (1995). Summary of an active flexible wing program. *Journal of Aircraft*, vol. 32, no. 1, pp. 10–15. ISSN 00218669.

Philpott, A.B., Sullivan, R.M. and Jackson, P.S. (1993). Yacht velocity prediction using mathematical programming. Tech. Rep. 1, University of Auckland.

Pinnell & Bax (2020). Pinnell & Bax Foils.
Available at: `https://www.pinbax.com/`

Pope, A. (1951). Basic wing and airfoil theory.

Prince Lund Engineering PLC (2020). Fiber Reinforced Polymers Characteristics and Behaviors.
Available at: `https://www.princelund.com/fiber-reinforced-polymers.html`

Rodriguez, A. (2007 jan). Morphing Aircraft Technology Survey. In: *45th AIAA Aerospace Sciences Meeting and Exhibit*. American Institute of Aeronautics and Astronautics, Reston, Virigina. ISBN 978-1-62410-012-3. ISSN 03760421.

Rogers, C., Barker, D. and Jaeger, C. (1988). Introduction to Smart Materials and Structures. Proceedings of U.S. Army Research Office Workshop on Smart Materials. *Technomic Publishing Co., Inc.*, pp. 17–28.

Sailing Waters Magazine (2020). How to sail into the wind.
Available at: `https://sailingwatersmag.com/how-to-sail-into-the-wind/`

Sanders, B.P., Crowe, R. and Garcia, E. (2004). Defense Advanced Research Projects Agency – Smart Materials and Structures Demonstration Program Overview. *Journal of Intelligent Material Systems and Structures*, vol. 15, no. 4, pp. 227–233. ISSN 1045-389X.

SchoolofSailing.net (2013). Points of Sail.
Available at: `http://www.schoolofsailing.net/Images/points-of-sail.jpg`

Segelsport Jess (2020). JESS Segelsport Race Boats.
Available at: `http://www.segelsportjess.de/`

Sinapius, M., Monner, H.P., Kintscher, M. and Riemenschneider, J. (2014). DLR's morphing wing activities within the European network. In: *Procedia IUTAM*, vol. 10, pp. 416–426. ISSN 22109838.

Skillen, M.D. and Crossley, W.A. (2008 feb). Modeling and Optimization for Morphing Wing Concept Generation II Part I : Morphing Wing Modeling and Structural Sizing Techniques. Tech. Rep. February, Purdue University, West Lafayette, Indiana.

Smith, J.W., Lock, W.P. and Payne, G.A. (1992 apr). Variable-Camber Systems Integration and Operational Performance of the AFTI/F-111 Mission Adaptive Wing. Tech. Rep., National Aeronautics anc Space Administration, Edwards, California.

Smith, S.B. and Nelson, D.W. (1990 nov). Determination of the aerodynamic characteristics of the mission adaptive wing. *Journal of Aircraft*, vol. 27, no. 11, pp. 950–958. ISSN 00218669.

Sofla, A.Y., Meguid, S., Tan, K. and Yeo, W. (2010 mar). Shape morphing of aircraft wing: Status and challenges. *Materials and Design*, vol. 31, no. 3, pp. 1284–1292. ISSN 02641275. `1045389X14521700`.

Southwest Airlines (2020). The Wright Brothers Warping Wing.
Available at: `https://community.southwest.com`

Thill, C., Etches, J., Bond, I., Potter, K.D. and Weaver, P.M. (2008 mar). Morphing skins. *The Aeronautical Journal*, vol. 112, no. 1129, pp. 117–139. ISSN 00019240.

Thornton, S. (1993). Reduction of structural loads using maneuver load control on the Advanced Fighter Technology Integration (AFTI)/F-111 mission adaptive wing. Tech. Rep., National Aeronautics anc Space Administration, Edwards, California.

Van Mannen, J. and Van Oossanem, P. (1988). *Principles of Naval Architecture Vol. II - Resistance, Propulsion & Vibration*, vol. II. The Society of Naval Architechts and Marine Engineers. ISBN 0939773015.

Vasista, S., Tong, L. and Wong, K.C. (2012). Realization of Morphing Wings: A Multidisciplinary Challenge. *Journal of Aircraft*, vol. 49, no. 1, pp. 11–28. ISSN 0021-8669.

Vidmar, P. and Perkovič, M. (2013). Optimization of upwind sailing applying a canting rudder device. *Ocean Engineering*, vol. 73, pp. 55–67. ISSN 00298018.

Viresh, W., Yong, C., Marcias, M., Frank, W. and Robert, K. (2009 may). Design and Verification of a Smart Wing for an Extremely-Agile Micro-Air-Vehicle. In: *AIAA/ASME/ASCE/AHS/ASC Structures, Structural Dynamics, and Materials Conference*, vol. 50. American Institute of Aeronautics and Astronautics, Palm Springs, California. ISSN 2009-2132.

Webb, L.D., Mccain, W.E. and Rose, L.A. (1988). Measured and Predicted Pressure Distributions on the AFTI / F-111 Mission Adaptive Wing. Tech. Rep., National Aeronautics and Space Administration, Edwards, California.

Weisshaar, T.A. (2006). Morphing Aircraft Technology – New Shapes for Aircraft Design. Tech. Rep., Purdue University.

Wigley, A.T. (2018). Shape Shifting Foils.

Wlezien, R., Horner, G., McGowan, A., Padula, S., Scott, M., Silcox, R. and Simpson, J. (1998). The Aircraft Morphing Program. In: *39th Structures, Structural Dynamics, and Materials Conference and Exhibit*.

Young, Y.L., Motley, M.R., Barber, R., Chae, E.J. and Garg, N. (2016 oct). Adaptive Composite Marine Propulsors and Turbines: Progress and Challenges. *Applied Mechanics Reviews*, vol. 68, no. 6, p. 060803. ISSN 0003-6900.

Zeiner-Gundersen, D.H. (2014 dec). A vertical axis hydrodynamic turbine with flexible foils, passive pitching, and low tip speed ratio achieves near constant RPM. *Energy*, vol. 77, pp. 297–304. ISSN 03605442.

Appendices

A Sailing

A.1 Background

A brief explanation of sailing terminology as well as the basic physics and forces involved will improve the readers comprehension of the thesis as well as the concepts discussed. The purpose of this this appendix subsection is simply to introduce potentially confusing sailing specific terms and not to expand too deeply into the physical interactions and aero-hydro dynamic theory that make sailing possible, that is covered in section 4.1 and subsection A.2.

Sailing involves a complex interaction between aerodynamic and hydrodynamic forces on the sails and hull of a sailing boat. All control is provided through human input often by means of complicated control systems. All propulsion is provided by the interaction of the sails with the wind and the hull and underwater appendages with the water. From this a number of sailing specific terms arise which are generally not common knowledge. Anderson (2008) provides a well written, easy to understand paper outlining the physics of sailing. To start with, Figure A.1 gives an illustration of a simple sailing dinghy with most of the basic components labeled.

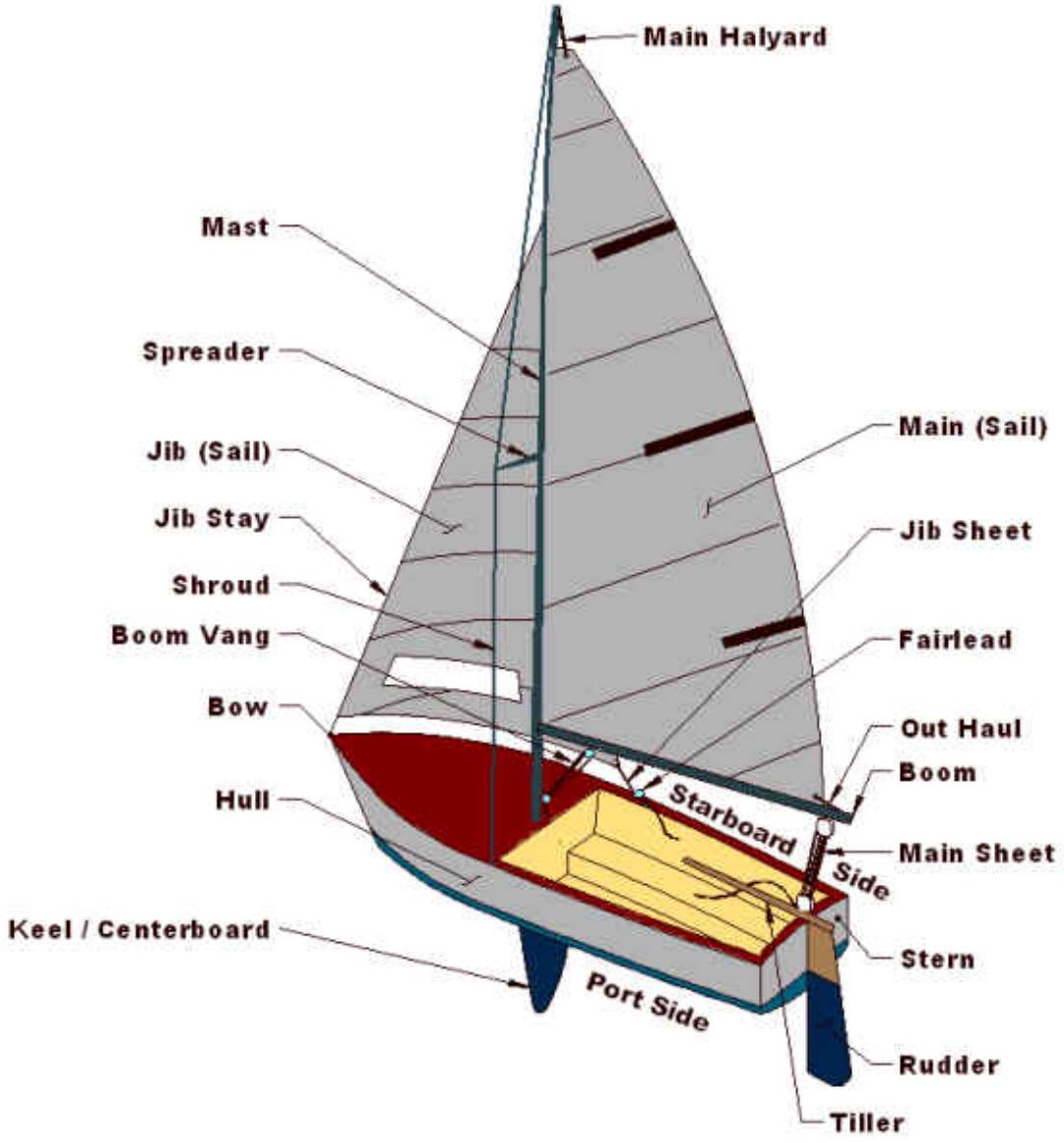

Figure A.1: Basic Sailing Boat Terminology (Gulf Port Yacht Club, 2019)

In order to understand why a morphing foil is desirable in a sailing application, specifically the centreboard of a high performance sailing dinghy, an understanding of the way sailing boats achieve certain courses, and the basic component forces involved is necessary. Sailing boats are steered by, among other complex interactions, constant control inputs from a *rudder*. The direction that the boat points

is called a *heading*, this is in contrast to the actual direction of travel of a boat through the water which is termed the boat's *course*. Changes in forces on the boat from environmental factors require constant changes in control (via the sails, rudder, crew weight and a number of other methods) to maintain a heading. A boats heading relative to the mean wind direction is termed a *point of sail* and the main points of sail are illustrated in Figure A.2. Sailing a course near to opposite the wind vector is considered *high* and *close* [1] to the wind, this is *above* a course that is in the same direction as the wind vector which is considered *low* and *away* from the wind.

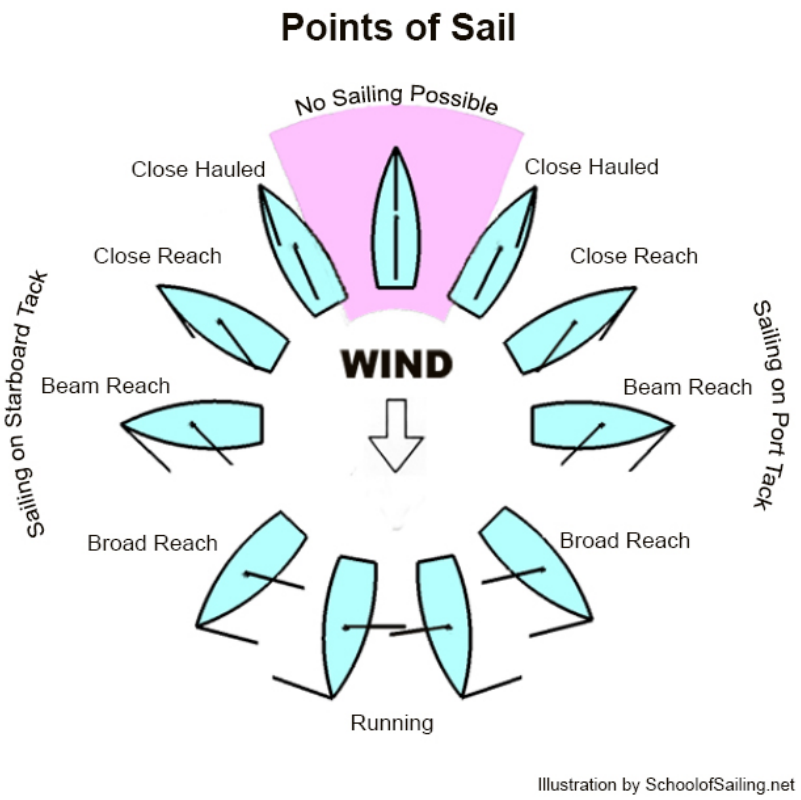

Figure A.2: Points of sail (SchoolofSailing.net, 2013)

To travel to a goal which is directly upwind a sailing boat will sail a *close hauled* course at roughly 45 degrees to the wind and *tack* [2] a number of times, allowing the

[1] Sailing at an acute angle between the wind direction and the direction of travel, also called *upwind* sailing

[2] When *tack* is used as a verb it means to transition between starboard and port tacks with the bow of the boat crossing the wind

boat to 'zig-zag' upwind. An illustration of this can be seen in Figure A.3. A new term *Velocity Made Good (VMG)* is now introduced. A boat's VMG is its relative velocity towards its desired goal. It should be clear to see from Figure A.2 that, unless the goal is within the *No-Go Zone* and the boat can sail directly towards the goal, a boat's VMG (Ignoring current, leeway which will still be introduced and other such complex factors and assuming the boat is sailing straight towards its goal) in this case is equal to its velocity. If the goal is directly upwind of the boat the best it can do is sail close hauled and tack as illustrated in Figure A.3. For a close hauled course the VMG of a boat is calculated as shown in Figure A.4 and Equation A.1.

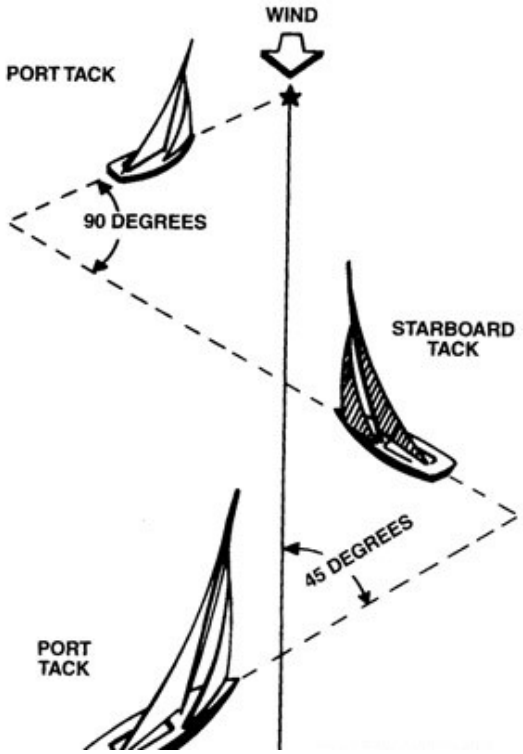

Figure A.3: Upwind Sailing (Sailing Waters Magazine, 2020)

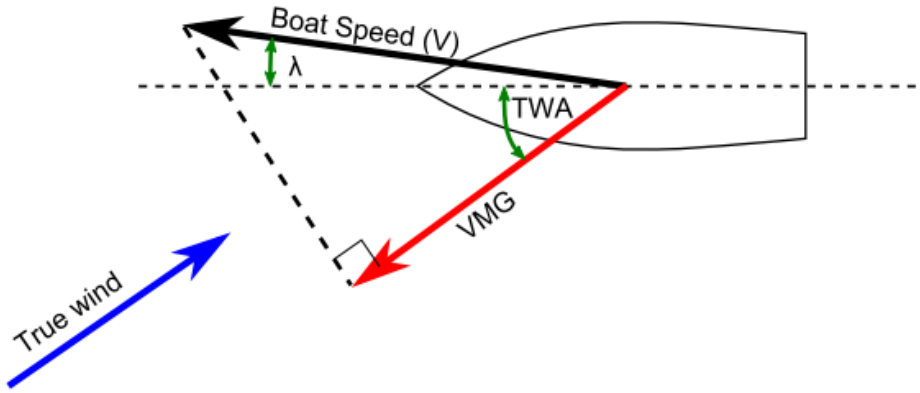

Figure A.4: Velocity Made Good (Knudsen, 2013)

$$VMG = V_s \cos(TWA + \lambda) \tag{A.1}$$

Finally the concept of *leeway* must be introduced. Due to the forces present on a boat that is sailing in any direction except directly downwind, it never travels a straight path through the water, rather it slips sideways to some extent. The course the boat travels is thus different from its heading, the angle difference in these courses is termed the *leeway angle* (λ). This leeway reduces VMG as well as reducing pure boat speed by increasing hydrodynamic drag on the hull and underwater appendages. Leeway is however necessary on conventional sailing boats as the hull and underwater appendages are (usually) symmetric about the centre line. The boat must therefore sail at a non-zero leeway angle in order to give the centreboard and hull an angle of attack relative to the flow and in turn allows the centreboard to generate lift countering the sideways component of the force generated by the sails. Figure 4.2 gives a basic force balance of a boat on a close hauled course. Since asymmetric profiles are capable of generating lift at zero and even negative angles of attack these would reduce and potentially eliminate leeway, drastically improving VMG and performance.(Anderson, 2008)(Gentry, 1981)

The practical implications of changing the profile shape of the centreboard to an asymmetric profile are that the boat still needs to be able to operate on both tacks, meaning that for an asymmetric centreboard to function it must be able to morph its camber line over the centre line to each side of the foil as illustrated in Figure 4.9.

Sailing races for high performance sailing dinghies (such as the 505 class) usually consist of a number of boats sailing around set marks in the water in a certain order. This requires boats to sail on all of the points of sail at some point in the race. Due to the nature of upwind sailing (tacking and zig-zagging), VMG is the lowest on this leg and consequently the most time in a sailing race is spent on the upwind leg yielding the most potential for improvement in overall time.

In conclusion, in order for a boat to sail around a course in the shortest possible time VMG must be improved, especially on the upwind leg. From Equation A.1, assuming the true wind speed and true wind angle remain constant, this can be achieved in three ways: (1) increasing boat speed while keeping leeway angle constant, (2) reducing leeway angle while keeping boat speed constant or (3) some combination of increased speed and reduced leeway. The way in which a boat may achieve these goals is presented in section 4.1.

A.2 Theory

The two main areas where forces act on a sailing boat are on the sails and superstructure as aerodynamic forces and on the hull and underwater appendages as hydrodynamic forces.

Aero-forces

The aerodynamic forces are largely responsible for the forward motion of the boat and are shown in Figure A.5. Although the hull, rigging, crew and superstructure all have aerodynamic effects, the forces from sails dominate. Conventionally, since the sails work as aerofoils, the aerodynamic force is divided into two components referenced to the direction of the apparent wind, an *aerodynamic lift force* (L) perpendicular to the apparent wind direction and an *aerodynamic drag force* (D) parallel to the apparent wind direction. These forces act through the *centre of effort* (CE) above the waterline (the location of which is affected by the sail trim) and, consequently create moments which will be considered in following sections.

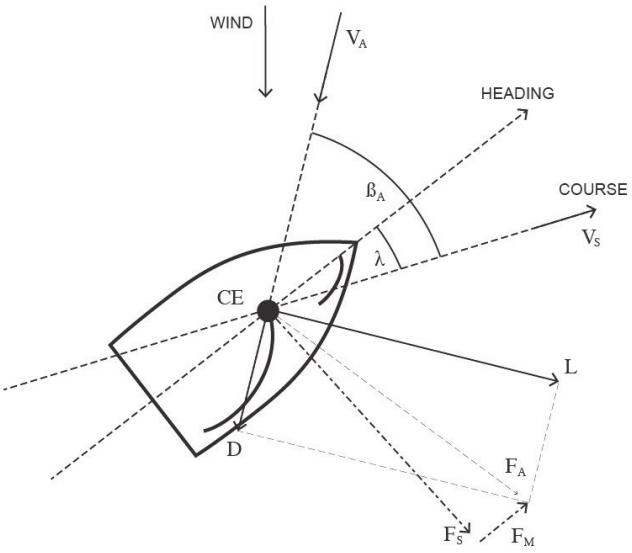

Figure A.5: Aerodynamic Forces on a Sailing Boat's Sails

The vector sum of $\vec{L}$ and $\vec{D}$ yields the total aerodynamic force on the sails, $\vec{F}_A$. In order to be of more use in a mathematical model the total aerodynamic force can be broken down into component vectors parallel with and perpendicular to the direction of the *boat velocity* (V_s): the *driving* or *motive force* (F_m) and the *aerodynamic side* or *lateral force* (F_s) respectively.

The reason behind continuing to use the lift and drag forces, even though they do not directly relate to the boats coordinate system, is that existing aerodynamic theory is then easily applied to the sails and, through trigonometry the forces can be broken into their useful vectors. Since the sails act as wings the lift and drag coefficients may be defined as follows:

$$\begin{aligned} L &= qAC_l, \\ D &= qAC_d, \end{aligned} \tag{A.2}$$

where

$$q = \frac{1}{2}\rho V_\infty^2, \tag{A.3}$$

Here C_l and C_d are functions of the *apparent wind angle* (β_A), the *sail trim angle* (δ_m), the *heel angle* (θ) and the sail shape. The dynamic pressure of the operating fluid is represented by q with a density (ρ) and free stream velocity (V_∞). As Philpott *et al.* (1993) states, these statements require further aerodynamic assumptions which are appropriate for use in this case. The sail shape factor represents both the planform (the shape designed by the sail maker) and a sail trim condition (sail twist and camber under control of the crew).

It is difficult to determine how the aerodynamic force coefficients depend upon the variables provided and this depth of calculation is far too involved for this project. Philpott *et al.* (1993) shows how the heel angle can be removed by assuming that the sails generate a force which acts in a plane normal to the mast and depends only on the component of apparent wind lying in this plane. The dependence of the coefficients on the remaining variables is one of the most difficult parts of all VPPs and Philpott *et al.* (1993) provides further information on existing research into this area.

In a high performance sailing dinghy the ideal sailing condition, maximising performance, is sailing at zero heel angle $\theta = 0$. Among other effects this maximises the component of the total aerodynamic force and consequently lift and motive force in plane with the water thus maximising the boat speed. For the purposes of this project it will simply be assumed that the boat will be sailed at a zero heel angle. The heel angle can easily be included in the following calculations through further application of trigonometry.

The motive and lateral forces can now be expressed in terms of the lift and drag forces and their angles, including apparent wind angle and leeway angle. This will put the aerodynamic forces in the same frame of reference as the hydrodynamic forces and will be useful in later calculations. F_m and F_s are expressed as follows:

$$\begin{aligned} F_m =& (L\cos\beta_A + D\sin\beta_A)\cos\theta\sin\lambda \\ &+ (L\sin\beta_A - D\cos\beta_A)\cos\lambda, \\ F_s =& (L\cos\beta_A + D\sin\beta_A)\cos\theta\cos\lambda \\ &- (L\sin\beta_A - D\cos\beta_A)\sin\lambda, \end{aligned} \tag{A.4}$$

Since we assumed earlier that the boat will only be sailed at zero heel angle, a new term: the *aerodynamic heeling force* or *aerodynamic overturning force* (F_{oa}),

is introduced. This is the force acting normal to the hull centre line and mast and not necessarily the boats direction of travel, and will be useful in the moment calculations to follow.

$$F_{oa} = L\cos\beta_A + D\sin\beta_A \tag{A.5}$$

Hydro-forces

In order to balance out the aerodynamic forces on the sails, the hull and underwater appendages (centreboard or keel and rudder) create both a lift and a drag force shown in Figure A.6. The lift force perpendicular to the boat's path through the water and, consequently the flow, is termed *hydrodynamic side or lateral force*(S) and the drag, parallel to the flow opposing the forward motion of the boat, *hydrodynamic drag force or resistance* (R). These hydrodynamic forces act through a point under the water surface termed the *centre of lateral resistance* (CLR). The hull and underwater appendages on a sailing boat are usually symmetric about the centre line and therefore rely on a non-zero leeway angle to provide an AoA great enough to produce the required S.

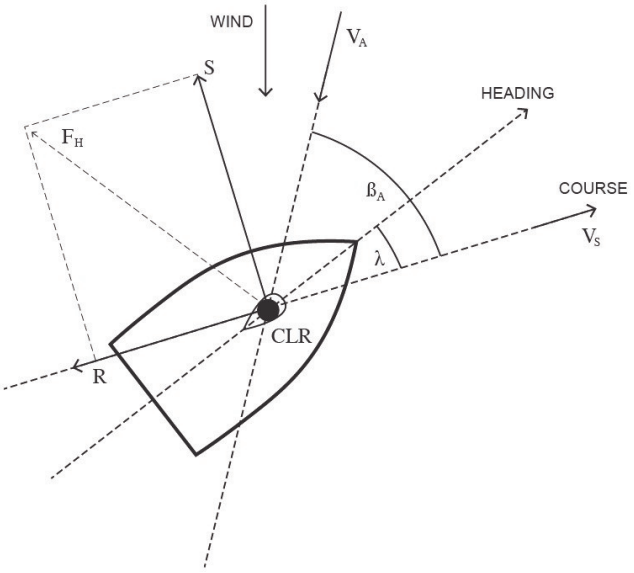

Figure A.6: Hydrodynamic Forces on a Sailing Boat's Hull and Underwater Appendages

Like the aerodynamic forces, the total hydrodynamic force is yielded by the vectorial,

$$\vec{F}_H = \vec{S} + \vec{R}, \tag{A.6}$$

These two force components can be modelled similarly to the aerodynamic counterparts. Additionally the hydrodynamic overturning force can be presented similarly to the aerodynamic overturning force:

$$F_{oh} = S\cos\lambda + D\sin\lambda \tag{A.7}$$

As a starting point, the resistance is modelled theoretically and often calibrated to fit experimental data. Many modern VPPs break the total resistance into a large number of more detailed resistance components that are added together to yield the total hydrodynamic resistance. In the case of Philpott *et al.* (1993) a simple, concise formulation is provided and used as a basis here. The drag components of the centreboard and rudder can simply be calculated using the corresponding

three-dimensional drag coefficients as outlined in Equation A.2.

The resistance of the hull is then split into three parts namely, upright resistance, heeled resistance and induced resistance. Induced resistance is the drag due to lift produced by the hull from the leeway, while heeled resistance is simply the extra drag arising from a non-zero heel angle and consists of a number of components too detailed to be mentioned here, Mason (2010) provides a more detailed, modern breakdown of these components. The induced and heeled resistance are usually combined in a single equation dependant on the leeway and heel angles as well as the boats speed, $F_i(\lambda, \theta, V_s)$.

This only leaves the upright resistance which is the hull drag at zero heel and zero leeway. This upright resistance can once again be broken up into components, in this case it is split into a frictional component arising from the water viscosity and a wave drag component giving the energy used to propagate waves away from the hull. Philpott *et al.* (1993) recommends a number of methods as the basis for this division.

The frictional resistance is understood well in theory and the frictional force acting on the hull can be derived as follows:

$$F_f = \frac{1}{2}\rho_w C_f A_w V_s^2, \tag{A.8}$$

In Equation A.8 A_w represents the hull's wetted surface area, ρ_w is the density of water and C_f is a coefficient of friction or resistance coefficient depending on boat velocity, waterline length and the water viscosity. Values for this coefficient can be found in the Delft Systematic Yacht Hull Series ($DSYHS$) presented in papers such as Vidmar and Perkovič (2013) and Day (2017). The wave drag component is derived from classical hydrodynamics such as presented in Hoerner (1965) as:

$$F_w = \frac{1}{2}\rho_w C_w A_w V_s^2, \tag{A.9}$$

where C_w is the wave drag coefficient depending on the hull shape (particulars of which can be found in the $DSYHS$) and the Froude number (Fr). Philpott *et al.* (1993) summarises that the relationship between wave drag and hull shape is not fully understood and that, in practice, coefficients are determined through model tow tank testing. Gerritsma and Keuning (1992) and Van Mannen and Van Oossanem (1988) provide generalised expressions for hull shape factors from

fitting curves to tow tank data.

Finally, the hydrodynamic side forces on the boat need to be taken into account. These side forces arise directly from the lift produced by the hull canoe-body (as is termed in classical hydrodynamics) and the lifting surfaces of the underwater appendages, usually a centreboard and a rudder. Papers such as that of Day (2017) provide comprehensive derivations and expressions for the side force of each component, specifically for a sailing dinghy, however a number of simplifying assumptions will be made here as used by Philpott *et al.* (1993). At small leeway and heel angles the hull produces little lift and can therefore be ignored in order to focus attention to the centreboard and rudder. In the case of the centreboard, it's span is restricted on one end by the hull surface which acts as an end plate, this has consequences when calculating the effective aspect ratio for the foil. The rudder will produce lift from the waterline to the depth it draws.

These side forces will act perpendicular to their velocity vector through the water and the vertical axis of the boat. Since the centreboard and rudder both act as wings, their forces can be expressed in terms of lift coefficients yielding the equation for hydrodynamic side force:

$$S = \frac{1}{2}\rho_w V_s^2 \left(C_{Lr} A_r + C_{Lk} A_k\right) \cos\theta, \tag{A.10}$$

In Equation A.10 the variables C_{Lr} and C_{Lk} represent the lift coefficients of the rudder and keel/centreboard respectively while A_r and A_k represent their respective surface areas. The lift coefficients of both the centreboard and rudder depend upon the properties of their shape and design as well as their AoA. The angle of attack of the centreboard (α_{keel}) can be calculated simply using trigonometry depending solely on the leeway and heel angles:

$$\alpha_{rudder} = \arctan\left(\cos\theta \tan\left(\lambda + \delta_r - \phi\right)\right), \tag{A.11}$$

$$\alpha_{keel} = \arctan\left(\cos\theta \tan\lambda\right), \tag{A.12}$$

The AoA and, consequently, lift coefficient for the rudder is a far more complicated calculation. Day (2017) provides comprehensive equations for the accurate calculation of rudder lift based on the work of Keuning and Verwerft (2009), these calculations take into consideration two main factors which change the rudder's effective AoA. The centreboard produces downwash from the lift it generates, reducing the rudder angle of attack, further the rudder angle (δ_r), which is an independent variable, affects α_{rudder}.

For a high performance sailing dinghy to be sailed at a steady state optimal performance, crews aim to eliminate the use and consequently the drag of the rudder, so much so that most competitive teams are able to sail a constant course entirely without the rudder, steering using a complex combination of sail and boat trim. Sailing a dinghy in such a way eliminates any potential induced drag produced by the rudder and for this reason it is possible to assume that the rudder produces zero lift in steady state operation. Practically this means that the rudder angle is equal to the leeway angle minus the downwash angle from the centreboard.

$$\delta_r = \arctan\left(\frac{\tan\alpha_{rudder}}{\cos\theta}\right) - \lambda + \phi \tag{A.13}$$

and since it will be assumed that $\alpha = 0$ and $\tan\alpha_{rudder} = 0$ it follows that

$$\delta_r = \phi - \lambda, \tag{A.14}$$

Consequently, following from the assumptions provided, the only remaining factor producing hydrodynamic lift is the centreboard.

A.3 Supplementary Information for section 4.2.1

The 505 class sailing dinghy is considered a high performance, highly powered, physically demanding boat sailed by two sailors or *crew*. Due to this the sailors are typically tall, and physically strong. [3] Helmsmen are seldom shorter then 1.6 m and lighter than 60 kg and crew are typically taller than 1.7 m and heavier than 90 kg, this correlates to the typical sailor weight parameters mentioned by the international 505 class association on their website, (505 International Class Association, 2020). Light sailor combinations will move their collective weight further out from centre line sooner, increasing their moment arm to achieve same righting moment as heavier sailor combinations up to a certain point. Once the light sailors are fully extended, as far away from the centre line as possible, they cannot move their weight further out to match the righting moment of heavier

[3] It must be noted that lighter crew combinations, including many female and younger sailors have achieved much success in the class. Modern, lower camber sail shapes, spanwise flexible centreboards and innovative control systems have made the class far more accessible to a wider range of sailors. These lighter crew combinations typically carry large performance penalties upwind due to limited righting moment, however these crews can make significant gains downwind where righting moment is not the limiting factor. The assumption of crew weight and height is based on optimal upwind performance across a range of operating conditions. Additionally the equations used in this model are not focused on the drag penalties associated with heavier crews which are assumed to be minimal for this study.

sailor combinations. Consequently lighter sailor combinations will suffer reduced performance in heavy wind upwind sailing, where righting moment is the limiting factor in performance, but will have increased performance in light wind sailing due to less mass to accelerate, less displacement and consequently less hull drag.

Sailors move their weight transversely using a number of systems on the boat. In lighter wind conditions sailors begin siting on centre line of the boat and then simply move within the hull of the boat, as the wind speed increases and more righting moment is required the crew uses a *trapeze* and the helm uses *hiking straps* in order to move their weight outboard. Figure 4.4 shows a crew trapezing and a helmsman hiking at near full extension. A number of assumptions on the COG of the sailors is made in line with the research presented in Davidovits (2019). Firstly it is assumed that the sailors are male, in line with the majority of 505 sailors. The normal standing COG for men is at 56 % of their height. When standing with arms extended above their head the COG moves to 66 % of their height. Further it is assumed that the crew, when trapezing is standing on the gunwale edge perpendicular to the mast and, at zero heel angle, parallel to the water surface. Typically for the helmsman hiking at full extension the gunwale lies just outboard of the knees. This leaves roughly 75 % of the body outboard of the gunwale, assuming the mass distribution along the body is roughly even (a valid assumption since the standing COG is at 56 %) the COG position can simply be multiplied by 75 % to find the helmsman COG position. The boat gunwale position can be used as a baseline for the sailors righting moment lever arm shown in Figure 4.3, adding the relevant sailor COG positions to this position will yield the total lever arm distance. The gunwale of a 505 is 0.94 m transversely away from the hull centre line, represented as D_{gun}, and is near parallel to the centre line in the region where the sailors are positioned. The moment arm for each sailor, y_c and y_h or generally, D_m, is then calculated as:

$$D_m = D_{gun} + COG\ \%_{position} * H_{sailor} * POS, \tag{A.15}$$

where COG % is defined by the above assumptions and h_{sailor} is the sailor's standing height. Vectors consisting of fractions of maximum extension, representing the relevant sailor positions across the wind range is set up, POS. There are position vectors for both helm and crew in both the heavy and light combinations. It can be seen that the crew (who's job on-board is to balance the roll moment) moves outboard before the helm and that the lighter sailor combinations have to move their collective weight outboard in lighter wind, increasing their moment arm and compensating for their lighter mass. Since the 505 dinghy's sail-plan is powerful it can be noted that from 14 kts wind speed both the heavy and light combinations use all of their available righting moment and must balance the roll

moments acting on the boat by de-powering or easing the sails. The position vectors are given in Table A.1.

Table A.1: Sailor Position Vectors

True Wind Speed [kts]	6	8	10	12	14	16	18	20
Position Vectors								
Heavy Helm	0	0	0.0625	0.25	0.5625	1	1	1
Heavy Crew	0	0.04	0.16	0.36	0.64	1	1	1
Light Helm	0	0.04	0.16	0.36	0.64	1	1	1
Light Crew	0.175	0.205	0.3275	0.575	0.95	1	1	1

To calculate the overturning force from the crew righting moment geometry of the boat providing the distances of the CE and CLR from a reference point must be found. Keuning and Vermeulen (2003) shows that it is reasonable to assume the CLR of a foil is located along the quarter chord line at 43 % of the total draft of the foil, similarly it can be assumed that the CE lies on the quarter chord line at 43 % of the sail hoist. This yields: $z_a = 2{,}75$ m for CE, and:

$$z_h = 0{,}458 + \left(\frac{4 * s}{3 * math{,}pi}\right) \tag{A.16}$$

for CLR where 0.458 m is the distance from the reference point to the bottom of hull where the foil root begins. All of the diagrams providing the boat geometry can be found on the international 505 class association website, (505 International Class Association, 2020). The equation for the distance of CLR uses the assumption that both the centreboard planform and spanwise lift distribution is elliptical, therefore the equation for geometric centre for an ellipse can be used, this equates to close to 43 % of the span.

A.4 Supplementary Information for the Fluid Dynamic Analysis

Moment Coefficient

Symmetric foils' lift force vector acts through a single point at all AoAs, the centre of pressure of the airfoil does not move significantly with AoA, this corresponds to a near zero C_m. Conversely, asymmetric foils experience a movement in centre of pressure forward or aft along the chord line with changes in AoA this movement is described by the C_m. The moment coefficient is equal to the pitching moment acting on the profile divided by the dynamic pressure, area and chord length

(Equation A.17), it provides an indication of the total pitching moment force acting on the profile and, consequently the boat. In principle this moment should be minimised to reduce the requirement of rudder input (see section 4.1) in order to balance the yaw moments acting on the boat.

$$C_m = \frac{M}{qAc} \tag{A.17}$$

All of the profiles are found to have C_ms around 0.1. The NACA 4410 profile has a C_m of 0,1027. Solving Equation A.17 for M the pitching moment is found to be 47.36 Nm , pitching the nose of the foil down, this would require a forward sweep of the centreboard to balance the yaw moments. Since the maximum centreboard lift is known the maximum forward sweep required is calculated as 2,97°. This is well within the achievable range of 505 centreboards. For the remainder of the design it is assumed that relatively small ($<= 0{,}1$) C_m values can easily be counteracted in operation by the sailors and therefore are excluded from consideration in the foil profile selection.

Flow Separation

The parameter governing the transition point of the onset of turbulence in XFoil, $Ncrit$, is highly dependent on specific flow conditions and surface roughness of the foil and therefore difficult to decide upon. The values for *dirty* or turbulent conditions ((Drela and Harold, 2001)) are used in the simulations as the flow conditions for the centreboard are affected by a number of inferences such as surface waves and other boats on the course. An $Ncrit$ value of 5 is used for all of the XFoil simulations.

The location of laminar flow separation or flow separation bubbles can be found by analysing the skin friction coefficients along the profile surface. If the friction coefficient is negative it indicates there is reverse flow in that area as a result of a region of flow separation. The values of C_f are found using XFoil for each foil profile. Although certain foil sections such as NACA 3710 produce the required C_l at relatively low AoA ($-0{,}3°$) with very low drag coefficients there is danger of flow separation occurring due to the position of maximum camber being relatively far back in the foil. This can be attributed to the delayed onset of turbulence on the top surface. In fact this trend can be seen when the position of maximum camber is moved to either end of the foil.

Pressure Distribution

Figure A.7 show the pressure distributions as pressure coefficient values over the top and bottom surfaces of the symmetric and cambered profiles respectively. These curves provide some insight into the way in which lift is generated in a symmetric foil versus an asymmetric foil. The symmetric foil at a non-zero *AoA* relies on a large pressure differential near the nose of the foil, mainly produced by a large negative pressure on the top surface where the flow is accelerated as it remains attached to the surface. The large negative pressure area is the cause of flow separation and stall as *AoA* increases, it also contributes to the increased drag experienced by the symmetric foil at this operating point. The asymmetric foil by comparison produces a more even pressure differential along the chord length of the foil, this is in part due to the low *AoA* but also due to the fact that the flow needs to *turn* along the whole length of the foil not only at a single point. The NACA 4410 profile will be far less susceptible to flow separation and stall in dynamic operation, while generating less profile drag.
The pressure distribution over the profile can be used to provide load cases and boundary conditions over the profile for future designs but is excluded from the FEM analysis in subsection 4.3.2.

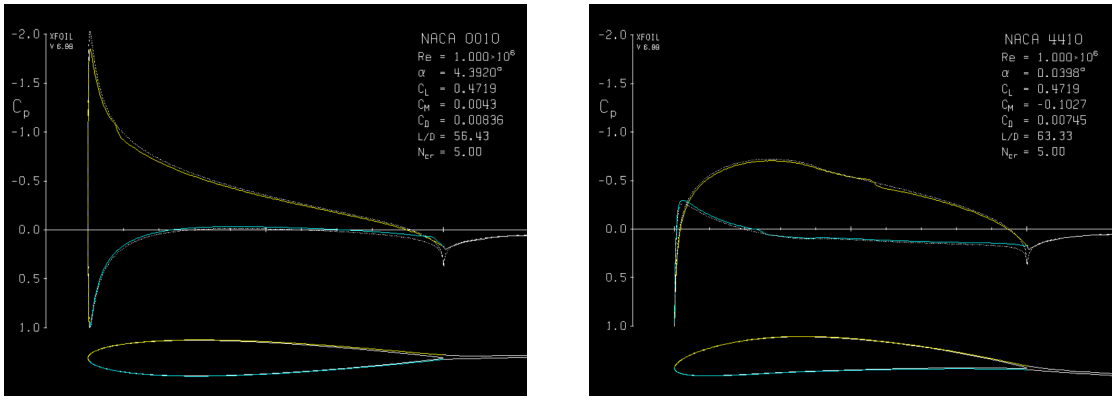

(a) NACA 0010 Pressure Distribution (b) NACA 4410 Pressure Distribution

Figure A.7: Symmetric vs Cambered Foil Pressure Coefficients

A.5 505 Geometry

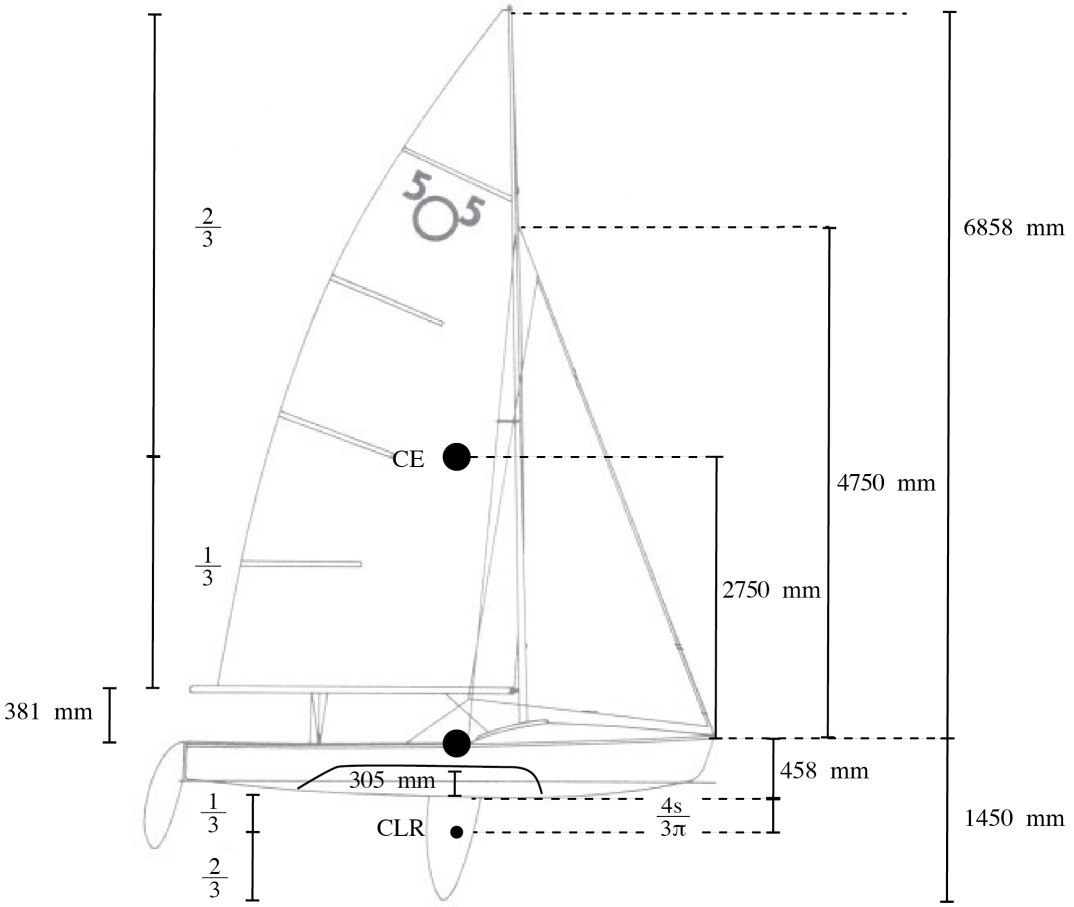

Figure A.8: 505 Dinghy CE, CLR Geometry

B Filtered Output of Populated Research Table fro Morphing Research Database

There is simply too much information present in the filtered research table to be presented well in this format. The filtered research table, shown in Table B.1 can be provided electronically if required.

Table B.1: Filtered Research Table

	Entry Information		Focus Area [FA]									Morphing Effect [MEF]		Physical Description [PD]				Axis Influenced [AXI]		Actuation [ACT]						Surface [SUR]	Sub-structure [SUB]		
			Field [FLD]			System [SYS]			Level [LVL]					Scale [SCL]		Degree of Shape Change [DSC]													
Mendeley Ref	Year	Research Title	Fluid Dynamics	Mechanics	System	Actuator	Surface	Sub-structure	SYS, SUB, COMP	Design Target [DT]		[property]	[effect]	[characteristic length]	[magnitude]	[shape change]	[nature of change]	[magnitude]	Deflection [D] x,y,z	Rotation [R] x,y,z	Actuation Load [AL]*	Actuation Frequency [AF]	Actuation Energy Source [AES]*	Sub-system Involved [ASI] Actuator, Surface, Sub-structure	Descriptor [DES act]	Descriptor [DES sur]	Descriptor [DES sub]	Operating Conditions [OPR]	
Cooper2006	2006	Adaptive Stiffness Structures for Air Vehicle Drag Reduction. (Rotating Spars Concept)	Y	Y		Y		Y	SUB	L/D	max	[Cl; Cd; Cl/Cd]	[0,2; -0,55; 0,24]	[chord]	0,25	Bending, Camber, Twist			Z	X, Y		2 Hz	0*	ACT, SUB	1	1	1; 8	Re	10^6
Diaconu2008	2008	Concepts for morphing aerofoil sections using bi-stable laminated composite structures. (TE Flap Concept)		Y			Y	Y	SUB; COMP	Camber Change	0,1			[chord]	[0,68]	Camber	Rotate; Bend	0,103	Z	Y	42 N*	inf	1*	SUB	1	1; 8; 9	8; 9; 11	Re	10^6
Diaconu2008	2008	Concepts for morphing aerofoil sections using bi-stable laminated composite structures. (Longitudinal Plate Concept)		Y			Y	Y	SUB; COMP	TE Rotation	0,11			[chord; TE chord]	[0,68; 0,102]	Camber (TE)	Rotate; Bend	0,089	Z	Y	24 N*	inf	1*	SUR; SUB	1	1; 8; 9	8; 9; 11	Re	10^6
Virosh2009	2009	Design and Verification of a Smart Wing for an Extremely-Agile Micro-Air-Vehicle		Y	Y	Y		Y	SUB	TE Rotation	0,33			[chord; TE chord]	[0,24; 0,1]	Camber (TE)	Rotate; Bend	0,13	Z	Y	20 N	1 – 5 Hz	1	ACT, SUR, SUB	2	10	10; 11	Re	10^5
Pool2009	2009	Development of a Simple Morphing Wing Using Elastomeric Composites as Skins and Actuators		Y		Y	Y		SUB	Camber Change	Max			[chord]	0,508	Camber (LE; TE)	Rotate	0,26; 0,17	Z	Y	450 N		1	ACT	2	1	2; 6		
Kota2013	2000	Mission Adaptive Compliant Wing - Design, Fabrication and Flight Test	Y	Y	Y	Y	Y	Y	SUB	L/D	Max	[Cl/Cd; Cd; AL]	[0,75; -0,25; -0,33]	[chord; TE chord]	[0,762; 0,229]	Camber (TE)	Rotate, Bend	0,22	Z	Y		3 Hz	1	ACT	1	1	1	Re	10^6
Eggleston2002	2002	Morphing Aircraft Design Team (Piezoelectric Actuator Concept)	Y	Y	Y	Y		Y	SUB; COMP	Cl; Cl_max	0,3; Max	[Cl; Cd]	[0,66; -0,8]	[chord; TE chord]	[0,3302; 0,0825]	Camber (TE), Twist	Rotate	0,11	Z	Y			1	ACT	2	1	10; 11	Re	10^5
Eggleston2002	2002	Morphing Aircraft Design Team (SMA Actuator Concept)	Y	Y	Y	Y		Y	SUB; COMP	Cl; Cl_max	0,3; Max			[chord]	0,3302	Camber; Twist	Rotate, Bend	0,11	Z	Y		0,5 - 1 Hz	1	ACT; SUB	2	1	10; 11	Re	10^5
Eggleston2002	2002	Morphing Aircraft Design Team (Conventional Actuator Concept)	Y	Y		Y	Y	Y	SUB; COMP	Cl; Cl_max	0,3; Max	[Cl; Cd]	[1,33; -0,5]	[chord; TE chord]	[0,3302; 0,248]	Camber; Twist	Rotate	0,11	Z	Y	0,93 Nm		1	ACT; SUB	1	1; 2	1	Re	10^5
Cadogan2004	2012	Morphing Inflatable Wing Development for Compact Package Unmanned Aerial Vehicles	Y	Y		Y	Y	Y	SYS; SUB	Roll Rate	45 deg/s	[Cl]	0,295	[chord; TE chord]	[0,4318; 0,095]	Camber (TE)	Rotate, Contract	0,033	Z	Y	3,3 bar	≈1 Hz	1	ACT	2	1; 10	6	Re	10^6
Daynes2009	2009	On a Bistable Flap for an Airfoil	Y	Y		Y		Y	SUB; COMP	Bistable Proof of Concept		[Cl]	0,25	[chord; TE chord]	[0,68; 0,136]	Camber (TE)	Rotate, Bend	0,11	Z	Y	670 N*	20 Hz	1*	ACT, SUB	1	1	8; 9; 11	Re	10^6
Kiceniuk1964	1964	Control and propulsion fluid foil		Y	Y	Y		Y	SUB	L/D; Control; propulsion	Increase					Camber; Twist	Bend		Z	X, Y			1	ACT, SUB	1	1; 2; 6	6		
WilliamDorfman1976	1976	Variable Foil Keel and Sailboat		Y	Y	Y	Y	Y	SUB	AoA; Cl	0; increase					Camber, Thickness	Bend		Z				1	ACT	1	1; 2	1	Sailing Boat Keels	
Wigley2018	2018	Shape Shifting Foils		Y	Y		Y	Y	SUB	Cd	decrease					Camber, Thickness	Rotate, Bend		Z	Y			1	ACT, SUB	1	1; 2	1	Sailing Boat Keels	

C Literature Study and Morphing Timeline

Morphing Aircraft History

Shape Morphing for use in aircraft specifically is not a new idea, in fact in 1903, the very first heavier-than-air craft successfully used foil morphing or *Wing Warping* as it was then known as a form of roll control (The equivalent of which would be ailerons in modern aircraft). The Wright Brothers' Wright flyer (Figure C.1) morphed both the leading and trailing edges of the wing as well as twisting the wing span-wise (Thill *et al.*, 2008).

Figure C.1: Wright Brothers Flyer Demonstrating Wing Warping (Southwest Airlines, 2020)

In the early to mid 20th century the payload and speed requirements on aircraft demanded stronger, stiffer wing structures with reduced aero-elastic feedback and the ability to withstand far greater wing loading. This led to *fixed* wings with discrete, mechanical control surfaces as we see in modern aircraft and the concept of foil morphing was put on hold due to a lack of feasible technology (Vasista *et al.*, 2012).

Parker (1920) presented one of the first formal studies on a concept for a variable-camber wing which morphed passively under aerodynamic load. The intention was for the wing to camber automatically with aerodynamic load, throughout the research this was, however found not to be feasible within the proposed design. The *Parker Variable Camber Wing* was an attempt by the then *National Advisory Committee for Aeronautics* (NACA) to address the ever increasing problem of speed differences between takeoff, landing and cruising speeds in early aircraft. It must be noted that this was before the invention of flaps [4] and to Parker a variable camber wing seemed far less of a challenge than increasing the surface area of the wing to perform the same function. In fact Parker writes, referring to the concept of increasing wing area during flight:

> "Unfortunately, mechanical difficulties prevent the realization of this method. These difficulties are so serious that there does not seem any prospect of their being overcome in the near future."

Parker's wing uses an internally hinged structure with a number of cables which are either under tension or slack depending on the configuration of the wing. Parker's concept is not unlike many modern patents making use of complex internally hinged structures, leading one to believe that there is far more space for innovation in this regard.

Between this time and WW2 many morphing concepts were proposed and some even tested, however very few actually made it to the production phase. The post WW2 pursuit of supersonic flight caused a resurgence in interest in some of these technologies as can be seen in the various well known wing sweep aircraft of the mid to late 20th century (Bell X-5, MiG 23, F-14 Tomcat etc.) (Jha and Kudva, 2004).

One of the first large scale morphing research programs was the *Mission Adaptive Wing* (MAW) research program run by NASA with involvement from Boeing and the United States Air Force (USAF). During this program the cross sectional shape, and more specifically the camber of a wing including spanwise differential camber is changed in flight. A segmented wing with a composite surface was deformed through an arrangement of internal rods and linkages actuated by hydraulic rams. More specifically, the MAW consists of leading and trailing edge variable camber sections which are deflected in flight either manually or through automatic, active flight control systems. Proof of concept models were developed and wind tunnel testing was performed before the MAW airfoil was flight tested

[4] Plain flaps had been used before to discretely increase wing camber but the *Fowler Flap*, the first flap to propose an increase in chord length was only invented in 1924, and tested by NACA in 1932 (Fowler, 1942).

on an modified advanced fighter technology integration (ATFI)/F-111 aircraft at low sub-critical to supercritical speeds. The program produced satisfactory results in terms of performance, significantly improving aerodynamic characteristics compared to the basic F-111A aircraft, however the increase in weight and complexity limited further development. The main aerodynamic improvements included increased roll control, reduced wing root bending moment, delayed shock onset and improved L/D throughout the flight envelope. Decamp and Hardy (1984), Larson (1987), Bonnema and Smith (1988), Webb *et al.* (1988), Smith and Nelson (1990), Goecke Powers *et al.* (1992), Smith *et al.* (1992) and Thornton (1993) report on the project during its various phases. The tests, however, encouraged further innovation in the field and within the organisations involved.

NASA had been involved in foil morphing from the infancy of the technology, together with Boeing and Lockheed Martin they performed many of the wind tunnel and flight tests for the MAW program. Much of the NASA research was only declassified after WW2 and as such didn't drive widespread innovation in the early phases of the technology.

The Active Flexible Wing (AFW) concept was designed by Rockwell International Corporation in the mid 1980s, this concept was the basis of a research program together with NASA beginning in 1986. Perry *et al.* (1995) summarises the program in its entirety and provides the overall vision of the concept and ensuing project: to embrace and exploit rather than avoid wing flexibility to provide weight savings and improve aerodynamics. Two wind tunnel tests demonstrated aeroelastic control through active, digital control of conventional control surfaces. The key program accomplishments included flutter suppression and both load contol and alleviation during maneuvers. The classification of aeroelastic tailoring as a morphing technology remains to be discussed, however this idea is at the heart of many modern morphing concept, notably passively actuated multistable composite based wings.

Beginning in 1996 and running until 2005 NASA was involved in a joint project with the US Air Force Research Laboratory and a number of industry partners called the *Active Aeroelastic Wing* (AAW) project which built upon the previous AFW project. The basis of this project was to exploit the wing flexibility in a controlled, tailored way in order to achieve an aerodynamic performance goal. The project culminated in two full scale series of flight tests on a modified F/A - 18 aircraft commencing in 2003 and 2005 respectively. The basis of this concept was intentional, tailored flexibility in the structural design of the wing enabling low weight solutions which were shown to improve performance. The project relied on

a reduced torsional stiffness F/A-18 wing with independently controlled leading edge and trailing edge flaps and other conventional control surfaces. Much of the focus on the project was on control law designed to optimize strategies for moving wing control surfaces in order to maximise aircraft roll rates. The project was largely successful proving the idea of tailored aeroelastic properties in the control and performance improvement of a wing.

Alongside the AFW and AAW projects the six year *Aircraft Morphing* project was started by NASA in 1998 as outlined by Wlezien *et al.* (1998). The broad aim was to couple research over a wide range of disciplines in order to integrate smart technologies into high payoff aircraft applications. The project focused on smart materials, adaptive structures and active flow control among others, all applications were high bandwidth closed loop devices with dynamic actuation, local sensing and feedback control. The Aircraft Morphing program was mainly aimed at exploring enabling technologies rather than producing a complete morphing concept, much emphasis was placed on the applicability of concept to a real world operational environment. Many of the concepts generated during this project were described as "... virtual shape change through micro flow control..." by McGowan *et al.* (2009) where flow separation and circulation areas were effectively *morphed* by synthetic jets providing the desired effect. Virtual shape change through micro flow control remains at the fringes of what can be considered morphing technologies.

For the sake of continuity in its research in many of these projects, NASA created a fixed definition of a morphing technology. McGowan *et al.* (2009) present it as follows: "efficient, multi-point adaptability". This is in contrast to the definition presented by Skillen and Crossley (2008) who, in a later NASA morphing wing project, defined morphing as: "...a “morphing wing” is an aircraft wing able to drastically change planform shape during flight – perhaps a 200 % change in aspect ratio, 50 % change in wing area, and a 20 degree change in wing sweep. Furthermore, a “morphing aircraft” refers to a conventional fixed-geometry aircraft structure with the fixed wing replaced with a morphing one. Other types of “morphing”, such as variable geometry airfoils, are not considered here." Here Skillen and Crossley (2008) outlines the field from a completely different angle to the majority of research, focusing on the planform changes of a wing of fixed profile shape rather than the more commonly used connotation of a change in airfoil profile or variable geometry specifically applied to the wing.

One of the main technical challenges identified by NASA during the period spanning these projects - brought to light by, among others Wlezien *et al.* (1998)

- was the large multidisciplinary nature of such morphing programs. To that end NASA developed an integrated *multidisciplinary analysis* method (MDA) specifically for aircraft with a large shape change (Chwalowski *et al.*, 2009). The goal of the process was to enable designers to compare several very different morphing designs early on in the design phase providing results which allowed a more confident design decision. The process effectively synthesised the aerodynamic and structural model results. Figure C.2 shows a flow diagram of the NASA MDA tool.

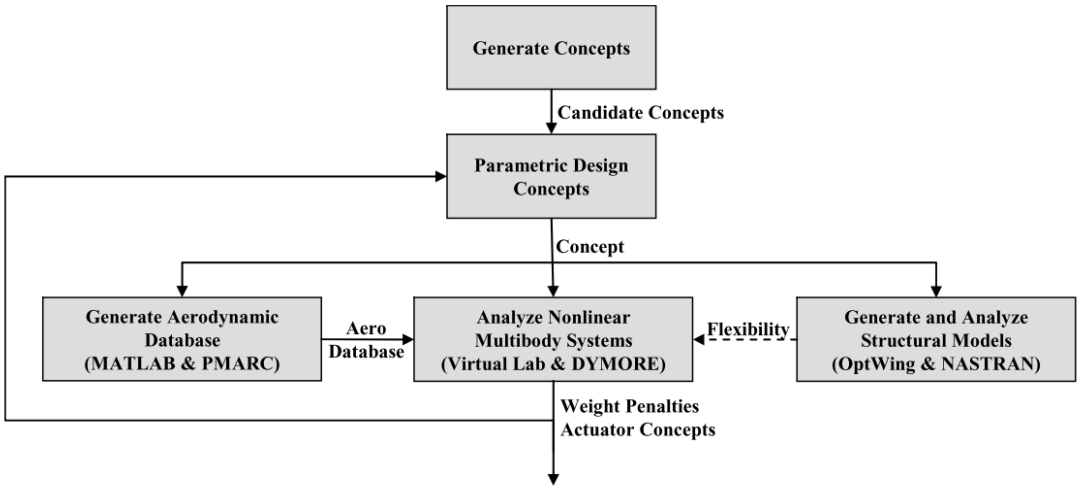

Figure C.2: NASA's MDA Overall Design Process (Chwalowski *et al.*, 2009)

Although most of the readily available literature originates in the US, the *Deutsches Zentrum für Luft- und Raumfahrt* (DLR; German Aerospace Centre) has long been investigating *adaptronics*, as Smart Structures are termed in Germany, directly related to the morphing of airframes (Sinapius *et al.*, 2014). The DLR initiated their national morphing wing program in 1995 and has continued research in the field together with European industry partners up to 2005 through a number of projects. These projects included a morphing smart trailing edge (The ADIF DLR project), a morphing smart winglet (IHK, German Aeronautics Research Program (LuFo) project), a smart leading edge and slat and, more recently a *droop nose* - a morphing LE structure for a civil aircraft wing (SmartLED, LuFo project and SADE project).

Sinapius *et al.* (2014) highlights the main technological challenges encountered by the DLR during the duration of the program, these are listed as:

- Highly elastic skin capable of both the required shape change and withstanding aerodynamic loads,
- Appropriate compliant mechanism or kinematics to deform skin/structure,
- Connection of compliant mechanism or kinematics to elastic skin,
- Actuator integration, both discrete and distributed.

These technological challenges are shared by much research in the field and are some of the main obstacles which need to be overcome in practical morphing designs.

The first of the DLR projects, ADIF, marks the beginning of the organisations morphing wing research in 1995. Similarly to the MAW NASA project the goal was to actively change the shape of a fixed wing during flight, in this case for application on a civil transport aircraft. Variable camber achieved by a morphing trailing edge as well as a local profile *spoiler* bump were the concepts investigated and are shown in Figure C.3.

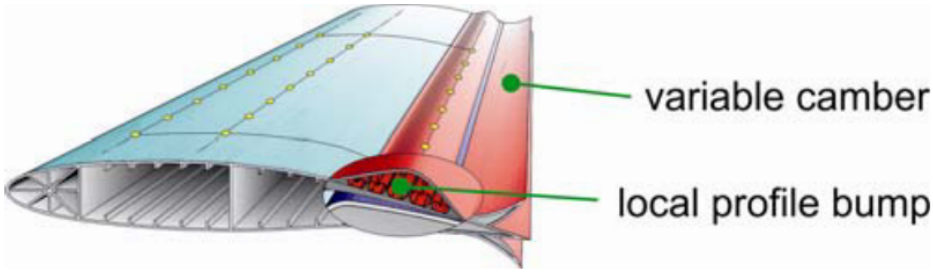

Figure C.3: ADIF Morphing Concepts (Monner *et al.*, 2000)

The flexible trailing edge aimed to provide a continuous, smooth chordwise and spanwise differential camber variation within the same structural system. Two different sub-structural approaches were taken, a finger concept consisting of separate plate like elements with revolute joints outlined by Monner (2001) and a so called *belt rib* concept consisting of a closed belt as the skin of the airfoil with the upper and lower parts of the belt connected by spokes shown by Campanile and Sachau (2000).

The finger concept by Monner *et al.* (2000) replaces the traditional inflexible internal ribs of a wing with flexible ribs comprising of a segmented internal plate like structure linked by revolute joints and actuated covered by a flexible outer surface.

Additionally Monner *et al.* (2000) suggest the implementation of a *local spoiler bump*, the purpose of which is to reduce or at least control transonic shock. The bump is not of interest to this project but the flexible trailing edge suggests many novel solutions to practical difficulties encountered with such a structure(Monner *et al.*, 2000).

Overlapping with the NASA morphing program the *Defence Advanced Research Projects Agency* (DARPA) of the US ran a smart wing program. According to Thill *et al.* (2008) their project was also mainly aimed at smart materials based control surfaces aimed at providing improved aerodynamic efficiency. Aeroelastic concepts were also explored and tests were conducted on a scale model aircraft in a wind tunnel. These concepts mainly composed of continuous, hinge-less control surfaces on the leading and trailing edges of the aircraft wing. These projects were the precursor of the larger *Morphing Aircraft Structures* (MAS) project.

DARPA used contractors such as NextGen Aeronautics and Lockheed Martin to develop the morphing concepts for the MAS program. The goal of the project is summarised by McGowan *et al.* (2009) as: "... to create and advance enabling technologies and ultimately design, build, and demonstrate a seamless, aerodynamically efficient, aerial vehicle capable of radical shape change." The resulting designs from this project were focused on folding wing approaches and a number of wind tunnel tests and remotely piloted vehicle tests were conducted. This project only dealt with changes in wing surface area and aspect ratio and no changes to the profile shape of the wings were considered.

The advent of *smart* materials and structures which grew significantly during the 1990s led to a renewed interest and a new approach to morphing. According to Thill *et al.* (2008), *Smart* materials represent a broad spectrum of materials which respond mechanically to a variety of external stimuli. These materials can be used in *smart* structures in which overall structural requirements, actuation and control are all embedded within the design of the structure. Often it is impossible to differentiate between subsystems due to the multi-functional nature of the structure. In this way actuation capability is integrated within the structure and, as set out by Barbarino *et al.* (2011*b*), this leads to significant benefits in weight, reliability and efficiency (both structural and aerodynamic). Chopra (2002) provide an excellent review of, what was in 2002, state of the art smart structures and integrated systems.

McGowan *et al.* (2009) outline the more futuristic approach to morphing research, much of this driven by the significant increase of research on smart materials

and structures which offer solutions to the previously unattainable design requirements and constraints. These smart material solutions fall far more in line with the pure idea of morphing and are considered in research to be at the centre of any future technologies. Smart materials do, however, have a number of disadvantages which often restrict their practical use according to Li *et al.* (2018). These include the relatively low strain output of Piezoelectric Materials or the slow actuation time of Shape Memory Alloys, due to this Li *et al.* (2018) suggest that cellular materials are more suitable for morphing wings.

Of all the smart materials, there are a few stand out candidates for this project. Shape Memory Alloys and Polymers (SMA and SMP), Piezoelectric Actuators (PZT), bi- or multi-stable composites and pneumatically actuated cellular structures are some of the main *smart* technologies which have been implemented in recent morphing concepts.

Hydrodynamic Applications History

There are a limited number of hydrodynamic applications of this concept available in literature and it must be noted that they are few and far between and an extensive search of a large number of publications is required to find appropriate, reliable literature on the topic. The most prolific source of literature on morphing applied to the hydrodynamic case is, unsurprisingly the US Patent office, where a number of shape morphing patents have been registered dating as far back as 1920. In fact, the first patent for a variable camber wing was registered in the US in 1916 Thill *et al.* (2008). Kiceniuk (1964) provide the first camber changing foil for use in a fluid specifically. The invention makes use of variable fluid pressure within a lattice structure internally within the foil in order to change the shape and camber, it is a rather novel idea and more elegant than most of the cable or linkage ideas to follow. The uses provided include control and propulsion.

In 1976 Dorfman *et al.* (1978) proposed a similar solution comprising of a foil with a narrow central core with moveable surfaces on each side attached to the leading and trailing edges. This surface would be actuated with an increase or decrease of fluid pressure within the chamber between surface and core either bulging outwards or lying against the core. It is difficult to envision the control as well as the morphed and un-morphed shapes of the foil being extremely accurate as there is no structure internally controlling this. The patent is however specifically presented for sailing boats' keels as is proposed in this project and in this regard it is of interest. The patent serves to provide a backing for the need for such technology.

Patents on inventions of morphing foils are not limited to the 20th century. In

the last decade there are a number of foil morphing patents, some dealing specifically with hydrodynamic applications. Many of these patents, such as the *Shape Shifting Foil* by Wigley (2018) rely on intricate internal structures or linkages and are mechanically operated.

D Code Aster Command File Code

```
# Code-Aster command file for surface model
# Requires .med file mesh & initial and final profile geometries as
# .txt files with normalised chord
# Alex Ham 11-05-2020

# 'NON' allows Salome read/write access
DEBUT(PAR_LOT='NON')    # Starting Salome

# Python Functions
# ----------------------------------------------------------------------
import numpy

# Read nodal points from files
coords_old = numpy.loadtxt('/home/alex/PycharmProjects/FEM-pipeline/
                first_geom', skiprows=1)
coords_new = numpy.loadtxt('/home/alex/PycharmProjects/FEM-pipeline/
                second_geom', skiprows=1)

x_old = coords_old[:, 0].tolist()
x_old.append(1.0)                       # Adding TE to list
   # Scale geometry to desired chord length
x_old_scaled = [0.3*x for x in x_old]
y_old = coords_old[:, 1].tolist()
y_old.append(0.0)                       # Adding LE to list
# Scale geometry to desired chord length
y_old_scaled = [0.3*y for y in y_old]
x_new = coords_new[:, 0].tolist()
x_new.append(1.0)                       # Adding TE to list
y_new = coords_new[:, 1].tolist()
y_new.append(0.0)                       # Adding LE to list

# dx distance of each node, unmorphed - morphed
dx = [0.3*(xn - xo) for xn, xo in zip(x_new, x_old)]
```

```
# dy distance of each node, unmorphed - morphed
dy = [0.3*(yn - yo) for yn, yo in zip(y_new, y_old)]

# Function to match relevant translation with input coordinates
def translate_x(X, Y, x_list, y_list, dx_list, dy_list):
    trans_x = 0
    for num1, num2, num3, num4 in zip(x_list, dx_list, y_list, dy_list):
        if abs(float(X)-num1) <= 1e-8 and abs(float(Y)-num3) <= 1e-8:
            #print('x = ', num1)
            #print('dx = ', num2)
            trans_x = num2
    return trans_x

# Function to match relevant translation with input coordinates
def translate_y(X, Y, x_list, y_list, dx_list, dy_list):
    trans_y = 0
    for num1, num2, num3, num4 in zip(x_list, dx_list, y_list, dy_list):
        if abs(float(X)-num1) <= 1e-16 and abs(float(Y)-num3) <= 1e-16:
            #print('y = ', num3)
            #print('dy = ', num4)
            trans_y = num4
    return trans_y

# Code-Aster solver commands
# ------------------------------------------------------------------

# Read existing mesh file in .med format
mesh = LIRE_MAILLAGE(FORMAT='MED',
                     UNITE=20)

# Mechanical, 1D Timoshenko straight Beam analysis (POI_D_T)
model = AFFE_MODELE(AFFE=_F(MODELISATION=('POU_D_T', ),
                            PHENOMENE='MECANIQUE',
                            TOUT='OUI'),
                    MAILLAGE=mesh)

# Assigning cross sectional properties to beam elements
elemprop = AFFE_CARA_ELEM(MODELE=model,
                          POUTRE=_F(CARA=('HZ', 'HY'),
                                    GROUP_MA=('Union_1'),
```

```
                                    SECTION='RECTANGLE',
                                    VALE=(1.450, 0.002)))

# Material properties, assumed to be linear isotropic
mater = DEFI_MATERIAU(ELAS=_F(E=70000000000.0,
                              NU=0.1))

# Assigning material to mesh and model
fieldmat = AFFE_MATERIAU(AFFE=_F(MATER=(mater, ),
                                 TOUT='OUI'),
                         MAILLAGE=mesh,
                         MODELE=model)

# Implementing python formulas for nodal translation
formulax = FORMULE(NOM_PARA=('X','Y',),
                   VALE='translate_x(X, Y, x_list, y_list, dx_list, dy_list)',
                   translate_x=translate_x,
                   x_list=x_old_scaled,
                   y_list=y_old_scaled,
                   dx_list=dx,
                   dy_list=dy)

# Implementing python formulas for nodal translation
formulay = FORMULE(NOM_PARA=('X','Y',),
                   VALE='translate_y(X, Y, x_list, y_list, dx_list, dy_list)',
                   translate_y=translate_y,
                   x_list=x_old_scaled,
                   y_list=y_old_scaled,
                   dx_list=dx,
                   dy_list=dy)

# Enforcing displacement at each node on the surface
# according to the python formulas
load = AFFE_CHAR_MECA_F(DDL_IMPO=(_F(DX=formulax,
                                     GROUP_NO=('Edge_nodes', )),
                                  _F(DY=formulay,
                                     GROUP_NO=('Edge_nodes', ))),
                        MODELE=model)

# Fixing the remaining degrees of freedom on the LE node
```

```
load0 = AFFE_CHAR_MECA(DDL_IMPO=(_F(DRX=0.0,
                                    GROUP_NO=('LE', )),
                                 _F(DRY=0.0,
                                    GROUP_NO=('LE', )),
                                 _F(DZ=0.0,
                                    GROUP_NO=('LE', ))),
                       MODELE=model)

# Setting up the solver and results file
# Assigning element properties to the relevant Code-Aster variable
reslin = MECA_STATIQUE(CARA_ELEM=elemprop,
# Assigning material properties to the relevant Code-Aster variable
                       CHAM_MATER=fieldmat,
                       # Assigning loads to solver
                       EXCIT=(_F(CHARGE=load), _F(CHARGE=load0)),
                       MODELE=model)

# Creation of a table to output the nodal displacement for each node
# in order to check BC's are enforced correctly
table = CREA_TABLE(RESU=_F(GROUP_NO=('Edge_nodes', ),
                           NOM_CHAM='DEPL',
                           NOM_CMP=('DX', 'DY'),
                           RESULTAT=reslin),
                   TITRE='depl_Tab',
                   TYPE_TABLE='TABLE')

# Specifying the specific output parameters required for post-processing
reslin = CALC_CHAMP(reuse=reslin,
                    CONTRAINTE=('SIEF_ELNO', 'SIEF_NOEU'),
                    # Principle stresses at Gaussian  points & Nodes
                    CRITERES=('SIEQ_ELGA', 'SIEQ_ELNO', 'SIEQ_NOEU'),
                    DEFORMATION=('DEGE_ELNO', 'DEGE_NOEU'),
                    FORCE=('FORC_NODA', ),
                    RESULTAT=reslin)

# Output results to .rmed file
IMPR_RESU(RESU=_F(RESULTAT=reslin),
          UNITE=80)

# Output table
```

```
IMPR_TABLE(FORMAT='TABLEAU',
           TABLE=table,
           UNITE=8)

FIN()
```